T H E S E

présentée

A L A F A C U L T E D E S S C I E N C E S

D E L ' U N I V E R S I T E D E G R E N O B L E

pour obtenir

LE GRADE DE DOCTEUR ES-SCIENCES-PHYSIQUES

par

Paulo COSTA RIBEIRO

APPARITION DU MAGNETISME SOUS L'EFFET DES INTERACTIONS DANS LES ALLIAGES DILUES DE Co PAR MESURE DE LEUR CHALEUR SPECIFIQUE NUCLEAIRE.

Soutenue le 5 Avril 1973 devant la Commission d'Examen

MM. L. NEEL Président

B. DREYFUS
F. GAUTIER
D. THOULOUZE
R. TOURNIER

Examinateurs

UNIVERSITE SCIENTIFIQUE

ET MEDICALE DE GRENOBLE

LISTE DES PROFESSEURS

Président : Monsieur Michel SOUTIF

Vice-Président : Monsieur Gabriel CAU

PROFESSEURS TITULAIRES

MM.	ANGLES D'AURIAC Paul	Mécanique des fluides
	AUBERT Guy	Physique
	ARNAUD Georges	Clinique des maladies infectieuses
	ARNAUD Paul	Chimie
	AYANT Yves	Physique approfondie
Mme	BARBIER Marie-Jeanne	Electrochimie
MM.	BARBIER Jean-Claude	Physique expérimentale
	BARBIER Reynold	Géologie appliquée
	BARJON Robert	Physique nucléaire
	BARNOUD Fernand	Biosynthèse de la cellulose
	BARRA Jean-René	Statistiques
	BARRIE Joseph	Clinique chirurgicale
	BENOIT Jean	Radioélectricité
	BESSON Jean	Electrochimie
	BEZES Henri	Chirurgie générale
	BLAMBERT Maurice	Mathématiques Pures
	BOLLIET Louis	Informatique (IUT B)
	BONNET Georges	Electrotechnique
	BONNET Jean-Louis	Clinique ophtalmologique
	BONNET-EYMARD Joseph	Pathologie médicale
	BONNIER Etienne	Electrochimie Electrométallurgie
	BOUCHERLE André	Chimie et Toxicologie
	BOUCHEZ Robert	Physique nucléaire
	BRAVARD Yves	Géographie
	BRISSONNEAU Pierre	Physique du Solide
	BUYLE-BODIN Maurice	Electronique
	CABANAC Jean	Pathologie chirurgicale
	CABANEL Guy	Clinique rhumatologique et hydrologie
	CALAS François	Anatomie
	CARRAZ Gilbert	Biologie animale et pharmacodynamie
	CAU Gabriel	Médecine légale et Toxicologie
	CAUQUIS Georges	Chimie organique
	CHABAUTY Claude	Mathématiques Pures
	CHARACHON Robert	Oto-Rhino-Laryngologie
	CHATEAU Robert	Thérapeutique

MM.	CHENE Marcel	Chimie papetière
	COEUR André	Pharmacie chimique
	CONTAMIN Robert	Clinique gynécologique
	COUDERC Pierre	Anatomie Pathologique
	CRAYA Antoine	Mécanique
Mme	DEBELMAS Anne-Marie	Matière médicale
MM.	DEBELMAS Jacques	Géologie générale
	DEGRANGE Charles	Zoologie
	DESSAUX Georges	Physiologie animale
	DODU Jacques	Mécanique appliquée
	DOLIQUE Jean-Michel	Physique des plasmas
	DREYFUS Bernard	Thermodynamique
	DUCROS Pierre	Cristallographie
	DUGOIS Pierre	Clinique de Dermatologie et Syphiligrap
	FAU René	Clinique neuro-psychiatrique
	FELICI Noël	Electrostatique
	GAGNAIRE Didier	Chimie physique
	GALLISSOT François	Mathématiques Pures
	GALVANI Octave	Mathématiques Pures
	GASTINEL Noël	Analyse numérique
	GERBER Robert	Mathématiques Pures
	GIRAUD Pierre	Géologie
	KLEIN Joseph	Mathématiques Pures
Mme	KOFLER Lucie	Botanique et Physiologie végétale
MM.	KOSZUL Jean-Louis	Mathématiques Pures
	KRAVTCHENKO Julien	Mécanique
	KUNTZMANN Jean	Mathématiques Appliquées
	LACAZE Albert	Thermodynamique
	LACHARME Jean	Biologie végétale
	LATREILLE René	Chirurgie générale
	LATURAZE Jean	Biochimie pharmaceutique
	LAURENT Pierre	Mathématiques Appliquées
	LEDRU Jean	Clinique médicale B
	LLIBOUTRY Louis	Géophysique
	LOUP Jean	Géographie
Melle	LUTZ Elisabeth	Mathématiques Pures
MM.	MALGRANGE Bernard	Mathématiques Pures
	MALINAS Yves	Clinique obstétricale
	MARTIN-NOEL Pierre	Séméiologie médicale
	MASSEPORT Jean	Géographie
	MAZARE Yves	Clinique médicale A
	MICHEL Robert	Minéralogie et Pétrographie
	MOURIQUAND Claude	Histologie
	MOUSSA André	Chimie nucléaire
	NEEL Louis	Physique du Solide
	OZENDA Paul	Botanique
	PAUTHENET René	Electrotechnique
	PAYAN Jean-Jacques	Mathématiques Pures

MM.	PEBAY-PEYROULA Jean-Claude	Physique
	PERRET René	Servomécanismes
	PILLET Emile	Physique industrielle
	RASSAT André	Chimie systématique
	RENARD Michel	Thermodynamique
	REULOS René	Physique industrielle
	RINALDI Renaud	Physique
	ROGET Jean	Clinique de pédiatrie et de puériculture
	SANTON Lucien	Mécanique
	SEIGNEURIN Raymond	Microbiologie et Hygiène
	SENGEL Philippe	Zoologie
	SILBERT Robert	Mécanique des fluides
	SOUTIF Michel	Physique générale
	TANCHE Maurice	Physiologie
	TRAYNARD Philippe	Chimie générale
	VAILLAND François	Zoologie
	VALENTIN Jacques	Physique nucléaire
	VAUQUOIS Bernard	Calcul électronique
Mme	VERAIN Alice	Pharmacie galénique
M.	VERAIN André	Physique
Mme	VEYRET Germaine	Géographie
MM.	VEYRET Paul	Géographie
	VIGNAIS Pierre	Biochimie médicale
	YOCCOZ Jean	Physique nucléaire théorique

PROFESSEURS ASSOCIES

MM.	BULLEMER Bernhard	Physique
	RADHAKRISHNA Pidatala	Thermodynamique

PROFESSEURS SANS CHAIRE

MM.	BEAUDOING André	Pédiatrie
	BERTRANDIAS Jean-Paul	Mathématiques Appliquées
	BIAREZ Jean-Pierre	Mécanique
	BONNETAIN Lucien	Chimie minérale
Mme	BONNIER Jane	Chimie générale
MM.	CARLIER Georges	Biologie végétale
	COHEN Joseph	Electrotechnique
	COUMES André	Radioélectricité
	DEPASSEL Roger	Mécanique des Fluides
	DEPORTES Charles	Chimie minérale
	DESRE Pierre	Métallurgie

MM.	GAUTHIER Yves	Sciences biologiques
	GEINDRE Michel	Electroradiologie
	GIDON Paul	Géologie et Minéralogie
	GLENAT René	Chimie organique
	HACQUES Gérard	Calcul numérique
	JANIN Bernard	Géographie
Mme	KAHANE Josette	Physique
MM.	MULLER Jean-Michel	Thérapeutique
	PERRIAUX Jean-Jacques	Géologie et minéralogie
	POULOUJADOFF Michel	Electrotechnique
	REBECQ Jacques	Biologie (CUS)
	REVOL Michel	Urologie
	REYMOND Jean-Charles	Chirurgie générale
	ROBERT André	Chimie papetière
	SARRAZIN Roger	Anatomie et chirurgie
	SARROT-REYNAULD Jean	Géologie
	SIBILLE Robert	Construction Mécanique
	SIROT Louis	Chirurgie générale
Mme	SOUTIF Jeanne	Physique générale

MAITRES DE CONFERENCES ET MAITRES DE CONFERENCES AGREGES

Melle	AGNIUS-DELORD Claudine	Physique pharmaceutique
Melle	ALARY Josette	Chimie analytique
MM.	AMBLARD Pierre	Dermatologie
	AMBROISE-THOMAS Pierre	Parasitologie
	ARMAND Yves	Chimie
	BEGUIN Claude	Chimie organique
	BELORIZKY Elie	Physique
	BENZAKEN Claude	Mathématiques Appliquées
Mme	BERTRANDIAS Françoise	Mathématiques Pures
MM.	BLIMAN Samuel	Electronique (EIE)
	BLOCH Daniel	Electrotechnique
Mme	BOUCHE Liane	Mathématiques (CUS)
MM.	BOUCHET Yves	Anatomie
	BOUSSARD Jean-Claude	Mathématiques Appliquées
	BOUVARD Maurice	Mécanique des Fluides
	BRIERE Georges	Physique expérimentale
	BRODEAU François	Mathématiques (IUT B)
	BRUGEL Lucien	Energétique
	BUISSON Roger	Physique
	BUTEL Jean	Orthopédie
	CHAMBAZ Edmond	Biochimie médicale
	CHAMPETIER Jean	Anatomie et organogénèse
	CHIAVERINA Jean	Biologie appliquée (EFP)
	CHIBON Pierre	Biologie animale
	COHEN-ADDAD Jean-Pierre	Spectrométrie physique
	COLOMB Maurice	Biochimie médicale
	CONTE René	Physique

MM.	CROUZET Guy	Radiologie
	DURAND Francis	Métallurgie
	DUSSAUD René	Mathématiques (CUS)
Mme	ETERRADOSSI Jacqueline	Physiologie
MM.	FAURE Jacques	Médecine légale
	GAVEND Michel	Pharmacologie
	GENSAC Pierre	Botanique
	GERMAIN Jean-Pierre	Mécanique
	GIDON Maurice	Géologie
	GRIFFITHS Michaël	Mathématiques Appliquées
	GROULADE Joseph	Biochimie médicale
	HOLLARD Daniel	Hématologie
	HUGONOT Robert	Hygiène et Médecine préventive
	IDELMAN Simon	Physiologie animale
	IVANES Marcel	Electricité
	JALBERT Pierre	Histologie
	JOLY Jean-René	Mathématiques Pures
	JOUBERT Jean-Claude	Physique du Solide
	JULLIEN Pierre	Mathématiques Pures
	KAHANE André	Physique générale
	KUHN Gérard	Physique
Mme	LAJZEROWICZ Jeannine	Physique
MM.	LAJZEROWICZ Joseph	Physique
	LANCIA Roland	Physique atomique
	LE JUNTER Noël	Electronique
	LEROY Philippe	Mathématiques
	LOISEAUX Jean-Marie	Physique Nucléaire
	LONGEQUEUE Jean-Pierre	Physique Nucléaire
	LUU DUC Cuong	Chimie Organique
	MACHE Régis	Physiologie végétale
	MAGNIN Robert	Hygiène et Médecine préventive
	MARECHAL Jean	Mécanique
	MARTIN-BOUYER Michel	Chimie (CUS)
	MAYNARD Roger	Physique du Solide
	MICOUD Max	Maladies infectieuses
	MOREAU René	Hydraulique (INP)
	NEGRE Robert	Mécanique
	PARAMELLE Bernard	Pneumologie
	PECCOUD François	Analyse (IUT B)
	PEFFEN René	Métallurgie
	PELMONT Jean	Physiologie animale
	PERRET Jean	Neurologie
	PERRIN Louis	Pathologie expérimentale
	PFISTER Jean-Claude	Physique du Solide
	PHELIP Xavier	Rhumatologie
Melle	PIERY Yvette	Biologie animale
MM.	RACHAIL Michel	Médecine interne
	RACINET Claude	Gynécologie et obstétrique
	RICHARD Lucien	Botanique
Mme	RINAUDO Marguerite	Chimie macromoléculaire

MM.	ROMIER Guy	Mathématiques (IUT B)
	ROUGEMONT (DE) Jacques	Neuro-Chirurgie
	STIEGLITZ Paul	Anesthésiologie
	STOEBNER Pierre	Anatomie pathologique
	VAN CUTSEM Bernard	Mathématiques Appliquées
	VEILLON Gérard	Mathématiques Appliquées (INP)
	VIALON Pierre	Géologie
	VOOG Robert	Médecine interne
	VROUSSOS Constantin	Radiologie
	ZADWORNY François	Electronique

MAITRES DE CONFERENCES ASSOCIES

MM.	BOUDOURIS Georges	Radioélectricité
	CHEEKE John	Thermodynamique
	GOLDSCHMIDT Hubert	Mathématiques
	YACOUD Mahmoud	Médecine légale

CHARGES DE FONCTIONS DE MAITRES DE CONFERENCES

Mme	BERIEL Hélène	Physiologie
Mme	RENAUDET Jacqueline	Microbiologie

Je tiens à exprimer ma gratitude à Monsieur le Professeur NEEL, Membre de l'Institut, pour l'honneur qu'il m'a fait en acceptant de présider le jury de cette thèse, ainsi qu'à Monsieur GAUTIER qui a bien voulu faire partie de ce jury.

Le travail exposé dans ce mémoire a été effectué au Centre de Recherches sur les Très Basses Températures dirigé alors par Monsieur le Professeur B. DREYFUS, qui a été à l'origine de ma venue à Grenoble, et maintenant par Monsieur le Professeur A. LACAZE. Qu'ils veuillent bien trouver ici l'expression de ma reconnaissance.

Je tiens à remercier Monsieur TOURNIER, Maître de Recherches au C.N.R.S., qui a bien voulu m'accepter dans le groupe Métaux Normaux, pour effectuer cette étude.

Je suis particulièrement reconnaissant envers Messieurs SOULETIE et THOULOUZE qui m'ont guidé de très près dans la réalisation de ce travail, par une présence constante et amicale et de fructueuses discussions.

Cette recherche n'aurait pas pu être réalisée sans l'aide précieuse et amicale de Monsieur PICOT dont la participation a été essentielle dans la réalisation des expériences décrites dans ce travail.

Je suis très reconnaissant à Monsieur PILON et à tous mes collègues du groupe Métaux Normaux pour leur collaboration et leur amitié, et particulièrement Monsieur SAINT-PAUL avec qui a été faite l'étude des alliages Pt-Co.

Mes remerciements au groupe de Métallurgie du Laboratoire qui a préparé et analysé les échantillons et au groupe calcul pour les conseils prodigués dans la réalisation des programmes de traitement des données.

A Mademoiselle FAURE-BRAC et Madame JULLIEN, mes remerciements pour avoir effectué rapidement la frappe de cette

thèse à partir de manuscrits pas toujours lisibles.

Enfin à tout le personnel du laboratoire ma reconnaissance pour ces cinq années de travail en commun.

T A B L E D E M A T I E R E S

I N T R O D U C T I O N

Nous présentons ici les résultats des mesures de chaleur spécifique à très basse température réalisées sur des alliages dilués contenant des impuretés de transition, principalement du Co, dissoutes dans différentes matrices.

La contribution nucléaire à la chaleur spécifique nous a permis d'étudier l'apparition des moments magnétiques par interaction entre les impuretés bien au-dessous de la température caractéristique T_K, dans des alliages de T_K élevée (Au-Co et Au-Co-Ni) et de T_K faible : Pt-Co et Zn-Mn. Des mesures effectuées sur le système Au-Co-Fe nous ont permis de confirmer et compléter les résultats obtenus sur l'Au-Co. La contribution des impuretés non magnétiques a été observée autour de T_K (Pt-Co) et bien au-dessous de T_K(Au-Co).

Le choix de ces alliages a été dicté par le besoin de disposer d'impuretés ayant un moment nucléaire élevé (Co ou Mn) et par le fait que d'autres mesures partielles suggéraient l'existence d'effets de concentration sur une gamme de température et de concentration compatibles avec nos possibilités expérimentales.

Une méthode d'acquisition et de traitement des données a été mise au point pour augmenter la précision des mesures, ce qui nous a permis, par exemple, de séparer la contribution de la matrice de celle des impuretés dans un échantillon de Cu-Mn.

Ce travail se présente sous la forme de publications déjà parues sur les systèmes Au-Co (chapitre IV) ou à paraître : Pt-Co (chapitre V), Au-Co-Fe (chapitre IV) et traitement des données (chapitre III), suivies de quelques résultats complémentaires sur les alliages Zn-Mn et Au-Co-Ni (chapitres V et IV). De ce fait une certaine redondance apparaît parfois, exigée

par le rappel de certains concepts à l'intérieur de chaque publication. Dans le chapitre I nous introduisons quelques concepts et problèmes liés à l'étude des alliages dilués et aux effets d'interaction entre impuretés, en récapitulant brièvement nos résultats. Enfin, au chapitre II , nous expliquons l'utilité de la chaleur spécifique nucléaire comme moyen expérimental pour étudier l'effet des interactions sur l'apparition du magnétisme.

C H A P I T R E I

LES ALLIAGES DILUES ET L'EFFET DES INTERACTIONS

A - IMPURETES MAGNETIQUES ET NON MAGNETIQUES DANS UN ALLIAGE DILUE

Le comportement magnétique des impuretés de transition dissoutes dans un métal a fait l'objet de nombreuses études aussi bien expérimentales que théoriques. Ces impuretés sont définies comme magnétiques ou non-magnétiques selon que la susceptibilité magnétique observée suit une loi de Curie (ou Curie Weiss) ou au contraire est "pratiquement" indépendante de la température. Cette définition opérationnelle de l'impureté magnétique rejoint le concept de "moment localisé" par opposition à un comportement d'électrons libres caractérisé par une réponse à un champ magnétique externe très peu dépendante de la température.

Une autre façon de définir les impuretés magnétiques consiste à utiliser le concept d'ordre magnétique (effets coopératifs). Ainsi on dira qu'un alliage contient des impuretés magnétiques si un ou plusieurs des phénomènes suivants, caractéristiques de l'ordre, sont observés :

1°) Une aimantation rémanente ;

2°) Un maximum dans la variation thermique de la susceptibilité ;

3°) Une anomalie de la chaleur spécifique dont le maximum dépend de la concentration.

4°) Un champ hyperfin au niveau des noyaux des impuretés en champ externe nul (effet Mössbauer, chaleur spécifique nucléaire) ou faible (orientation nucléaire).

Historiquement, l'observation de trois autres phénomènes a été associée empiriquement aux précédents et a aussi été utilisée comme critère pour déterminer l'existence d'impuretés magnétiques dans un alliage :

5°) Un minimum de la résistivité électrique ;

6°) Un terme linéaire en T dans la chaleur spécifique à basse température, dont l'amplitude est indépendante de la concentration d'impuretés ;

7°) Une susceptibilité indépendante de la concentration à basse température.

Un ensemble de résultats expérimentaux a mis en évidence qu'une même impureté, magnétique dans une matrice, pouvait ne pas l'être dans une autre.

En utilisant le concept d'état lié virtuel pour décrire l'écran créé pour compenser le défaut de charge de l'impureté et en faisant intervenir l'énergie d'échange intra-atomique, Friedel a étudié les conditions de découplage des deux directions de spins et donc d'apparition d'un moment localisé. Il a pu ainsi faire une classification des résultats expérimentaux concernant différents alliages, dans un tableau où la ligne de séparation entre alliages magnétiques et non magnétiques est fonction du niveau de Fermi de la matrice d'une part et de la position de l'impureté dans la série de transition d'autre part[1].

Anderson a repris le modèle de Friedel et a montré que pour une impureté avec une seule orbitale d plongée dans une mer d'électrons libres, l'énergie de répulsion Coulombienne entre 2 électrons localisés sur l'impureté était suffisante pour faire apparaître un moment localisé si la condition (1) (type Stoner) était satisfaite :

$$U \cdot \rho_d(\epsilon_F) \geq 1 \qquad (1)$$

U est l'énergie de Coulomb et $\rho_d(E_F)$ la densité d'état au n de Fermi. L'extension de ce résultat au problème des cinq o d fait intervenir l'intégrale d'échange intra-atomique J dan condition précédente [2] :

$$(U + 4J)\rho_d(\epsilon_F) \geq 1 \qquad (2)$$

L'approximation de Hartree-Fock utilisée n'est cependant valable que si :

$$U \cdot \rho_d(\epsilon_F) < 1 \qquad (3)$$

et le traitement d'Anderson n'est correct que dans la région où l'impureté n'est pas magnétique. Néanmoins, il fait apparaître les paramètres fondamentaux du problème et permet de comprendre la tendance à l'apparition d'un moment localisé.

Certains faits expérimentaux restaient cependant inexpliqués. Par exemple, la température 0 de la loi de Curie-Weiss suivie par les impuretés magnétiques :

$$\chi = \frac{C}{T + \theta} \qquad (4)$$

n'était pas proportionnelle à la concentration d'impuretés comme prévu par un modèle de champ moléculaire. De plus, pour des alliages très peu concentrés la valeur de 0 observée était indépendante de la concentration [3] montrant par là que ce paramètre ne provient pas des interactions entre impuretés magnétiques mais est une propriété intrinsèque à une impureté noyée dans les électrons de conduction (effet à une impureté).

La loi empirique donnée par (4) a été déduite des développements du modèle introduit par Kondo dans le but d'expliquer un autre fait expérimental, connu de longue date : le minimum observé à basse température sur la résistivité électrique des alliages contenant des impuretés magnétiques. Traitant au-delà de l'approximation de Born l'hamiltonien d'échange s-d entre le spin S de l'impureté et le spin s de l'électron de conduction, Kondo a trouvé une divergence logarithmique dans la résistivité pour des températures inférieures à la température caractéristique T_K du système, donnée par :

$$k T_K = D\, e^{-1/|J| \cdot N(0)} \qquad (5)$$

où J est la constante de couplage d'échange et N(O) la densité d'état dans la bande de largeur 2D, par atome[4].

Le modèle de Kondo part de l'existence d'un "bon spin" localisé sur l'impureté, pour laquelle la condition (2) serait donc satisfaite et prévoit encore la formation d'un état singulet, dit de "spin compensé" pour $T \ll T_K$, où l'impureté aurait un comportement non magnétique (χ indépendant de T). Les paramètres U, J et ρ n'étant pas directement accessibles à l'expérience, une hypothèse a été avancée selon laquelle la condition (2) pourrait être satisfaite pour tous les alliages dilués, et les alliages connus comme non magnétiques seraient tout simplement ceux qui seraient dans l'état de "spin compensé", c'est-à-dire, ceux pour lesquels T_K serait bien supérieure à la gamme de température couverte par les mesures expérimentales[5].

Parallèlement au modèle de Kondo, a été développé le modèle de fluctuations locales de spin (LSF), où les paramètres U, J et ρ sont supposés tels que la condition de validité de Hartree-Fock (équ. 3) soit remplie, c'est-à-dire les deux directions de spin de l'état lié virtuel ne sont pas découplées,

mais des fluctuations locales de spin se produisent de sorte que pour $T > T_{SF}$, l'impureté se comporte comme si elle était magnétique. La température caractéristique étant définie d'après la relation :

$$1/kT_{SF} = \frac{\pi \rho(E_F)}{1 - U\rho(E_F)} \qquad (6)$$

Le modèle LSF permet de décrire certains résultats expérimentaux comme la susceptibilité, la chaleur spécifique et la résistivité de certains alliages et particulièrement de ceux à base de métaux renforcés d'échange. L'équivalence entre les 2 modèles a été montré pour des alliages non-magnétiques[6][7].

Le concept d'alliage magnétique a donc été rendu plus complexe du fait de l'introduction d'un paramètre supplémentaire, la température. Ainsi le comportement "magnétique" d'une impureté dépend non seulement de l'impureté et de la matrice considérées mais aussi de la gamme de température couverte par la mesure.

D'autre part les développements du modèle de Kondo et de LSF ont prévu des nouvelles lois de variation pour la susceptibilité, résistivité et chaleur spécifique qui se sont avérées être d'une vérification expérimentale difficile, car théorie et expérience traitaient des problèmes différents. En effet, les modèles théoriques sont construits à partir d'une condition impossible à réaliser expérimentalement : une seule impureté dans une mer d'électrons de conduction. Les conditions expérimentales exigent cependant l'étude de concentrations finies où les effets d'interaction entre les impuretés modifient les données du problème. A cause de la nature "itinérante" des électrons qui donnent origine au magnétisme dans les métaux, il n'est pas effectivement évident qu'on puisse séparer le problème en deux : formation des moments et par la suite interaction entre eux, donnant origine aux phénomènes d'ordre magnétique. Cette difficulté a été néan-

moins progressivement levée d'une part avec l'augmentation de la sensibilité des appareils de mesure permettant de travailler sur des échantillons à très faible concentration et d'autre part avec l'étude expérimentale des effets d'interaction entre impuretés sur l'apparition d'un moment magnétique.

Dans notre travail, nous présentons les résultats d'une telle étude sur quelques alliages. Si à l'heure actuelle il est difficile de décider du modèle le plus correct, si toutefois il existe une différence entre les deux, pour décrire le comportement d'un alliage donné (Kondo ou fluctuations locales de spin) il est néanmoins certain que la température caractéristique T_K déterminée aux concentrations évanescentes a une signification expérimentale bien définie. Ainsi les valeurs de T_K déterminées à partir de la susceptibilité $\left(\chi \sim \frac{C}{T+T_K} \right)$, de la résistivité $\left(\rho = \rho_0 \left[1 - (T/T_K)^2 \right] \right)$, du maximum de l'anomalie de chaleur spécifique (effet à une impureté observée par la superposition des courbes dans un diagramme $\Delta C/c\,(T)$) correspondent bien entre elles pour un alliage donné. Les valeurs de T_K pour les différents alliages dilués varient de plusieurs ordres de grandeurs et il est possible de classer ces alliages suivant leur T_K et par rapport à la gamme de température couverte par une expérience donnée. Ainsi, pour nos mesures situées entre 10^{-2} K et 1 K, nous pouvons classer les alliages étudiés en trois catégories :

$T_K \gg 1$ K	Au-Co, Au-Co-Ni
10^{-2} K $\lesssim T_K \lesssim 1$ K	Pt-Co, Zn-Mn
$T_K \ll 10^{-2}$ K	Cu-Mn

Cette classification correspond à celle utilisée par Coles[8] qui classe les impuretés comme :

1°) portant un moment zéro ($T_K \sim 10^3$ K)

2°) portant un moment intermédiaire ou Kondo ($T_K \sim 1$ K)

3°) portant un bon moment ($T_K \sim 10^{-3}$ K)

Les effets d'interaction entre impuretés se traduiront par un comportement différent pour chacun de ces 3 groupes. Dans le dernier cas peu examiné dans ce travail, l'impureté est bien magnétique et les interactions entre les impuretés sont caractérisées par des oscillations de densité de spin des électrons de conduction (RKKY) menant à une distribution de champ moléculaire P(H) et à un terme linéaire en chaleur spécifique dont l'amplitude est indépendante de la concentration en impuretés (superposition des courbes dans un diagramme réduit)[9].

B - LES EFFETS D'INTERACTION

L'existence des effets d'interaction sur le comportement magnétique des impuretés a été suggérée pour la première fois pour expliquer des effets non linéaires en concentration, observés sur des alliages de Cu-Ni. L'observation d'un terme de susceptibilité en 1/T dont le coefficient variait comme le cube de la concentration a été associé à l'existence d'un découplage de spin pour le groupement de 3 atomes de Nickel voisin[1].

L'importance de l'environnement immédiat de l'impureté sur son comportement magnétique et l'apparition discontinue des moments localisés ont été mis en évidence par Jaccarino et Walker pour expliquer la variation du moment moyen du Fe dans la matrice Nb_{1-x} Mo_x et du Co dans Rh_{1-x} Pd_x. L'augmentation graduelle du moment de ces impuretés avec la concentration de Mo ou Pd avait été interprétée comme un changement continu de la largeur Δ de l'état lié virtuel, quand les propriétés moyennes de la matrice Nb-Mo ou Rh-Pd variaient[10]. Cependant, Jaccarino et Walker ont signalé l'impossibilité de faire la distinction dans une mesure macrosco-

pique entre une situation où toutes les impuretés possèdent le même moment et celle où quelques impuretés possèdent le moment maximum et les autres un moment zéro selon leur environnement. En montrant que la dépendance de la valeur moyenne du moment magnétique porté par le Fe (ou Co) était proportionnelle à la probabilité d'un atome de Fe (ou Co) d'avoir au moins 7 atomes de Mo (ou 11 atomes de Pd) parmi ces premiers voisins, ils ont conclu que les moments magnétiques apparaissaient d'une façon discontinue[11]. Ce modèle de "tout ou rien" ou 1-0, a été récemment confirmé par des mesures microscopiques de RMN faites sur le ^{59}Co dissous dans le Nb-Mo[12].

Du point de vue théorique les effets d'interaction entre impuretés ont été étudiés par divers auteurs. L'hamiltonien d'Anderson a été généralisé au cas de deux impuretés[13][14]

$$H = \sum_{k,\sigma} \varepsilon_k n_{k\sigma} + \sum_{i=1,2} E_{d_i} n_{i\sigma} + \sum_{i=1,2} U n_{i+} n_{i-} + \sum_{\alpha \neq \beta,\sigma} C^*_{\alpha\sigma} C_{\beta\sigma}$$

Le premier terme de H représente l'énergie cinétique des électrons de conduction, le second et le troisième l'énergie des électrons d dans l'état lié d_i initial. Le quatrième terme contient un terme de mélange s-d :

$$H_{mel} = \sum_{i,k,\sigma} V_{k d_i} C^*_{k\sigma} C_{d_i\sigma} + c.c.$$

et un terme d'interaction directe d-d :

$$H_{d-d} = \sum_{i \neq j,\sigma} V_{d_i d_j} C^*_{d_i\sigma} C_{d_j\sigma} + c.c.$$

En négligeant ce dernier terme, dans le calcul de l'énergie d'interaction, Caroli a montré l'importance du couplage de double résonance entre impuretés magnétiques à travers la bande de conduction.

Ses résultats suggèrent la possibilité d'une modification de la densité d'état $\rho_d(E_F)$ d'une impureté non magnétique par la présence d'autres impuretés distantes de la première et qui pourraient permettre à celle-ci de franchir la limite de Stoner. Les effets de longue distance bien que plus généraux **seront repris** plus loin. Nous aborderons d'abord les effets d'interaction à courte distance où le terme négligé par Caroli, d'interaction directe d-d peut être non négligeable.

EFFET D'INTERACTION ENTRE IMPURETES PROCHE VOISINES

L'apparition discontinue des moments magnétiques localisés est justifiée dans le cadre du modèle d'Anderson où le moment varie rapidement de zéro à sa valeur à saturation pour une faible variation de $(U + 4\ J)/\Delta$[15]. Il est possible de prévoir que l'environnement immédiat de l'impureté que ce soient des atomes différents dans le cas d'une matrice binaire ou d'autres impuretés du même type dans le cas classique, peut changer la valeur de Δ et faire apparaître (ou disparaître) un moment localisé sur l'impureté.

Le terme d'interaction directe d-d décrit plus haut a été considéré par Alexander et Anderson[13] et ensuite par Morya[15] qui a montré que près de la limite critique d'apparition d'un moment (eq. 1), la valeur du moment peut changer de beaucoup par l'existence de ce terme. Par contre le moment n'est pas beaucoup influencé par l'impureté voisine s'il se trouve être saturé. Son modèle serait valable pour l'interaction entre impuretés de différents types et la condition pour l'apparition d'un moment serait plus ou moins favorisée suivant que les couches d des impuretés seraient demi-pleines ou plus que demi-pleines.

Pour les impuretés avec des couches d plus que demi-pleines (Fe, Co, Ni) l'interaction favorise l'apparition d'un moment si l'impureté se trouve dans une situation où la condition de Stoner est proche d'être réalisée dans la matrice noble en question (condition limite dans le tableau de Friedel). Des

résultats du même type ont été retrouvés pour les alliages à base de Cu dans un modèle qui tient compte de la structure de bande de la matrice[16].

Le cas du Co dissout dans l'Au ou Cu se trouve dans cette situation limite et paraît mettre en évidence l'existence d'effets d'interactions à travers la dépendance en concentration observée expérimentalement (voir chapitre IV). Ceci serait en accord avec les prévisions de Morya où l'interaction entre 2 impuretés de Co intervient pour favoriser la réalisation de la condition de Stoner. En effet, les résultats obtenus en aimantation[17] sur le Cu-Co permettent d'associer un comportement magnétique à certains groupes d'atomes de Cobalt.

Nous avons étudié ici d'une façon systématique la dépendance en fonction de la concentration de la chaleur spécifique nucléaire de l'alliage Au-Co (chapitre IVa). Les résultats obtenus ont permis d'associer la présence de moments localisés (jusqu'à 20 mK) aux groupes d'au moins 3 atomes de Co proches voisins pour lesquels la condition de Stoner serait donc réalisée. D'après la contribution linéaire en température à la chaleur spécifique, nous avons déterminé les températures de fluctuation de spin associées aux paires et aux atomes isolés de Co (50 et 700 K respectivement).

Ces résultats ont été confirmés par l'analyse de mesures d'aimantation faites sur les mêmes échantillons[18] et l'existence d'un T_{SF} très élevé pour les impuretés isolées a été retrouvée récemment par des mesures de RMN[19]. Pour démontrer l'existence de réponses magnétiques différentes propres aux paires et aux atomes isolés de Cobalt, nous avons "soumis" ces configurations d'impuretés au champ moléculaire créé par le Fe dans l'Au,

en étudiant la chaleur spécifique nucléaire de l'alliage Au-Co-Fe en fonction de la concentration de Co et de Fe. L'analyse des résultats obtenus paraît confirmer l'existence de ces 2 températures T_{SF} de l'ordre de 16 et 240 K proches de celles déterminées par l'aimantation (chapitre IV b).

Récemment, Parlebas[16] a étudié dans l'approximation Hartree-Fock la structure électronique d'une paire d'impuretés en utilisant une structure réaliste des bandes "s" et "d" hybridées pour les alliages de Cuivre. Il est intéressant de constater qu'il a pu ainsi déterminer pour la paire et les atomes isolés de Co dans le cuivre des températures de fluctuation de spin de 7 et 700 K respectivement.

Mais si ces mesures effectuées sur l'Au-Co confirment la prévision qualitative de Morya, l'existence de tels effets d'interaction entre impuretés de type différent dans un alliage ternaire d'Au-Co-Ni n'a pas été observée (chapitre IV c).

Dans le cas où le moment de l'impureté est bien saturé (T_K très faible) comme pour le Mn dans l'Au ou Cu, certains résultats paraissaient montrer une éventuelle variation du moment du Mn. Ainsi, pour des concentrations très élevées de Mn dans l'Au (composés définis) les mesures de chaleur spécifique nucléaire mettent en évidence une décroissance du champ hyperfin avec la concentration de Mn[20]. De même, des mesures de champ hyperfin du Mn dans le Cu faites sur des échantillons contenant de l'ordre de quelques ppm de Mn (par orientation nucléaire) et de l'ordre du % de Mn (chaleur spécifique nucléaire) donnaient des valeurs très différentes. Des mesures plus précises de chaleur spécifique nucléaire faites sur un échantillon de Cu-$Mn_{0.9}$ % ont permis de séparer la contribution de la matrice de celle des

impuretés et de vérifier ainsi que le champ hyperfin sur le Mn est le même que celui observé par orientation nucléaire (290 ± 10 kOe contre 280 ± 10 kOe déterminés par orientation nucléaire) (chapitre III).

EFFET D'INTERACTION ENTRE IMPURETES A GRANDE DISTANCE

Expérimentalement, des effets d'interaction à longue distance ont été mis en évidence sur des alliages comme Cu-Fe et Au-Fe[21][22]. Aux limites des faibles concentrations, les "paires" d'atomes de Fe, distantes de plusieurs distances interatomiques présentent un comportement magnétique à des températures bien inférieures au T_K des impuretés isolées (magnétisme résiduel). Ces études ont permis de séparer les effets à une impureté des effets d'interaction, traduits expérimentalement par des effets de concentration (aimantation à saturation, constante de Curie, etc... qui varient comme le carré de la concentration). Des calculs de températures caractéristiques des paires T_K et T_{SF}, ont été effectués dans le cadre des modèles Kondo[23] et fluctuation de spin[24][16].

De tels effets d'interaction entre impuretés à longue distance, se traduisant expérimentalement par des effets non linéaires en concentration, sont observés autour d'une concentration critique, définie comme celle pour laquelle $T_{ordre} = T_K$. Ce critère empirique qui suggère la destruction de l'état considéré quand l'énergie de l'effet coopératif d'ordre est équivalente à l'énergie de l'état de "spin compensé", donne approximativement l'ordre de grandeur des concentrations intéressantes à étudier. Ainsi, T_{ordre} étant situé en général autour de 10 K par % pour des alliages avec T_K = 1 K, les effets de concentration doivent être perçus autour de c = 0,1 % at.

Nous présentons dans ce contexte le résultat de l'étude sur le système Pt-Co, dont la concentration critique et les mesures connues permettaient de croire à l'existence des effets de concentration dans une gamme de concentration et de température sensible à notre appareil (chapitre V). La dépendance en c^2 de la chaleur spécifique nucléaire pour les faibles concentrations de Co, nous a permis d'associer un moment magnétique aux paires de Co situées en deça d'une distance critique de l'ordre de 8 Å. Ainsi même dans un alliage dont la matrice est renforcée d'échange, le magnétisme apparaît au-dessous de T_K comme pour les alliages à base de métaux nobles (Cu-Fe, Au-Fe) avec le carré de la concentration totale. Les mesures de Saint-Paul au-dessus de 0,3 K présentées au même chapitre, ont permis d'identifier l'existence de l'anomalie associée à l'effet à une impureté autour de T_K = 1,2 K.

Finalement, l'étude de 4 échantillons de Zn-Mn, malgré des problèmes de métallurgie et de sensibilité de la mesure, a permis de vérifier que, comme pour le Pt-Co, le champ hyperfin qui apparaît lorsque les impuretés deviennent magnétiques par interaction est proche de celui obtenu dans la limite des très faibles concentrations par l'application d'un champ externe saturant l'impureté. Pour les 2 échantillons les moins concentrés, la présence de l'anomalie associée à l'effet à une impureté a été détectée au-dessous de 0,2 K.

R E F E R E N C E S

1 - A. BLANDIN et J. FRIEDEL, J. Phys. Radium 20, 160 (1959)

2 - P.W. ANDERSON, Phys. Rev. 124, 41 (1961)

3 - KNAPP , J. Appl. Phys. 38, 1267 (1967)

4 - J. KONDO, Progr. Theoret. Phys. (Kyoto) 32, 37 (1964)

5 - J.R. SCHRIEFFER, J. Appl. Phys. 38, 1143 (1967)

- M.D. DAYBELL and W.A. STEYERT, Rev. Mod. Phys. 40, 380 (1968)

6 - P. LEDERER and D.L. MILLS, Solid State Commun. 5, 131 (1967)

and Phys. Rev. 165, 837 (1968)

7 - N. RIVIER and M.J. ZUKERMANN, Phys. Rev. Letters 21, 904 (1968)

8 - COLES, International Symposium on Amorphous Magnetism.

WAYNE STATE UNIVEPSITY (1972)

9 - J. SOULETIE and R. TOURNIER, J. Low Temp. Phys. 1, 95 (1969)

10 - A.M. CLOGSTON et al, Phys. Rev. 125, 541 (1962)

11 - V. JACCARINO and L.R. WALKER, Phys. Rev. Letters, 15, 258 (1965)

12 - K.C. BROG and Win. H. JONES, Jr, Phys. Rev. Letters, 24, 58 (1970)

13 - S. ALEXANDEP and P.W. ANDERSON, Phys. Rev. 133, A1594 (1964)

14 - B. CAROLI, J. Phys. Chem. Solids 28, 1427 (1967)

15 - T. MORYA, Proceeding of International School of Physics, Enrico Fermi Course 37, Academic Press (1968)

16 - J.C. PARLEBAS, Thèse Université de Strasbourg (1972)

17 - R. TOURNIER, Thèse Université de Grenoble (1965)

18 - E. BOUCAI et al, Phys. Rev. B3, 3834 (1971)

19 - A. NARATH and D.C. BARHAM, à paraître dans Phys. Rev. B.

20 - P. LYMAN, W. PROCTOR and R.G. SCURLOCK, Proc. 11th Int. Conf. Low Temp. Phys. p. 519

21 - J.L. THOLENCE and R. TOURNIER, Phys. Rev. Letters 25, 867 (1970)

22 - J.L. THOLENCE and R. TOURNIER, Suppl. J. Physique 32, C1-211 (1971)

23 - K. MATHO and M.T. BEAL-MONOD, Phys. Rev. B. 5, 1899 (1972)

24 - P. LEDERER, Thèse Université de Paris (1967).

C H A P I T R E II

LA CHALEUR SPECIFIQUE NUCLEAIRE

Le couplage entre les électrons et les noyaux donne naissance à un écartement des niveaux d'énergie de ces derniers. La contribution nucléaire à la chaleur spécifique provient du changement de la population de ces niveaux avec la température et est caractérisée par une anomalie de Schottky (nombre fini de niveaux dont l'écartement est indépendant de la température). L'écartement des niveaux étant typiquement de l'ordre du millidegré, cette anomalie n'est observée que pour $T < 1$ K.

Dans le cas des alliages dilués il existe au moins 2 types de noyaux : ceux de l'impureté et ceux de la matrice. La chaleur spécifique nucléaire mesurée sera alors la somme d'une contribution des impuretés et d'une contribution de la matrice. Pour les alliages considérés dans ce travail, la contribution des impuretés était toujours prépondérante et celle de la matrice ne représentait que de l'ordre de quelques pour cent (Au-Co) à 20 % de la contribution des impuretés (Cu-Mn).

Chacune de ces deux contributions peut avoir deux origines : magnétique ou quadrupolaire électrique. En effet, le couplage entre électrons et noyaux est décrit par l'Hamiltonien hyperfin magnétique qui tient compte des interactions magnétiques entre spin et moment orbital électronique avec le spin nucléaire et l'hamiltonien hyperfin quadrupolaire électrique qui traduit

l'interaction entre les gradients de champ électrique créés par les électrons et le moment quadrupolaire du noyau. Le terme hyperfin provient historiquement de l'observation d'une structure hyperfine dans le spectre optique.

- Couplage magnétique

L'hamiltonien d'interaction magnétique entre un noyau et un électron s'écrit[1] :

$$H_H = -g\, g_I\, \mu_0\, \mu_I \left\{ 8\pi/3\, \delta(r)\, \vec{S}.\vec{I} + \frac{\vec{L}.\vec{I}}{r^3} - \frac{\vec{S}.\vec{I}}{r^3} + \frac{3(\vec{S}.\vec{r})(\vec{I}.\vec{r})}{r^5} \right\} \quad (1)$$

où $\vec{L}$, $\vec{S}$ et $\vec{I}$ sont les opérateurs moment angulaire, spin électronique et spin nucléaire ; μ_0 et μ_N sont les magnétons de Bohr et nucléaire ; g et g_I sont les facteurs d'écartement spectroscopique électronique et nucléaire.

Le premier terme qui contient la fonction de Dirac, caractérise l'interaction de contact de Fermi entre les noyaux et les électrons dont la probabilité de présence sur les noyaux est différente de zéro, c'est-à-dire les électrons s des couches internes de l'atome, polarisés par la présence d'un spin sur les couches externes (polarisation de "coeur") où les électrons de conduction de la matrice polarisés par la présence d'impuretés magnétiques[2]. La polarisation de "coeur" sera responsable de la contribution à la chaleur spécifique des impuretés magnétiques et la polarisation des électrons de conduction produira la contribution magnétique de la matrice, dans le cas d'un alliage avec une matrice noble.

Les autres termes de (1) qui caractérisent l'interaction du moment orbital L et du spin électronique S avec le noyau, sont négligeables devant le premier terme, dans le cas des impuretés de transition. L'hamiltonien (1) peut s'écrire dans le cas plus général comme l'interaction entre le moment magnétique nucléaire

et un champ effectif, H_{eff}, produit par l'électron à l'emplacement du noyau, représenté par l'opérateur vectoriel, proportionnel au spin électronique total J :

$$\vec{H}_{eff} = g\mu_0 \left\{ 8\pi/3\ \delta(r)\ \vec{S} + \frac{\vec{L}}{r^3} - \frac{\vec{S}}{r^3} + \frac{3\vec{r}\,(\vec{S}\cdot\vec{r})}{r^5} \right\} \qquad (2)$$

On peut ainsi écrire sous la forme d'un hamiltonien Zeeman :

$$H_H = -\gamma_N \hbar\, \vec{I}\cdot\vec{H}_{eff}$$

ou encore

$$H_H = -\mu_I \cdot H_{eff}/I \cdot I_z \qquad (3)$$

le moment nucléaire $\vec{\mu}_I = g_I \mu_N \vec{I}$ et H_{eff} étant pris dans la direction z.

La chaleur spécifique nucléaire (C.S.N.) décrivant la variation des populations entre les valeurs propres de H_M permet de déduire l'espacement entre ces niveaux d'énergie. Historiquement, la C.S.N. a été une des premières techniques utilisées pour la mesure de H_{eff}. Dans le problème des alliages dilués, elle a été utilisée comme sonde du magnétisme électronique, du fait de la proportionalité entre le moment magnétique électronique et le champ effectif H_{eff}. Du Chatenier et Miedema[3] l'ont utilisée pour répondre à la question impureté magnétique ou non et ainsi remplir le tableau de Friedel(*). Thoulouze[4] l'a employée pour étudier les oscillations de densité de spin produites sur les électrons de conduction de la matrice par les impuretés magnétiques.

(*) L'observation expérimental d'un H_{eff} sous champ externe nul, par C.S.N., effet Mössbauer ou autre technique, est le reflet d'un ordre magnétique (voir chapitre V) et permet dans le cas d'un alliage dilué d'affirmer l'existence d'impuretés magnétiques au même titre que l'observation d'une aimantation rémanente.

- Couplage électrique

L'hamiltonien d'interaction électrique entre le gradient de champ électrique produit par les électrons et le moment quadrupolaire du noyau s'écrit :

$$H_Q = \sum_{jk} \left(\partial^2 V / \partial x_j \partial x_k\right)_{r=0} Q_{jk} \qquad (4)$$

où l'opérateur tensoriel $\left(\partial^2 V / \partial x_j \partial x_k\right) = V_{x_j x_k}$ est le tenseur gradient de champ électrique à l'origine et Q_{jk} est l'opérateur qui représente le moment quadrupolaire associé à la distribution de charges nucléaires. Avec un choix convenable des axes (4) s'écrit :

$$H_Q = \frac{e^2 q Q}{4I(2I-1)} \left\{ 3I_z^2 - I(I+1) + \eta/2 \left(I_+^2 - I_-^2\right) \right\} \qquad (5)$$

où $eq = V_{zz}$ et $\eta = \dfrac{V_{xx} - V_{yy}}{V_{zz}} = 0$ pour un environnement à symétrie axiale du noyau.

Contrairement à l'hamiltonien magnétique, les niveaux d'énergie déduits de (5) ne sont pas également espacés (à cause du terme en I_z^2). Mais comme dans le cas précédent la mesure de la C.S.N. de substances non magnétiques a permis de mesurer les gradients de champ électrique créés au niveau des noyaux par le champ cristallin dans des substances non magnétiques[5].

- La C.S.N. dans l'étude des effets d'interaction

Avant de donner l'expression plus générale de l'anomalie de Schottky nucléaire tenant compte des niveaux d'énergie donnés par (3) et (5), plaçons nous dans un cas plus simple où la contribution quadrupolaire électrique est négligeable et à une température T bien supérieure à a/k, où a est l'espacement entre les niveaux Zeeman produits par le champ H_{eff}. L'aimantation nucléaire suit alors une loi de Curie :

$$\chi_N = N \mu^2 / 3kT$$

où N est le nombre de noyaux et μ leur moment magnétique. L'énergie de ces noyaux sera :

$$E = - \chi_N \cdot H_{eff}^2$$

$$E = - N \mu^2 H_{eff}^2 / 3kT$$

et la chaleur spécifique nucléaire :

$$C_N = N \mu^2 H_{eff}^2 / 3 k T^2 \qquad (6)$$

Cette expression simplifiée de la C.S.N. contient les principaux éléments qui justifient l'emploi de cette technique expérimentale dans l'étude des effets d'interaction sur l'apparition du magnétique dans les alliages dilués :

1°) La dépendance en T^{-2} nous permet de séparer aisément la contribution nucléaire des autres contributions présentes à basse température, qui proviennent des électrons, de l'anomalie d'ordre entre impuretés magnétiques ou de celle due aux phénomènes Kondo ou L.S.F. des impuretés non magnétiques.

2°) La dépendance en H_{eff}^2 la rend surtout sensible aux grandes valeurs de champs hyperfins et donc aux moments localisés dont la valeur est proche de la saturation. L'existence d'impuretés non magnétiques faiblement polarisées par le champ moléculaire (moments induits) ne sera pas détectée par la C.S.N., ce qui justifie encore l'utilisation du modèle 1 - O pour l'interprétation des résultats. De plus la direction z étant définie pour chaque site, contrairement à l'aimantation la C.S.N. détecte aussi bien les impuretés couplés ferromagnétiquement que celles couplées

antiferromagnétiquement (les 2 types de couplage pouvant exister dans le type d'ordre dominé par les interactions R.K.K.Y.).

3°) La dépendance en μ^2 fait que la chaleur spécifique mesurée représente principalement la contribution des impuretés, si nous choisissons des alliages tels que le moment nucléaire des impuretés est bien plus grand que ceux de la matrice.

4°) La proportionalité au nombre de noyaux N qui voient le champ hyperfin H_{eff}, permet de compter les impuretés magnétiques.

- Expression générale de la C.S.N.

L'expression générale de la C.S.N. en fonction des niveaux nucléaires W_i déduits de (3) et (5), s'écrit à partir de la fonction de partition du système :

$$C_N = R/k^2T^2 \cdot \frac{\sum_i \sum_j (W_i^2 - W_i W_j) \cdot e^{-(W_i + W_j)/kT}}{\sum_i \sum_j e^{-(W_i + W_j)/kT}} \qquad (7)$$

où k est la constante de Boltzman et R la constante des gaz parfaits.

Ou encore :

$$C_N = R \left\{ \frac{\sum_i (W_i/kT)^2 e^{-W_i/kT}}{\sum_i e^{-W_i/kT}} - \left[\frac{\sum_i W_i/kT \, e^{-W_i/kT}}{\sum_i e^{-W_i/kT}} \right]^2 \right\} \qquad (8)$$

Il est pratique d'exprimer les niveaux W_i en fonction du paramètre d'interaction magnétique a' et de la constante de couplage quadrupolaire P ; déduits de (3) et (5) :

$$W_i/k = -a' I_z + P \left[I_z^2 - \frac{1}{3} I(I+1) \right] \qquad (9)$$

avec

$$a' = \mu_I \cdot H_{eff} / kI$$

(espacement Zeeman exprimé en température)

et

$$P = \frac{3 e^2 Q q}{4kI(2I-1)}$$

(demi-espacement entre les niveaux $\pm 1/2$ et $\pm 3/2$ exprimé en température)

où $I_z = -I, -I+1, \ldots + I$

où on a supposé $\eta = 0$.

Finalement le développement en série de (8) pour

$$T >> |P - a'| \qquad (10)$$

nous donne :

$$C_N = A T^{-2} + B T^{-3} + C T^{-4} \qquad (11)$$

avec

$$\frac{A}{R} = \frac{1}{3} a'^2 I(I+1) + \frac{1}{45} P^2 I(I+1)(2I-1)(2I+3)$$

$$\frac{B}{R} = -\frac{1}{15} a'^2 P I(I+1)(2I-1)(2I+3)$$

$$\frac{C}{R} = -\frac{1}{30} a'^4 I(I+1)(2I^2+2I+1)$$

Dans le cas des alliages dilués contenant des impuretés magnétiques, les calculs de Thoulouze[4] montrent que la contribution quadrupolaire électrique de la matrice est faible devant la contribution magnétique.

Le gain de précision acquis lors de l'utilisation de la nouvelle méthode de dépouillement décrite au chapitre III, a montré que la série (11) n'était pas suffisante pour décrire les résultats expérimentaux qui, dans le cas des alliages de Pt-Co et Cu-Mn, sont bien reproduits par une anomalie Schottky (8) purement magnétique, une fois retranchée la contribution de la matrice.

Dans le cas de l'Au-Co, la mesure a été faite avec la méthode de dépouillement graphique traditionnelle et les résultats ont donc été traités en utilisant uniquement le terme en T^{-2}. Mais la variation avec la concentration du coefficient de ce terme permet d'affirmer que la contribution électrique est négligeable (chapitre IV).

Pour la série Au-Co-Fe, la présence de toute une distribution de champ hyperfin ne permet pas la vérification de l'existence de contribution quadrupolaire électrique qui a été néanmoins négligée vue son absence dans l'Au-Co.

- R E F E R E N C E S -

-:-:-:-:-:-:-:-:-:-

1 - R.E. WATSON and A.J. FREEMAN, Phys. Rev. 123, 2027 (1961)

2 - HYPERFINE INTERACTIONS, ed; J. FREEMAN et B. FRANKEL, Academic Press (1967)

3 - F.J. CHATENIER and A.R. MIEDEMA, Physica 32, 403 (1966)

4 - D. THOULOUZE, Thèse Université de Grenoble (1968)

B. DREYFUS, J.C. MICHEL and D. THOULOUZE, J. Applied Phys. 39, 1320 (1968)

5 - N. E. PHILIPS - C.R.C. Critical Reviews in Solid State Sciences 2, 467 (1971)

C H A P I T R E III

ALLIAGE AVEC $T_K << 10^{-2}$ K : Cu-Mn

METHODE D'ACQUISITION ET DE TRAITEMENT DES DONNEES DE CHALEUR SPECIFIQUE - CHALEUR SPECIFIQUE NUCLEAIRE DU Cu-Mn

(à paraître)

A METHOD FOR THE ACQUISITION AND THE TREATMENT OF SPECIFIC HEAT DATA - NUCLEAR SPECIFIC HEAT OF Cu-Mn

P. COSTA-RIBEIRO[*] [‡], B. PICOT, J. SOULETIE and D. THOULOUZE --

Centre De Recherches sur les Très Basses Températures, C.N.R.S., B.P. 166, Centre de Tri 38042 GRENOBLE-CEDEX, France.

[*] In partial fulfilment of a thesis

[‡] C.A.P.E.S. Fellow (Brazil)

A B S T R A C T

For the purpose of measuring the nuclear specific heat of dilute systems between 16 mK and 100 mK we have developed an improvement to the adiabatic method which is of interest in all cases where a long response time is present : use is made of the knowledge of the evolution of the temperature T vs time and of the time derivation of T vs T. This method was adapted in an automatic system of acquisition and treatment of the data using the possibilities of a computer. The gain in accuracy allows to determine higher order times in the development of the high temperature nuclear Schottky tail. An application is made to the case of Cu-Mn where the contribution of the Cu nuclei is separated from that at the Mn nuclei, where $H_{eff} \sim 280 \pm 10$ kOe in agreement with nuclear orientation data.

I - INTRODUCTION

We present a system of acquisition and treatment of data which was developped for the measurement of the specific heat in the range from 20 mK to 100 mK, and was used in the study of the nuclear specific heat of dilute alloys (Pt-Co[1], Au-Co-Fe[2] and Cu-Mn).

The apparatus described in a former paper[3] is capable of cooling a sample down to about 15 mK by the successive demagnetization of two salt pills. The sample is then isolated, by decreasing the field on a supraconducting thermal switch (a tin wire : ℓ = 2 cm and $\varnothing$=0.5 mm). The heat leak $\dot{q}$ to the sample has been made as small as 1 erg/min. by taking special care in protecting the apparatus from external perturbations (vibrations, electromagnetic radiations, etc..). The temperature is given by the magnetic susceptibility of a small sphere constituted by 5 CMN slabs glued to the sample holder with Apiezon N grease.

II - THE ADIABATIC METHOD ; DIFFICULTIES INHERENT TO THE LOW TEMPERATURE RANGE

A graphic of the temperature of the sample versus time, typical of a specific heat experiment, is schematized (fig. 1) in a somewhat ideal case : large diffusivity of the sample and instantaneous response of the thermometers. An additional controlled power $\dot{Q}$ is superimposed from t_A to t_B to $\dot{q}$, the heat leak to the sample, which is responsible for the drifts observed before t_A and after t_B :

$$T_F - T_I = \int_{t_I}^{t_A} \frac{\dot{q}}{C_p}\,dt + \int_{t_A}^{t_B} \frac{\dot{q}+\dot{Q}}{C_p}\,dt + \int_{t_B}^{t_F} \frac{\dot{q}}{C_p}\,dt \quad . \quad (1)$$

We may choose indistinctly different heating periods, following then other paths from T_I to T_F, and in the limit one such as IA'B'F where the additional energy ΔQ is given instantaneously at the time

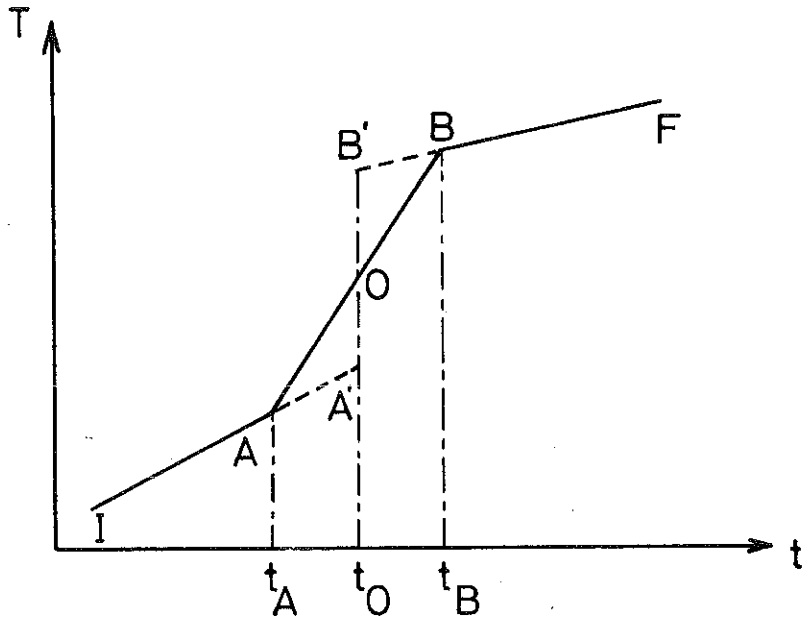

FIG. 1

$t_o = t_{A'} = t_{B'}$:

$$T_F - T_I = \int_{t_I}^{t_A} \frac{\dot{q}}{C_p}\,dt + \int_{t_A}^{t_{A'}} \frac{\dot{q}}{C_p}\,dt + \frac{\Delta Q}{C_p} + \int_{t_{B'}}^{t_B} \frac{\dot{q}}{C_p}\,dt + \int_{t_B}^{t_F} \frac{\dot{q}}{C_p}\,dt \ . \qquad (2)$$

The first and last integrals correspond to the drifts IA and BF ; the second and fourth integrals correspond to the extrapolations AA' and BB' of those drifts. The specific heat at t_o is $C_p = \frac{\Delta Q}{\Delta T}$, where $\Delta T = T_{B'} - T_{A'}$. But the path IA'B'F (eq. 2) is equivalent to IABF (eq. 1), with $\Delta Q = \dot{Q}dt$, only if t_o is chosen in such a way that the energies exchanged with the outside are the same, that is, if the areas below IABF and IA'B'F' are equal (equality of the triangles OB'B and OA'A, known as the rule of areas)[4]. With a fast response time, the temperature change corresponding to $\dot{q}$ remains small between t_I and t_F. Then the specific heat and the heat leaks may be considered constant and the drifts are approximately linear functions of time, from I to A' and from B' to F (eq. 1). In that case the extrapolation is easily made graphicaly.

Unfortunately such is not the situation in the specific heat measurements at very low temperature, when thermal contact resistances exist between sample, sample holder and thermometer. With a CMN as the thermometer, time constants as large as 6 minutes were found at 20 mK. In fig. 2 a mutual inductance bridge reading, typical of a low temperature measurement (20 mK to 70 mK), is plotted versus time ($M = a/T+b$, a and b beeing determined from a calibration in the helium range). Some typical difficulties arise then :

- From t_A to t_E, the instant where the internal thermal equilibrium is recovered, the temperature of the thermometer will differ from the temperature of the sample : this will make almost inoperant the application of the areas rule in the

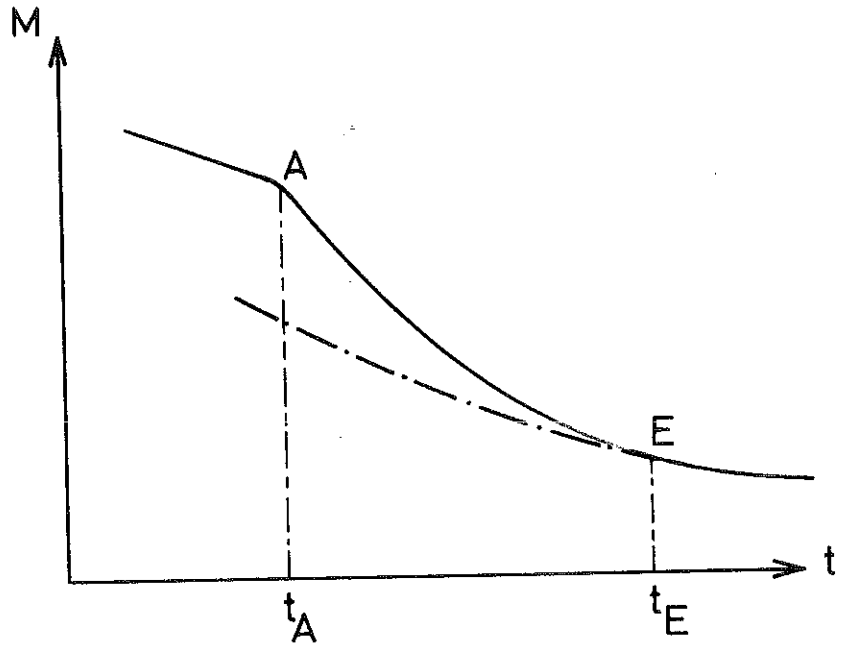

FIG. 2

determination of the instant t_o where ΔT should be measured.

- In this time scale the temperature change produced by the natural heat leak $\dot{q}$ results comparable to and even larger than the externaly supplied $\Delta\dot{Q}$. C_p and $\dot{q}$ are no more constants and the temperature drifts are no more linear. But even if C_p and $\dot{q}$ remain reasonably constant over a large period of time, the $1/T$ law followed by the thermometer will lead to non linear drifts of the inductance bridge signal. This makes a graphical extrapolation rather difficult.

- The time t_E from which this extrapolation is made is not easily determined on such a graphic as in fig. 2.

In the following we will attach ourselves to solve the last two problems (determination of t_E and extrapolation of the drifts) and will estimate the errors attached to some uncertainty in the choice of t_o. The method proposed below for low temperature calorimetry with a CMN may be useful as well when faster thermometers are used, but other difficulties inherent to the sample are present, such as a large T_1 (for nuclear specific heat) or a bad diffusivity (for insulating or amorphous systems).

III - THE DETERMINATION OF t_E

Curve A of fig. 3a schematizes the evolution of the temperature versus time due to $\dot{q}$ only ("free run"). $\dot{q}$ depends on T, the temperature of the sample, and on the temperature T_s of the screens with which the sample may exchange heat, by residual gaz conduction, solid conduction and so on. C_p depends on T only and from its definition

$$\dot{q}(T,T_s) = C_p(T)\,\frac{dT}{dt} \quad . \tag{3}$$

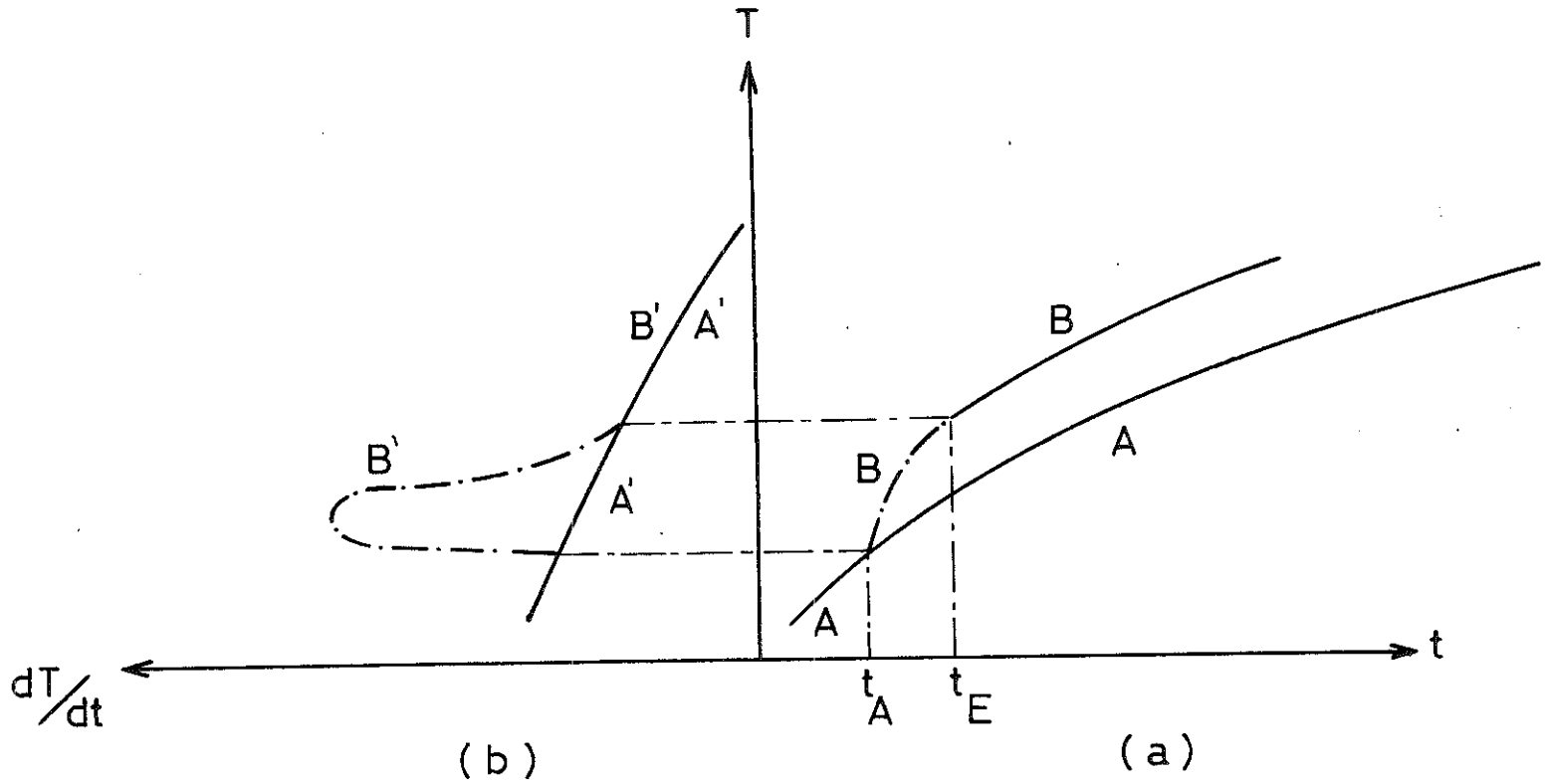

FIG. 3

All the screens which surround the sample have been thermally anchored to the salt and by construction of the apparatus T_s is expected (and observed) to remain reasonably constant over a run. Then $\frac{dT}{dt}$ depends on T only and the curve $\frac{dT}{dt}(T)$ is a unique curve for a state of "dynamic equilibrium" characterised by the leaks $\dot{q}(T,T_s)$ to the sample ; The curve A' of fig. 3b, schematizes the evolution of $\frac{dT}{dt}$ versus the temperature, corresponding to the path A of fig. 3a.

Now, when at t_A a heat pulse is applied to the sample, paths B (fig. 3a) and B' (fig. 3b) will be described which differ from A and A'. However, after a transient period necessary for the total quantity of heat introduced to diffuse in the sample and in the thermometer, the system will come back at time t_E to the same dynamic equilibrium than before, characterised by $\dot{q}(T)$ and $\frac{dT}{dt}(T)$. On fig. 3b the curves A' and B' coincide before t_A and after t_E ; over a complete run, discrete parts of A' are obtained and the total curve may be easily recovered by smooth interpolations between these parts : t_E is the instant at which B' reaches back this interpolated curve of "dynamic equilibrium".

The same considerations which are valid for T and $\frac{dT}{dt}(T)$ are also valid for M and $\frac{dM}{dt}(M)$ to which we have a direct access. Moreover dM/dt is a more physical quantity since, as shown in ref. 5 and 6, it is proportional to the heat leaks to the sample if the specific heat is proportional to T^{-2} (as is generaly the case at low temperature) :

$$\dot{q} = \frac{A}{T^2}\frac{dT}{dt} = -A\frac{d}{dt}\left(\frac{1}{T}\right) = -\frac{A}{a}\frac{dM}{dt} \quad . \qquad (4)$$

In practice, simultaneously with M versus time, we record, on an XY recorder, $\frac{dM}{dt}(M)$ which happens to be very linear over a complete run from 20 to 100 mK. This makes the determination of t_E particularly easy during the experiment.

On fig. 4 a typical XY graphic of dM/dt versus M is shown over two runs. The return to dynamical equilibrium is followed over several heat pulses. The obvious advantage of working with $\frac{dT}{dt}(T)$ rather than with T(t) in the determination of t_E relies on the fact that the discontinuities, even when smoothed by large time constant effects, remain more apparent on the time derivative.

IV - THE EXTRAPOLATION OF THE DRIFTS

The extrapolation of M(t) can be also achieved using the knowledge of dM/dt. This was the basis of a graphical method proposed in reference 6. In our case dM/dt is observed to be a linear function of M, a result which does not correspond to any obvious physical law : for example the Newton law would predict $\dot{q}$, i.e. dM/dt, to be a linear function of T not of M. However, the empiric law

$$\frac{dM}{dt} = - \alpha M + \beta \ , \qquad (5)$$

has been found experimentaly to be the best law to describe the heat leaks of our apparatus in the range of temperature of interest. This, although possibly casual, is fortunate since this simple law provides not only the method for the determination of t_E (as explained above) but also gives an analytic law for the extrapolation of the drifts : by integration we have at "equilibrium"

$$M = \gamma \, e^{-\alpha t} + \beta/\alpha \ . \qquad (6)$$

With this in mind, the determination of the specific heat follows from fig. 3. The coefficients α and β are obtained from the graphic of $\frac{dM}{dt}$ (M) (curve A' in fig. 3b) using altogether the data at equilibrium preceeding and following a heat pulse. Then two values for the integration constant γ are determined, one before and the other after a heat pulse by using the data of M(t) at equilibrium (curve A and B in fig. 3a). The drifts at equilibrium are extrapolated from both sides over the phase of non equilibrium and the temperature difference at any chosen

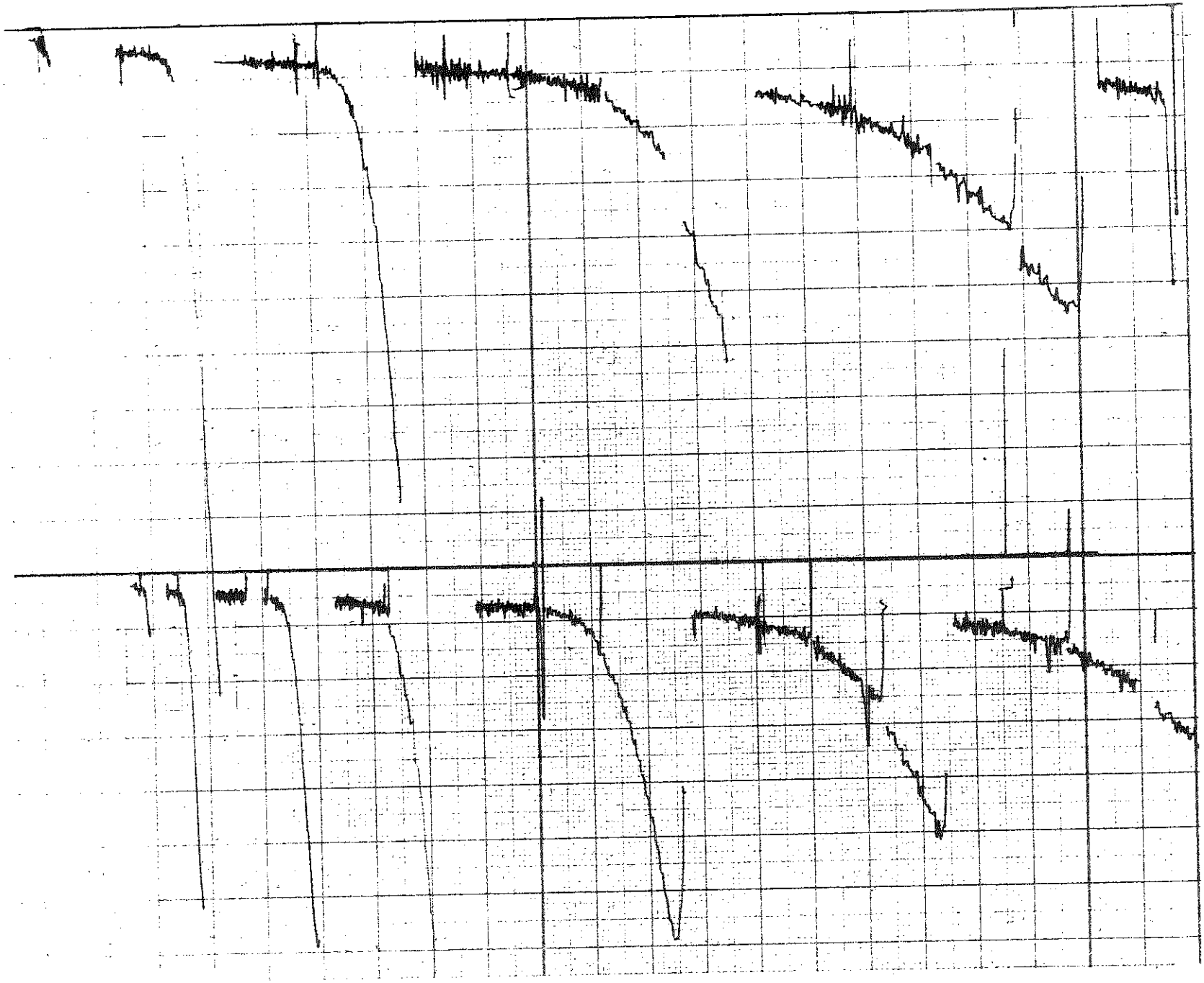

FIG. 4

time t_o may be calculated. From the above, computations appear appropriate for the treatment of the data and suggest the adoption of a system for the automatic acquisition of those data which would make these computations more straightforward.

IV - THE ACQUISITION OF THE DATA

To perform the specific heat determination according to the method described above, the knowledge of the following data are needed :

1°) Evolution of M(t) ;

2°) Appreciation of the equilibrium state ;

3°) Determination of the heating energy supplied to the sample.

- The problem of the evolution of M(t) is solved by punching the value of M at regular time intervals (every 10 seconds in our case). In the mutual inductance bridge (constructed in the laboratory and commercialized by S.E.I.N.) M is opposed by discrete values M_b and the difference between M and M_b is amplified and recorded. The bridge settings (the indications of a commercial A.O.I.P. six decades resistance box) were coded ; a Solartron 1604 numerical voltmeter reads the unbalance V. A data transfer unit (D.T.U. Schlumberger) enables to punch a "word" composed of an analogic part (the indications V of the voltmeter) followed by a digital part (the indication M_b of the bridge).

An intervention of the operator is necessary to change M_b to another value M_b' when V becomes too large (approaching the linearity limit of the bridge). In the treatment of the data, small extrapolations from both sides will allow to associate a variation ΔV of the voltmeter reading to a known variation ΔM_b in the bridge settings and hence establish the correspondance between M and V :

$$M = M_b + V \left(\frac{\Delta M_b}{\Delta V}\right) . \qquad (7)$$

- The direct appreciation of the equilibrium state on the graphic of $\frac{dM}{dt}(M)$ on the XY recorder (fig. 4) was left to the operator. A parameter X, which is punched together with the digital part of the "word", has the value 1 in the equilibrium state and is automatically turned to 0 (non equilibrium) when the heating is started (time t_A). It is manually turned back to 1 at the time t_E, when dM/dt becomes again a linear function of M on the XY recorder (fig. 4). It is the knowledge of the value of this punched parameter X that will define for the computer the state of dynamical equilibrium.

- A second channel of the D.T.U. is used to punch the value of the heating current (measured by the voltmeter on an equivalent circuit) and the time of the heating (indicated by a coded Schneider timer) after the end of the heating period and before t_E. A third channel is used to punch the values of a resistance thermometer fixed in the sample holder. This enables the calibration against the CMN thermometer of resistance thermometers for other experiments in the laboratory.

Figure 5 shows a block diagram of the acquisition data system. A group of relays enables the introduction in the D.T.U. of the "digital part" of the punched "word" ; they are triggered by the D.T.U. after the analogic part of the "word" has been punched. An external clock commands the lecture of the above channels each 10 seconds, giving the time basis for the treatment of the data.

VI - THE TREATMENT OF THE DATA

Figures 6, 7 and 8 show the elements of the treatment of the data for one typical run.

- Curve b in fig. 6 shows the restitution by the computer of the $\frac{dM}{dt}(M)$ curve also obtained during the experiment by

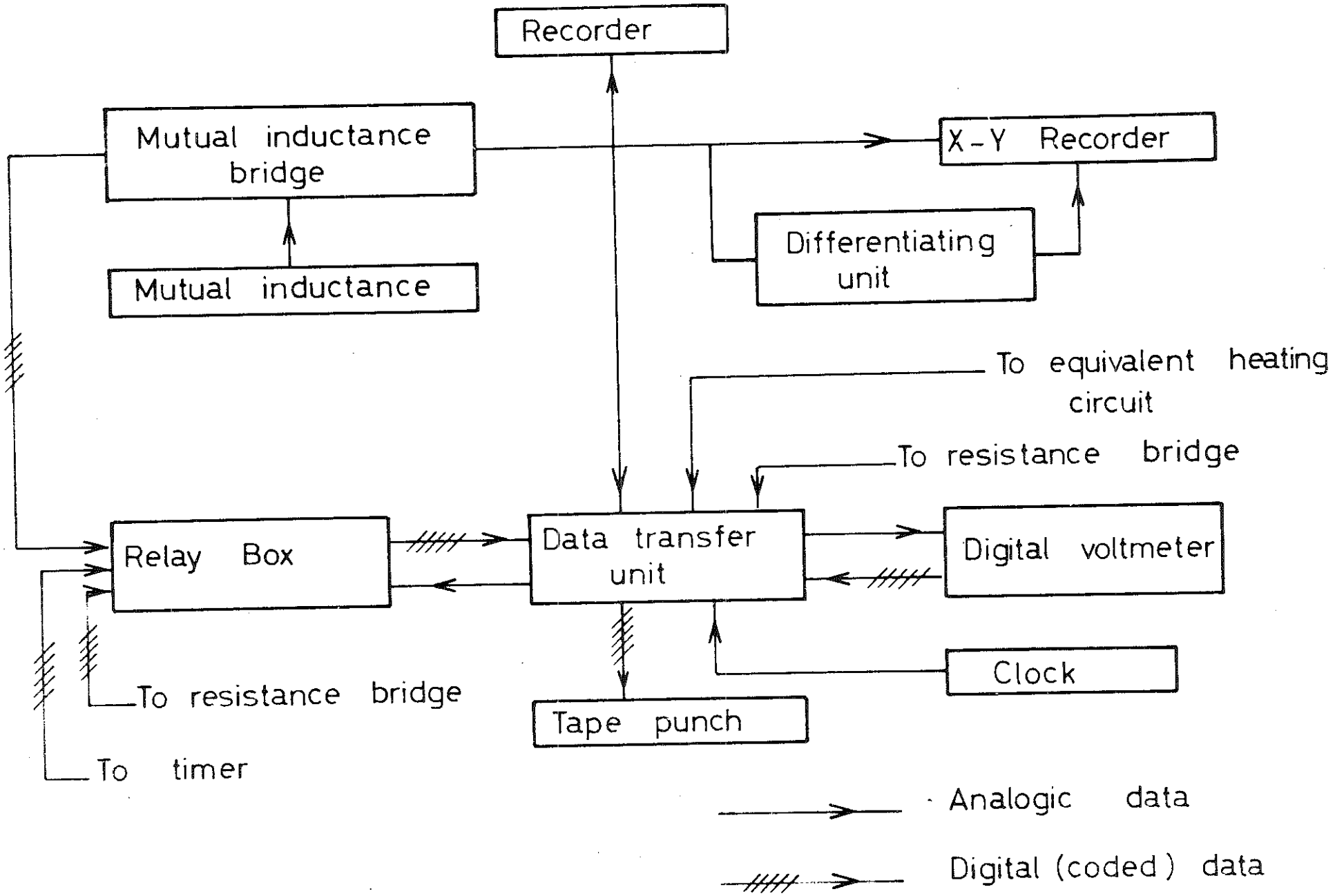
Recorder
Mutual inductance bridge
X-Y Recorder
Mutual inductance
Differentiating unit
To equivalent heating circuit
To resistance bridge
Relay Box
Data transfer unit
Digital voltmeter
Clock
To resistance bridge
Tape punch
To timer
Analogic data
Digital (coded) data

FIG. 5

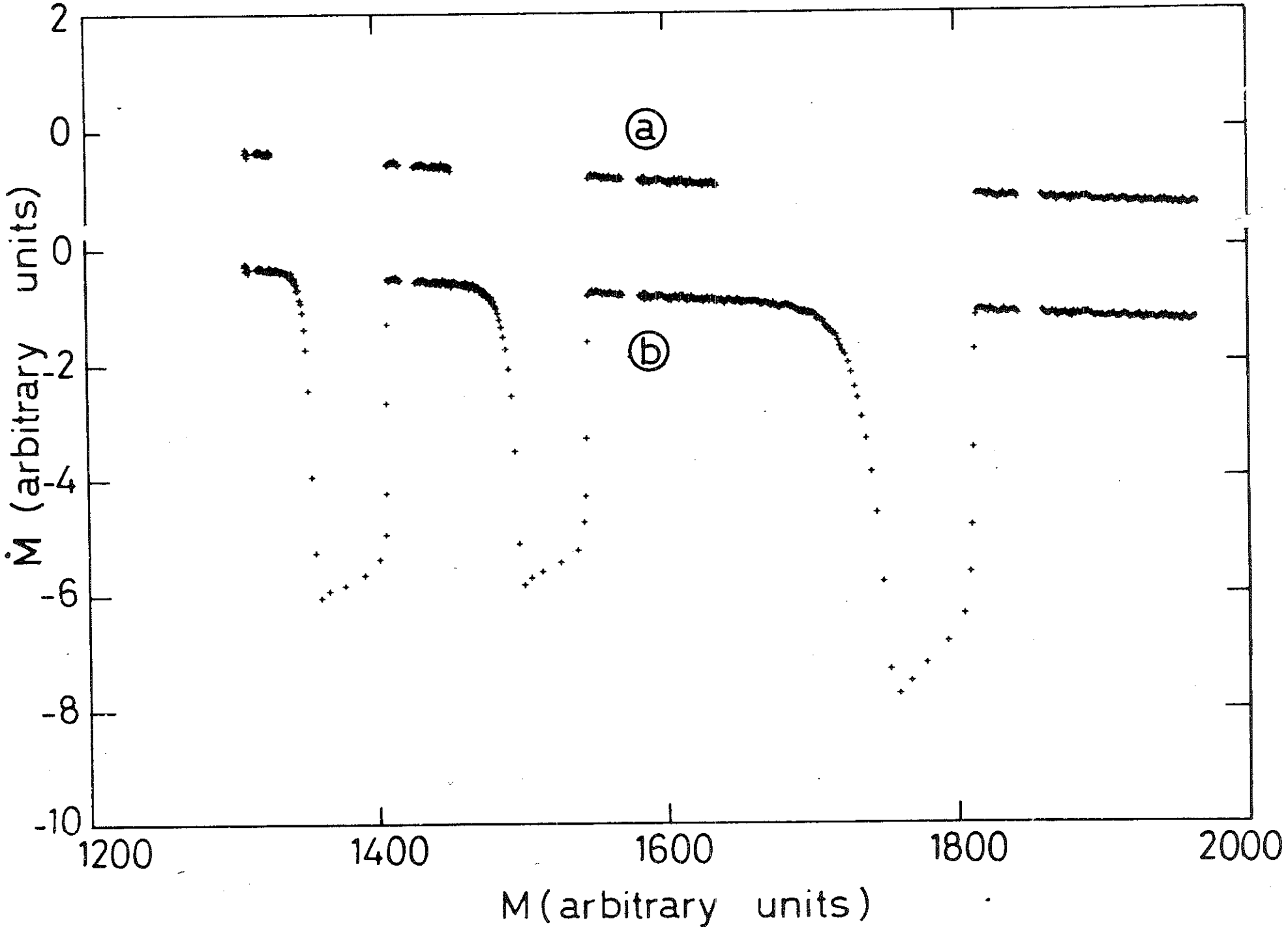
2
0
0
-2
-4
-6
-8
-10
Ṁ (arbitrary units)
ⓐ
ⓑ
1200
1400
1600
1800
2000
M (arbitrary units)

FIG. 6

the XY recorder (fig. 4).

- Curve a in fig. 6 shows the portions of this $\frac{dM}{dt}(M)$ curve which are retained i.e. the portions at equilibrium ($X = 1$). α and β the coefficients of equation (5) are calculated as explained before by fitting with a straight line (using the least mean square procedure) the two successive portions corresponding to the "equilibrium" data which immediately preceede and follow each heating of the sample.

- In fig. 7, a part of a typical run M(T) is restituted (corresponding to the curve b in fig. 6). The steps produced by the supplied energy are clearly seen (the achievement of equilibrium is not so easily detected as in fig. 4 or 6). The blank spaces in fig. 7 correspond to the few points where an intervention of the operator was necessary to change the bridge settings ($x = 2$)[7]. The values of α and β beeing known, the different values of γ (eq. 6) are calculated using a least mean square procedure with the data of the M(t) curve at dynamic equilibrium.

- Fig. 8 shows the actual values of M and the extrapolations for a typical determination of a specific heat point. From the values of M, the temperature T is recalculated using the calibration law $M = \frac{a}{T} + b$ and the specific heat is obtained.

VII - ESTIMATION OF THE ERRORS

a) Uncertainty due to the determination of t_o

According to equation 6, the difference ΔM between the two extrapolated drifts of fig. 8 is at the time t_o :

$$\Delta M = e^{-\alpha t_o} (\gamma_A - \gamma_B) , \qquad (8)$$

where γ_A and γ_B are the integration constants calculated as described in the previous section. Making use of $M = \frac{a}{T} + b$:

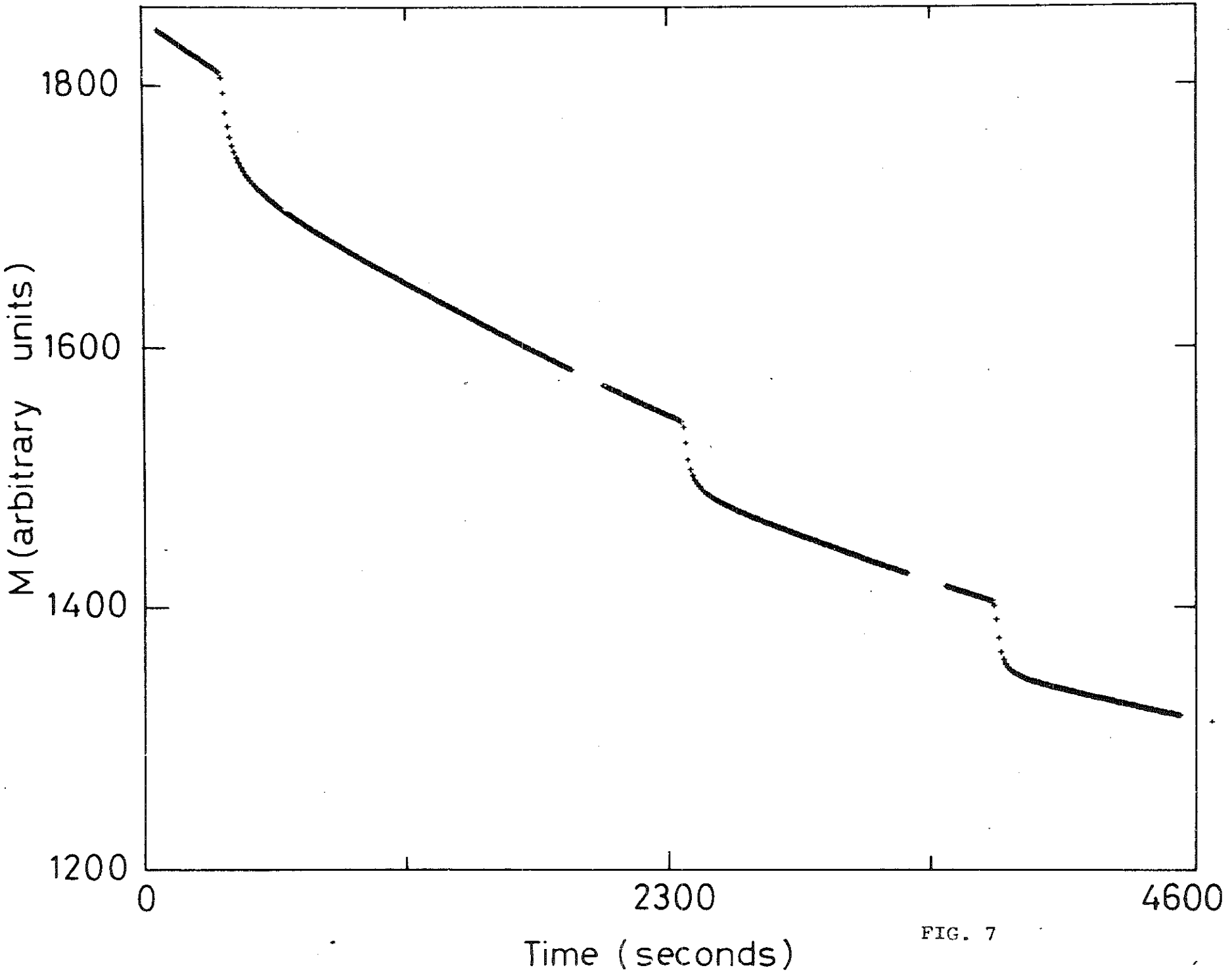
1800
1600
1400
1200
M (arbitrary units)
0
2300
4600
Time (seconds)

FIG. 7

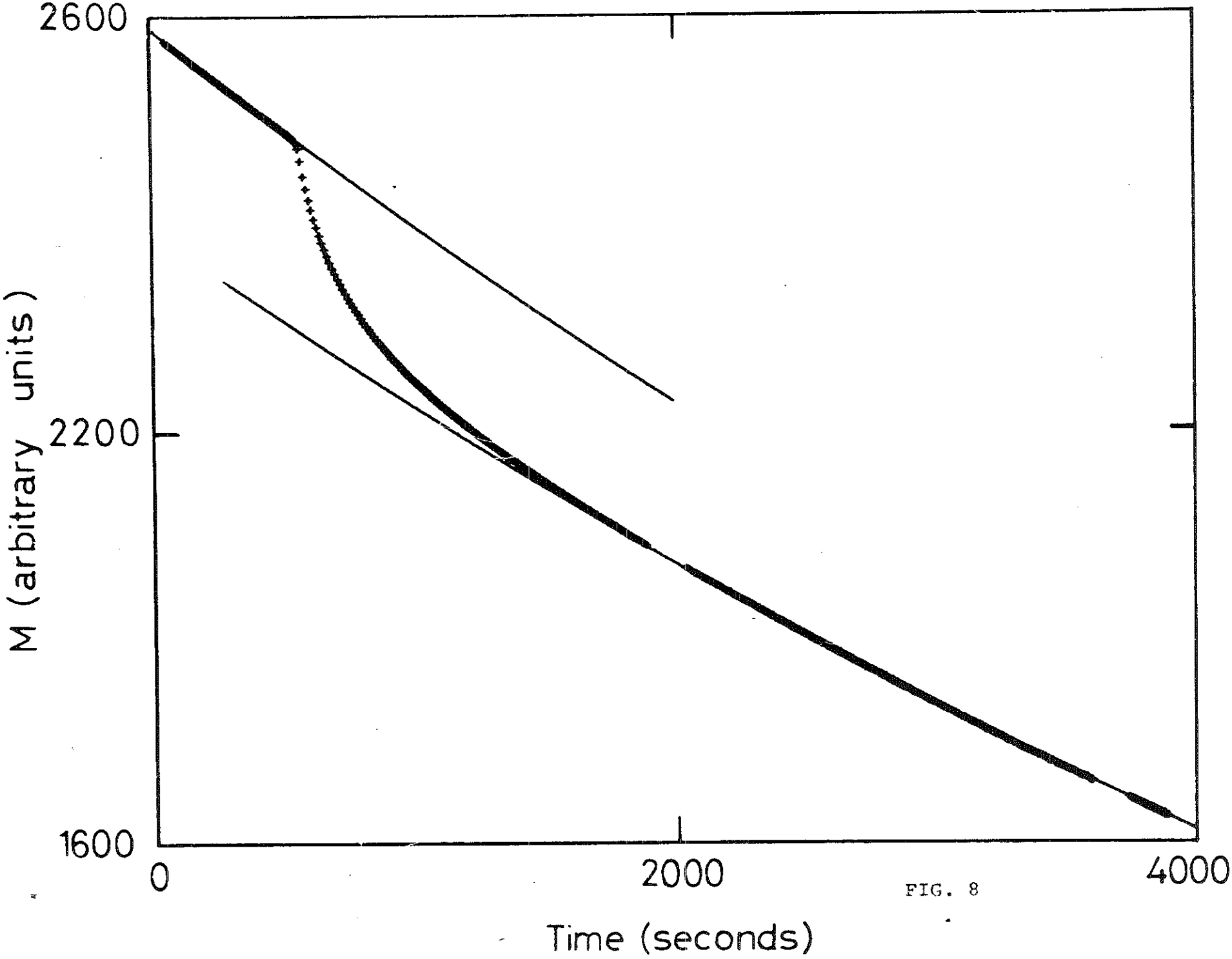

FIG. 8

$$\frac{\Delta T}{\bar{T}} = \frac{\Delta M}{\bar{M} - b} \quad , \tag{9}$$

and so $\Delta T = \bar{T}^2 \frac{\Delta M}{a}$.

The calculated specific heat will then be :

$$C_p = \frac{a}{\bar{T}^2 \, e^{-\alpha t_o} \, (\gamma_A - \gamma_B)} \cdot \Delta Q, \tag{10}$$

ΔQ being the energy supplied and $\bar{T}$ the mean temperature $\frac{T_{A'} + T_{B'}}{2}$.

At temperatures lower than 50 mK, the specific heat is dominated by the nuclear contribution and $C_p = A/T_M^2$. From equation (10) we see then that the evaluation of A is dependent on the correct choice of t_o. If any other time t'_o is choosen between t_A and t_E, the corresponding determination of A will be A' such that

$$\frac{A'}{A} = e^{-\alpha(t_o - t'_o)} ,$$

so that

$$\frac{\Delta A}{A} \simeq \alpha(t_o - t'_o) . \tag{11}$$

The values of α determined experimentaly are the greater, the smaller the heat capacity (in agreement with equations 4 and 5) and were found to be of the order of 10^{-4} s^{-1} for the smallest heat capacity measured.

For practical reasons t'_o has been systematicaly chosen at the end of the heating period, which was of the order of 20 seconds at the lowest temperatures. So $t'_o = t_A + 20$ s. The error $\Delta A/A$ depends on the difference between this value and the actual t_o.

b) <u>estimation of t_o</u>

According to (4) and (5), the observed heat leak $\dot{q}$ is proportional to M ; we are then tempted to use the areas rule

in the graphic M(t) (of M versus time) to determine t_o for the same reason which justifies its application in the graphic T(t) when $\dot{q}$ is proportional to T. On doing so we will make the wrong assumption that the temperature of the CMN and the temperature of the sample are the same during the transient period after heating. We shall come back to this last point later.

For small heat capacities, the approach to the dynamical equilibrium has been observed to follow an exponential law in the graphic M(t). In that case, the application of the rule of areas leads to choose t_o at $t_A + 0.7\ \tau$, where τ is the time constant of the exponential law. But in the limit of very small heat capacities (when $\Delta A/A$ is larger because α is larger), the time constant τ of this exponential law is dominated by the response time of the CMN and has been found to be[8] :

$$\tau_o = 3.T^{-3} \text{ ms} \quad , \tag{12}$$

τ_o increasing rapidily when the temperature decreases, for a given value of α, $\Delta A/A$ will be larger for the lowest temperatures. At 20 mK, for instance, according to (12) $t_o \simeq t_A + 400$ s.

Coming back now to the existence of a temperature difference between the CMN and the sample, during the transient period, we must observe, as in fig. 8, that the temperature of the thermometer approaches the equilibrium drifts by values smaller than the extrapolated drifts. Such an "underheating" of the thermometer implies an "overheating" of the sample. But, as shown in ref. 4, the rule of areas applied in the case of an "overheating" of the sample would lead to a choice of t_o nearer to t_A than the value of $0.7\ \tau$ calculated above. Then according to (11) :

$$\frac{\Delta A}{A} < 10^{-4}\ (400 - 20) \quad ,$$

that is :

$$\frac{\Delta A}{A} < 4\ \% \quad .$$

c) error due to the large time constant τ_o

The existence of a large time constant for the thermometer, will introduce a difference between the temperatures of the sample and of the thermometer, even when the system is in dynamic equilibrium. The error on C_p due to the existence of this difference may be estimated, assuming the system is a first order one. The error δM introduced during the measurement of M will be

$$\delta M = \dot{M} \cdot \tau \ , \tag{13}$$

τ being the time constant of the system (thermal and electronic).

The error $\delta(\Delta M)$ in the evaluation of ΔM produced by the supplied heat is (fig. 1) :

$$\delta (\Delta M) = \delta M_{A'} - \delta M_{B'} = (\dot{M}_{A'} - \dot{M}_{B'})\tau \ . \tag{14}$$

But :

$$M = \frac{a}{T} + b \ , \tag{15}$$

and so $$\frac{\delta(\Delta M)}{M - b} = \frac{\delta(\Delta T)}{\overline{T}} \ . \tag{16}$$

By another hand the supplied heat being known to better than 1 %

$$\frac{\delta C_p}{C_p} = \frac{\delta(\Delta T)}{\Delta T} \ , \tag{17}$$

During the experiment, the heat supplied is such that $\frac{\Delta T}{\overline{T}} \sim 10$ %, so :

$$\frac{\delta C_p}{C_p} \sim 10 \ \frac{\delta(\Delta T)}{\overline{T}} \ . \tag{18}$$

According to eq. (14), (16) and (18) :

$$\frac{\delta C_p}{C_p} = \frac{10\tau \ (\dot{M}_{A'} - \dot{M}_{B'})}{(\overline{M} - b)} \ . \tag{19}$$

But making use of (5) :

$$\frac{\delta C_p}{C_p} = \frac{10\ \tau\alpha\ \Delta M}{(\bar{M} - b)} , \qquad (20)$$

or

$$\frac{\delta C_p}{C_p} = \tau\alpha , \qquad (21)$$

with the values of α and τ given above we find for 20 mK and small heat capacities

$$\frac{\delta C_p}{C_p} < 3\ \% .$$

d) random errors

As shown in fig. 7, a typical run from 16 to 70 mK will allow the determination of 4 to 6 values of $C_p(T)$. Then another cycle is started by cooling the sample via the supraconducting thermal switch. In a typical experiment 3 to 7 runs are made below 100 mK and the scatter of the experimental points is a good estimation of the random errors. With the method described in this paper, the scatter has been reduced to a few percent for the different runs, as may be seen in the measurements of the Au-Co-Fe[2] and Pt-Co[1] systems. The standard graphical method of linear extrapolation of the drifts leads to a much larger scatter, in the same experimental conditions, as may be seen in the results obtained for the Au-Co[2] system. Thanks to this method, the (terms in $1/T^4$, $1/T^6$...) of the nuclear Schottky anomalies have been observed for the first time in dilute alloys containing 3d transition impurities[1].

VIII - NUCLEAR SPECIFIC HEAT OF Cu-Mn ALLOYS

Nuclear orientation measurements yield for the hyperfine field H_{eff} on the Mn nuclei in Cu-Mn alloys a value of 280 $\pm$10 kOe[10], in desagreement with the estimation of H_{eff} = 430 kOe from the low temperature specific heat[11]. The presence of a large contribution of the matrix, which could not be separated from the

impurity contribution in the specific heat measurement, was advanced as an explanation for an overestimation of H_{eff}.

As a test to the accuracy of the method discussed above we have measured between 20 mK and 100 mK the specific heat of a Cu-Mn sample of nominal concentration 1 at %, with the aim to separate if possible the impurity contribution from the host contribution.

The 14 g sample (Ø = 7 mm, ℓ = 20 mm) was prepared by the metallurgical group of our laboratory, from 99.999 % Asarco copper (Ø = 3/8 ") and 99.99 % Johnson Matthey manganese. The specimen was induction melted by a semilevitation technique on a water cooled base plate and cast in a water cooled copper mold[12]. The actual concentration, determined by absorption spectroscopy, was 0.901 at. % Mn.

The nuclear specific heat, $C_{nuclear}$, is plotted versus temperature in fig. 9 (circles). $C_{nuclear}$ has been obtained from the experimental results by substracting a linear contribution γT, with γ = 3.7 mJ/K^2.mole, due to the electronic contribution of the host (0.7 mJ/K^2.mole) and to the magnetic ordering contribution of the electronic spins (3 mJ/K^2.mole)[13]. In fact this γT term corresponds to a small correction on the experimental values attaining 5 % at 0.1 K and completely negligible in the lower temperature range.

The Schottky anomalies, expected from the Zeeman splitting of the Mn nuclear levels, are also plotted in this figure for 3 different values of the hyperfine field : 280 (curve A), 325 (curve B) and 430 kOe (curve C), with the concentration c = 0.9 at%. The following conclusion can be drawn :

1°) For temperatures higher than 50 mK (the range where

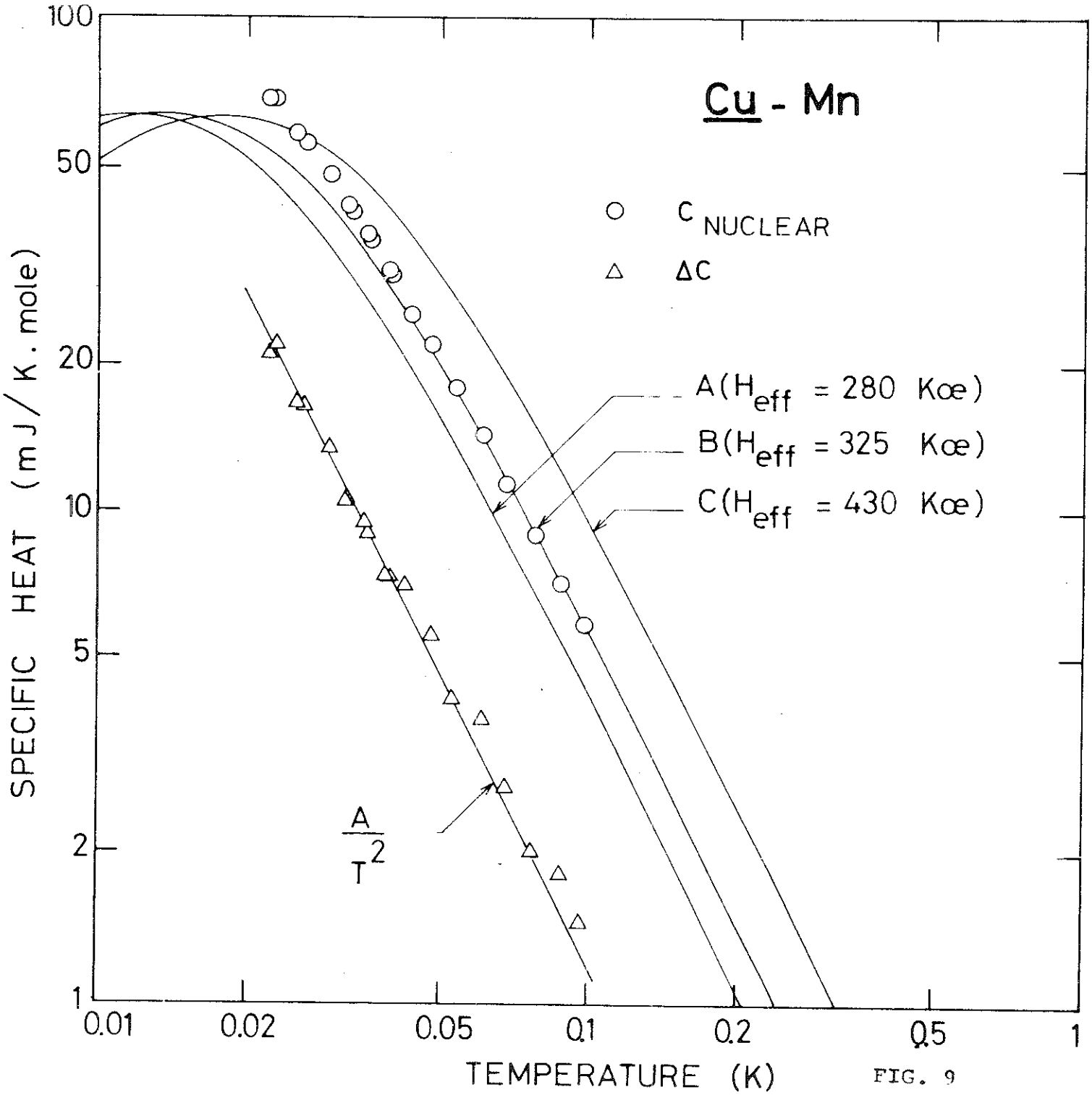
Cu - Mn
C NUCLEAR
ΔC
A(H eff = 280 Kœ)
B(H eff = 325 Kœ)
C(H eff = 430 Kœ)
A/T²
SPECIFIC HEAT (mJ/K.mole)
TEMPERATURE (K)
100
50
20
10
5
2
1
0.01
0.02
0.05
0.1
0.2
0.5
1

FIG. 9

Du Chatenier and Miedema experiments were performed) the observed specific heat is best described by the high temperature tail of the Schottky anomaly calculated with H_{eff} = 325 kOe (curve B) and not with H_{eff} = 430 kOe (curve C), as stated in ref. 11.

2°) Below 50 mK it appears that curve B cannot account for the experimental data and so the experimental points cannot be described by a single Schottky anomaly.

3°) The experimental values are always higher than curve A, which would correspond to the contribution of Mn impurities with H_{eff} as determined by nuclear orientation in a sample containing a few p.p.m. of Mn.

The excess $\Delta C = C_{nuclear} - C_{curve\ A}$ is plotted in the same figure (triangles), and is well described by an AT^{-2} law in the whole temperature range, with A = 12.0 mJ K/mole. Taking in account the experimental error, an acceptable ΔT^{-2} law is yet obtained attributing to the impurities an H_{eff} between 280 and 295 kOe, leading values of A between 12 and 9 μJ.K/mole. The permanence of such a T^{-2} law down to 20 mK requires a small value of the nuclear level splitting and so H_{eff} (for large H_{eff} a departure to the T^{-2} asymptotic behaviour should be observed, as in the case of curves A, B and C). On another hand, the great value of A requires a large number of nuclei probing this small hyperfine field. We are then led to conclude that this contribution comes from the host nuclei.

For 1 mole of Copper :

$$A = R\ \frac{I(I+1)}{3}\ \frac{\gamma^2 \hbar^2}{k^2}\ \overline{H_{eff}^2}\ , \qquad (22)$$

where I and γ are respectively the spin and gyromagnetic ratio of Copper nuclei, $\overline{H_{eff}^2}$ the mean value of the square of the hyperfine field induced on those nuclei, and the other constants have their usual meaning. Let H_{eff_i} be the hyperfine field induced

by a manganese atom of the ith shell containing z_i sites on one copper nucleus at the origin, the above expression becomes [14] :

$$A = c(1 - c)R \frac{I(I + 1)}{3} \frac{\gamma^2 \hbar^2}{k^2} \sum_i z_i H^2_{eff_i} , \qquad (23)$$

where c is the manganese concentration and (1 - c) the concentration of copper nuclei . The contact hyperfine field H_{eff_i} may be expressed as a function of the spin polarization $n(r_i)$ of the conduction band at the site i by [15] :

$$H_{eff_i} = \frac{\xi}{2g_I} a_A \Omega_o n(r_i) , \qquad (24)$$

where Ω_o is the atomic volume and where we assume for the other parameters in copper the values[16,17]

$$\xi = \langle |\Psi(0)|^2 \rangle_F / \langle |\Psi(0)|^2 \rangle = 0.33$$

$$a_A = 0.190 \text{ cm}^{-1}$$

$$g_I = 7.39 \times 10^{-24} \text{ erg.G}^{-1}$$

Following Friedel the asymptotic form of the spin polarization amplitude $n(r_i)$ will be[18] :

$$n(r_i) = - \frac{5}{4\pi^2 r_i^3} \sin(\phi^+ - \phi^-) \cos (2k_F + \phi^+ + \phi^-) , \qquad (25)$$

where ϕ^+ and ϕ^- are the phase shifts for spin up and spin down directions. Assuming the Mn ions carry 4 μ_B :

$$\phi^+ = 0$$
$$\phi^- = \pi/5$$

The summation in (23) happens to converge rather quickly and needs not to be extended farther than the first neighbour shells. Calculations up to the 20th neighbour yield for A the value of 1.5 μJK/mole.

In this calculation the contribution of the first four shells is preponderant and the use of the asymptotic expression (25) may be of doubtfull validity at such distances. A calculation made by Parlebas[19], taking in account the band structure of Cu leads, for the spin polarisation amplitude on the first heigbour shells, to values that are equal or somewhat smaller than those given by (25). On the other side the calculations of **Geldart**[20] using the Anderson model for a free electron gas and taking into account the magnetic ion structure yield for the first impurity neighbours values of n(r) which are considerably larger than those given by (25). Using his values up to the 3rd neighbour shell and (25) after that, A is found to be 6 μJ.K/mole. The theoretical predictions are then too small by a factor of 2 to 7, corresponding to a factor 1.5 to 3 on the amplitude of the oscillations. This is not a very large discrepancy considering the approximations involved and specialy the questionable validity of (23) where correlations effects have been neglected.

IX - CONCLUSION

In low temperature calorimetry where the contact resistances added to the bad diffusivity of the CMN introduce large thermal response times, the time derivative of the mutual inductance bridge signal $\dot{M}$ seems to be a very useful parameter. For small heat capacity samples, the time constant of the system composed by the sample - sample holder and the CMN is given by the CMN time constant which in our case follows the law $\tau=3.T^{-3}$ ms, in the temperature range between 20 mK and 100 mK, attaining thus about 6 minutes at 20 mK. In that time scale the temperature drifts are no more linear and the recovery of thermal dynamic equilibrium after a heat pulse is not easily detected in the graphic of M vs.time. The recording of $\dot{M}$ versus M, made during the experiment, enables to appreciate more easily the state of dynamic equilibrium and may be a useful technique in other specific heat

measurements at any temperatures but when problems of bad diffusivity are present.

For the extrapolation of the non linear temperature drifts a more complex machinery is necessary. The graphical method must be substituted by a computer treatment of the data describing the evolution of M versus time. Here also $\dot{M}$ is a useful quantity since, when measuring nuclear specific heat, the sample heat leak $\dot{q}$ responsible for the temperature drifts, is proportional to $\dot{M}$. The observation that for our apparatus $\dot{M}$ or $\dot{q}$ is proportional to M enables to use a simple analytical law to perform the extrapolation of the drift. The data acquisition system builded using commercial apparatus, on which only minor modifications have been introduced, yields a straightforward and rapid treatment of the data by a computer.

The above method reduces largely the systematic and random errors introduced by the linear graphical extrapolation method making possible, for example, the observation of higher order terms in T^{-2} in the series representing the nuclear Schottky anomaly of dilute alloys containing transition impurities. This fact allows to separate the impurity contribution from the host contribution to the nuclear specific heat of a Cu-Mn alloy. The experimental results are analysed as the sum of a Schottky anomaly due to the impurities, corresponding to the hyperfine field of 280 kOe found by nuclear orientation, and a host T^{-2} term, the amplitude of which is found to be in the range predicted by theoretical estimations.

A K N O W L E D G E M E N T S

We thank the metallurgical group of the laboratory for the preparation of the Cu-Mn sample and the data processing group for advices.

FIGURE CAPTIONS

-:-:-:-:-:-:-:-:-:-

Fig. 1 - Schematized graphic of the temperature versus time, typical of a specific heat determination, in the simple case when the diffusivity is large and a fast response thermometer is used.

Fig. 2 - Evolution of the inductance bridge signal M ($M = A/T + b$) versus time when a heat pulse is applied to the sample at t_A. After a transient period, dynamic equilibrium is recovered at t_E. The dotted line shows the extrapolation backward in time made from the drifts after t_E.

Fig. 3 - The evolution of the temperature T versus time t (fig. a) and the corresponding time derivative of T versus T (fig. b), for two cases : free run (curves A and A') and specific heat measurement (curve B and B'). Before t_A (begining of the heat pulse) and after t_E (recovery of dynamic equilibrium) curves A' and B' coincide.

Fig. 4 - The recording of M (vertical axis) versus M (horizontal axis) made on a X-Y recorder for 2 distinct runs during an experiment. A large departure from a linear $\dot{M}(M)$ variation, characteristic of the state of dynamic equilibrium (curve A' of fig. 3), is observed when a heat pulse is applied. This linear $\dot{M}(M)$ variation is recovered after a transient period the larger the lower the temperature (right side of the figure).

Fig. 5 - Block diagram of the data acquisition system.

Fig. 6 - $\dot{M}$ versus M as given by the computer from the data punched during the experiment (curve b). This figure is the restitution of a part of fig. 4. The points that are out of equilibrium are not well described here since $\dot{M}$ has been defined by $\frac{M(t + 100) - M(t)}{100}$. Curve (a) shows the part of figure (b) retained by the computer in the extrapolation of the drifts.

Fig. 7 - A part of a run of M versus time restituted by the computer. The three steps shown correspond to the same three specific heat point as in fig. 6 ($34 < T < 93$ mK).

Fig. 8 - The evolution of M versus time during a typical specific heat determination at 23 mK (crosses) and the extrapolations made by the computer (continuous line).

Fig. 9 - The specific heat as a function of temperature in a log-log plot for the Cu-Mn sample. The nuclear specific heat (circles) is obtained from the experimental results by substracting the γT contribution. Curves A, B and C are Schottky anomalies corresponding to H_{eff} = 280 , 325 and 430 kOe. The excess ΔC of the nuclear specific heat above curve A, follows a T^{-2} law (triangles) and is the contribution attributed to the host nuclei.

R E F E R E N C E S

(1) P. COSTA-RIBEIRO, J. SAINT-PAUL and D. THOULOUZE (to be published)

(2) P. COSTA-RIBEIRO, J. SOULETIE, D. THOULOUZE and R. TOURNIER Journal de Physique, Supplément au n°2-3, 32, C1 753 (1971)

P. COSTA-RIBEIRO, J. SOULETIE and D. THOULOUZE - Phys. Rev. Lett. 24, 900 (1970)

(3) J.R.G. KEYSTON, A. LACAZE and D. THOULOUZE - Cryogen. 8, 295 (1968)

(4) KEESOM and KOK - Leiden comm. 219 (C)
PARKINSON and QUARRINGTON - Proc. Phys. Soc. A 67, 569 (1954)

(5) A.R. MIEDEMA and T. HASEDA - Proceedings of I.I. 2 - London (1961) - Edited by A. Van Itterbeck - Pergamon Press

(6) WEATHLEY et al. - Physics 1, 337 (1965)

(7) The time response of the electronic being not instantaneous, a wrong value of M may eventualy be punched due to this intervention. This is why the operator indicates his intervention by turning to 2 the parameter X. The values of M punched during this phase are not taken in account by the computer, but enable to preserve the time basis.

(8) For low temperatures $M \sim a/T$ and so τ_o is also the time constant in the graphic of T versus time, exhibiting the same T^{-3} dependance already noticed in reference 9.

(9) P.E. GREGERS-HANSEN, M. KRUSIUS and G.R. PICKETT - Phys. Rev. Lett. 27, 38 (1970)

(10) I.A. CAMPBELL, J.P. COMPTON, I.R. WILLIAMS and G.V.H. WILSON - Phys. Rev. Lett. 19, 1319 (1967)

J. FLOUQUET - Phys. Rev. Lett. 25, 288 (1970)

(11) F.J. DUCHATENIER, A.R. MIEDEMA - Physica 32, 403 (1966)

(12) O. BETHOUX, J. FERRARI, B. CORNUT - Rev. Appl. Phys. 5, 865 (1965)

(13) N.E. PHILLIPS - C.R.C. Critical Reviews in Solid State Sciences 2, 467 (1971)

(14) B. DREYFUS and D. THOULOUZE - J. Applied Phys. 39, 1320 (1968)

(15) B. CAROLI and A. BLANDIN - J. Phys. Chem. Solids 27, 503 (1966)

(16) A. NARATH - Phys. Rev. 165, 506 (1968)

(17) W.D. KNIGHT - Solid State Physics, vol. 2, F. SEITZ and D. TURNBULL (Academic Press, N.Y. 1956) Chapt. 2.

(18) A. BLANDIN et J. FRIEDEL - J. Phys. Rad. 20, 160 (1959)

(19) J.C. PARLEBAS - Thesis (unpublished) Université de Strasbourg France (1972)

(20) D.J.W. GELDART - Phys. Lett. 38 A, 25 (1972).

C H A P I T R E IV

ALLIAGES AVEC T_K >> 1 K : Au-Co, Au-Co-Fe, Au-Co-Ni

A - EFFET DES INTERACTIONS SUR L'APPARITION D'UN MOMENT MAGNETIQUE SUR LE Co PAR MESURE DE CHALEUR SPECIFIQUE NUCLEAIRE D'ALLIAGES Au-Co

(publié dans Phys. Rev. Letters 24, 900, 1970)

B - CHALEUR SPECIFIQUE NUCLEAIRE ET SUSCEPTIBILITE D'IMPURETES DE Co NON MAGNETIQUES POLARISEES PAR DES IMPURETES DE Fe DANS LES ALLIAGES Au-Co-Fe

(à paraître)

C - ABSENCE D'EFFET D'INTERACTIONS IMPORTANTES ENTRE Co et Ni DANS L'Au.

INTERACTION EFFECTS ON THE APPEARANCE OF A MAGNETIC MOMENT ON Co, THROUGH NUCLEAR SPECIFIC HEAT MEASUREMENTS ON Au-Co ALLOYS[*]

P. COSTA-RIBEIRO[†‡], J. SOULETIE AND D. THOULOUZE

Centre de Recherches sur les Très Basses Températures,

C.N.R.S. CEDEX N°166, 38 - GRENOBLE-GARE, FRANCE.

The specific heat of Au-Co alloys down to 0.02K is reported. The nuclear term (AT^{-2}) is due to the magnetic Co atoms which are found to be those included in groups of three and more neighbours. The low temperature linear term (γT) is the sum of the contributions of the magnetic Co groups, non magnetic pairs and isolated atoms. We estimate fluctuation temperatures of 50K for the pairs and 700K for the isolated atoms.

---

[*] Part of this work was supported by D.R.M.E.

[†] In partial fulfilment of a thesis

[‡] C.A.P.E.S. - Ford Foundation Fellow

The available data on the Au Co system show that at low concentrations the alloys are non-magnetic while phenomenons which are generally considered as characteristic of the existence of a localized magnetic moment on the impurity are found at higher concentrations of Co.

- Firstly, the resistivity shows a flat $\rho(T)$ behaviour for the low concentrations but a large minimum is observed for concentrations over 0.1% [1].
- Secondly the magnetization[2] is Pauli like and remains small compared to alloys of the Cu Mn type, for the low concentrations, but for concentrations over 1% a romanent magnetization and a susceptibility maximum are observed.
- Thirdly, above 1 K, specific heat measurements[3] show an electronic term, concentration dependent, for concentrations below 3%, but for increasing concentrations a tendency towards a concentration independent behaviour is observed.

Similar remarks can be made for the Cu Co[4] system. In the early classification of Blandin and Friedel this has been considered a critical case, i.e. one for which the criterion for magnetism is almost realised : $U\rho(E_F)-1\sim 0$ [5]. ($\rho(E)$ is the density of states in the unsplit virtual bound state for one spin direction).

The theory of localized spin fluctuations[6] has given rise to the notion of a fluctuation temperature T_{SF} [7] $\left(\frac{1}{KT_{SF}} \frac{\Pi \rho(E_F)}{\rho(E_F)}\right)$ which would separate a non magnetic state (well below T_{SF}) and a state where the impurity would exhibit all the properties of

a magnetic impurity [8]. Caroli has shown $\rho(E_F)$ to be sensitive to the interactions with other impurities [9]. Thus the fluctuation temperature should depend on the interaction ; Lederer has shown that the susceptibility is different for an isolated impurity and an interacting pair [10]. Such an analysis is particularly convenient in the case of Co (where $1-U\rho(E_F)\sim 0$) since a moderate interaction may be sufficient to make T_{SF} change by several orders of magnitude. Recently Tournier and Blandin[4] interpreted magnetic results on the Cu Co system with this argument, attributing a lower fluctuation temperature to the groups of two atoms than to the isolated impurities and a localized moment to the Co atoms involved in groups of three and more atoms.

We report here specific heat measurements between 0.02K and 0.3K on Au Co alloys. The nuclear moment of Co being very large ($4.6\mu_N$), the hyperfine T^{-2} contribution will be mainly produced by the effective field H_{eff} of the ordered magnetic Co atoms on their own nucleus and hence will be proportional to the concentration C_m of magnetic impurities. Then the hyperfine contribution allows one to enumerate the magnetic impurities. In addition, the term linear in temperature will provide some indication about the ordering of the magnetic impurities, and the contributions of the non magnetic atoms.

The samples used for this experiment were prepared

from 99.999% Au and 99.999% Co. The constituants were melted in alumina crucibles under atmosphere of purified hydrogen, and held 4 hours at 1150°C. After removal of the crucible, the alloys (Ø7 mm, $\ell \sim 20$mm) were annealed 24 hours at 950°C and quenched in a flow of gaseous hydrogen of 120 bars. This procedure gives roproducible results and is more efficient than quenching in water. After quenching, the alloys were kept at 77K and heated to room temperature only for the time necessary to assemble the apparatus. The weighed constituants were such as to produce 0.75, 1, 1.5, 2, 3, 4, and 6 at % alloys. A very extensive magnetic study (0.04K to 100K and 0 to 70 kOe) has been made on the same samples and will be published elsewhere [11]. The specific heat was measured with an apparatus using the technique of double stage demagnetization [12].

In fig.1 we have plotted $C_p(T)$ curves for five of the seven samples measured. Each curve was observed to fit laws of the type $C_p = AT^{-2} + BT$ within experimental error, below the ordering temperature T_c which was determined from a $C_p\ T^2(T^3)$ diagram. The values of A and B determined by a least squares method are plotted as a function of concentration in fig.2.

The nuclear term appears to vary almost as the third power of the concentration. This suggests that a magnetic moment may be associated with groups of 3 or more atoms. More precisely let $N_1 = c\,(1-c)^{12}$, $N_2 = 12\,c^2\,(1-c)^{18}$, $N_3 = c^3\left[24.(1-c)^{22} + 36\,(1-c)^{23} + 90\,(1-c)^{24}\right]$ be the probabilities for a Co atom to be isolated or included in groups

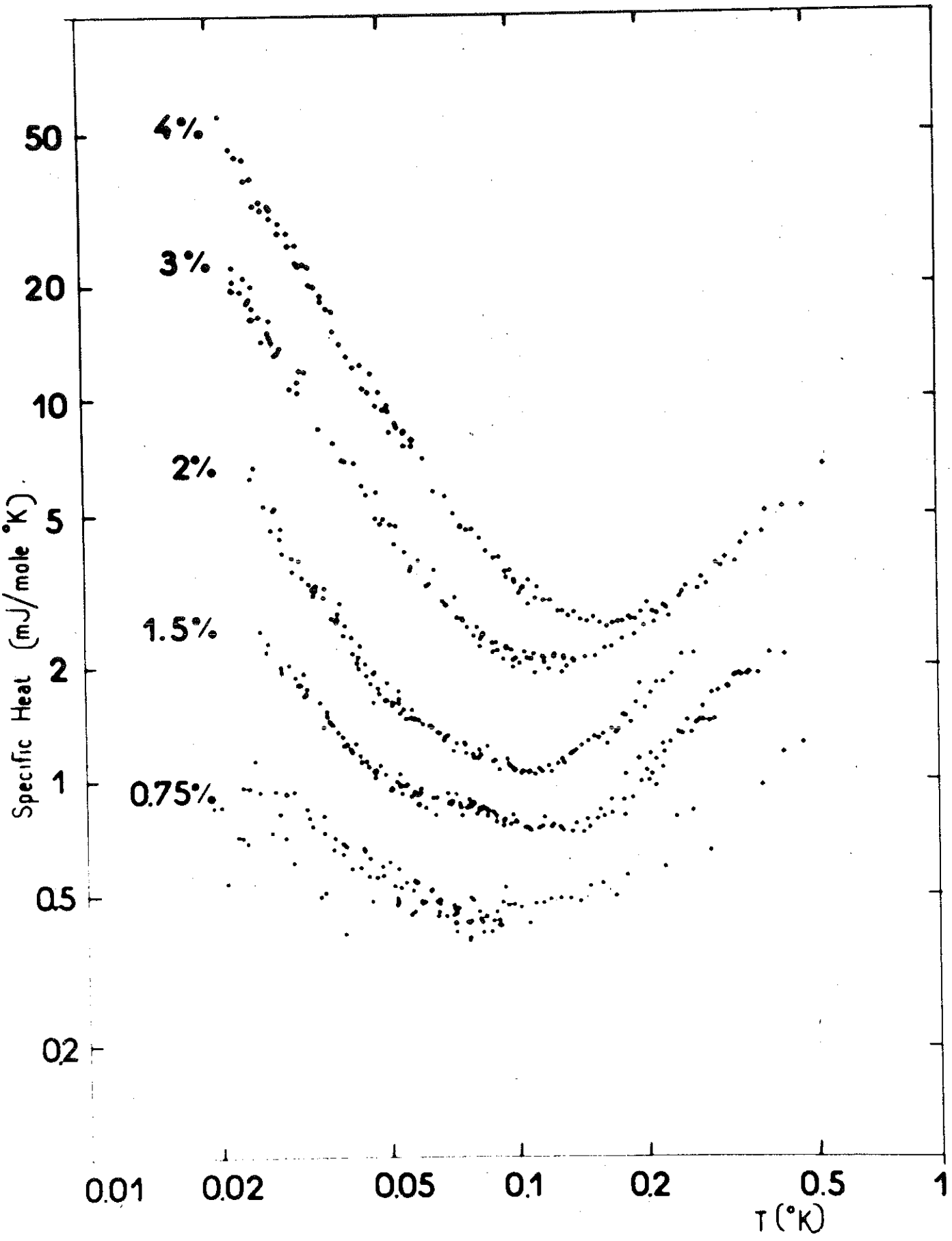
4%
3%
2%
1.5%
0.75%
50
20
10
5
2
1
0.5
0.2
Specific Heat (mJ/mole °K)
0.01
0.02
0.05
0.1
0.2
0.5
1
T (°K)

FIG. 1

of two or three atoms respectively (c is the concentration); then $X_2 = c - N_1$, $X_3 = c - (N_1+N_2)$, $X_4 = c-(N_1+N_2+N_3)$ are the concentrations in atoms of Co which are in groups of <u>at least</u> two, three or four atoms respectively. Assuming the value of the hyperfine field to be the same for each magnetic Cobalt, the variation of the coefficient A of the T^{-2} term with the concentration should reflect the variation of the number of magnetic carriers. On fig. 2 we observe that the best fit of the A(c) law is obtained with X_3 (c), <u>so that a magnetic moment is associated with all Co atoms which are included in groups of at least 3 atoms</u>.

From the expression

$A = [c - (N_1+N_2)]\ R\ [I\ (I+1)/3]\ \gamma^2 \hbar^2\ H_{eff}^2/k^2$ we calculate for the hyperfine field on the nucleus the value $H_{eff} \sim 190$kOe. This value is not very different from the value of 225kOe which is observed in hexagonal Co [13].

But we have neglected the hyperfine specific heat of <u>the matrix</u>. One term is due to the hyperfine field induced by the spin density oscillations (RKY) of conduction electrons produced by the <u>magnetic</u> Cobalt, and so is <u>proportional to X_3 (c)</u>. Assuming this term has the same magnitude for Co as for Fe or Cr impurities in the same matrix [14], we calculated that the value of H_{eff} would be lowered by 1.5% only. Another term (quadrupolar) is due to the electric field gradients associated to the charge density oscillations (Friedel oscillations) produced by <u>all</u> the Co impurities and is

therefore proportional to c. The fact that we observed a c^3 variation shows that, in our concentration range, this contribution is negligible. However, it may be responsible of some deviation such as is observed for the 0.75% and 1% alloys which give results somewhat higher than the theoretical expectation (fig.2). (But the experimental accuracy is poor for the small concentrations and further analysis cannot be made).

Now we turn to the linear term in temperature BT, corrected from the contribution of the Au matrix. We assume two different values T_1 and T_2 of the fluctuation temperature of the non magnetic impurities depending whether they are isolated or are in pairs. From the spin fluctuation theory[6,7] they will then contribute [15] $\gamma_1 T$ (for $T \ll T_1$) and $\gamma_2 T$ (for $T \ll T_2$) with $\gamma_1 = N_1 \frac{\pi R}{T_1}$ and $\gamma_2 = N_2 \frac{\pi R}{T_2}$ respectively per mole of alloy. The magnetic impurities interacting through long range oscillations of the $\cos(2k_F r+\varphi)/r^3$ form will contribute a $\gamma_3 T$ term which is concentration independent[16] in the range $T<T_o$ where T_o, the order temperature, is proportional to their concentration : $X_3(c)$ in this case.

In the insert of fig.2 the values of B are given for $T < T_o$ (T_o is estimated to be around 8×10^{-2}K for the 1.5 at.% alloy from our results). Hence $B = \gamma_1 + \gamma_2 + \gamma_3$. On the same graph measurements of B by Crane[3] at $T \sim 6$K, i.e. much greater than T_o are also given. In this case $B = \gamma_1 + \gamma_2$. Our results differ from Crane's results by an almost constant term of the order of 5 mJ/mole K^2 which is of the right order of magnitude

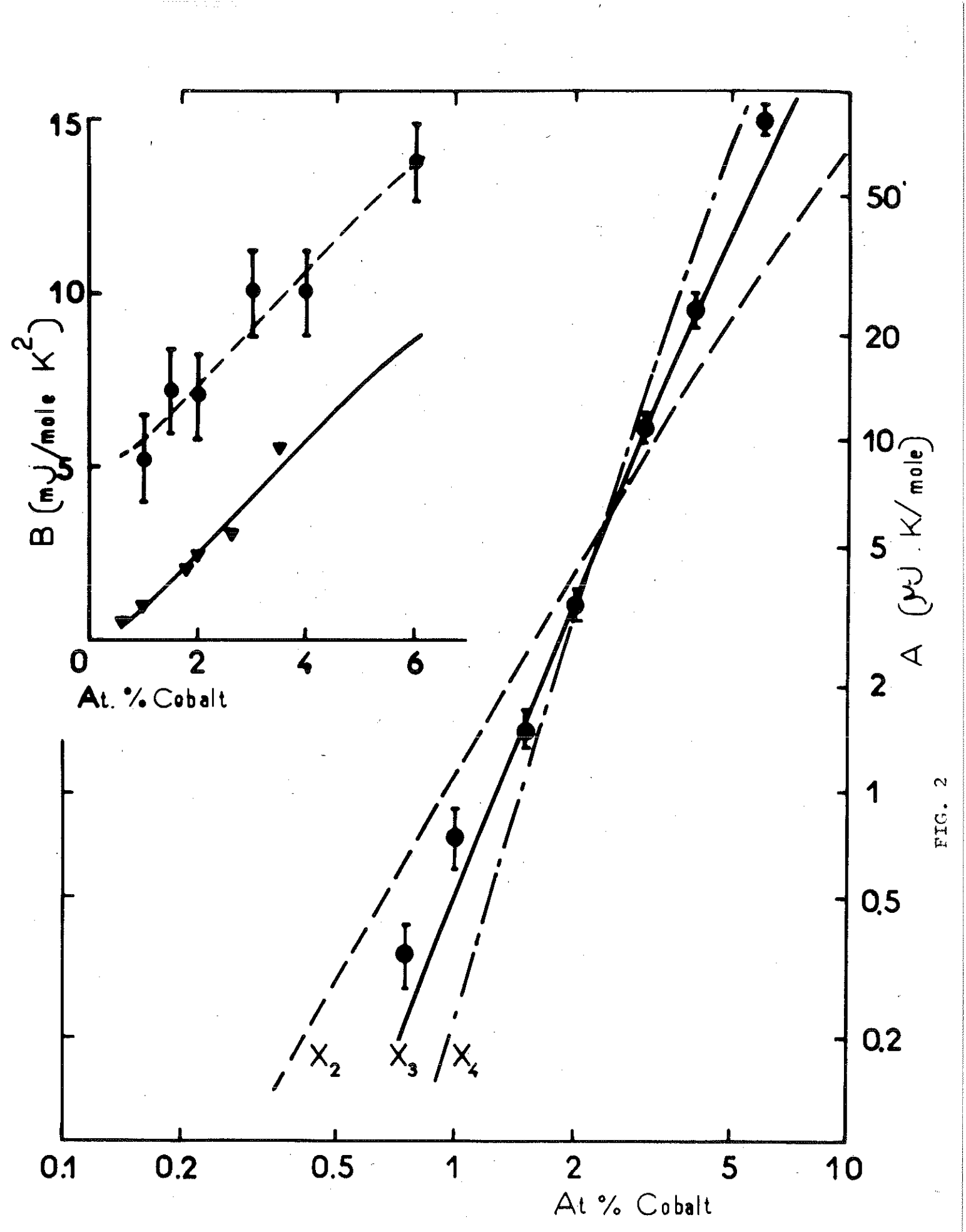
15
10
5
B (mJ/mole K²)
0
2
4
6
At. % Cobalt
50
20
10
5
2
1
0.5
0.2
A (μJ . K/mole)
X2
X3
X4
0.1
0.2
0.5
1
2
5
10
At % Cobalt

FIG. 2

for γ_3 (a term of 3.7 mJ/mole K^2 is observed in Cu Mn and 3 mJ/mole K^2 in Au Fe [16]).

We can estimate γ_1 and γ_2 more accurately from Crane's results. He fitted the variation of his B term with the concentration by the empirical law 800 $c^{1.5}$ mJ/mole K^2. An equally good fit is obtained with $B = \gamma_1 + \gamma_2 \sim 38N_1 + 520N_2$ mJ/mole K^2 which implies from what has been said above $T_1 \sim 700K$ and $T_2 \sim 50K$. It is interesting to note that there exists a logarithmic behaviour of the resistivity proportional to c, around 700K [17] and that new results [18] show another change of regime below 20K, where the slope of the increase is proportional to a power 1.5 of the concentration. (Here also this may hide an $\alpha N_1 + \gamma N_2$ variation which may be understood as evidence for short range interactions).

Thus, our measurements on the Au Co system confirm the model proposed for the Cu Co alloys[4]. The agreement is still better : this is not surprising since Au Co being a better solid solution, segregation effects are expected to be of less importance. Our paper supports the suggestion[4] that interaction effects should be of quite general importance in systems near the limiting condition for the appearance of a magnetic moment on the impurities.

We thank Dr. Tournier for advice and M. Picot for assistance in performing experiments. We also are grateful to the metallurgical group of the laboratory for preparing the samples.

FIGURE CAPTIONS

FIG. 1 - Measured specific heat of Au Co alloys versus temperature for different Co concentrations.

FIG. 2 - The A coefficient of the T^{-2} term of Cp versus per cent Cobalt (for the 0.75, 1, 1.5, 2, 3, 4 and 6 at.% we find respectively .35, .75, 1.5, 3.4, 11.0, 23.4 and 82.3 μJ.K/mole). The solid line shows the best fit of our data with a $X_3(c)$ law, yielding H_{eff}= 190 kOe. The dashed lines were obtained trying to fit the results with an $X_2(c)$ law and H_{eff} = 100 kOe, and an $X_4(c)$ law and H_{eff} = 370 kOe.

The insert shows the B coefficient of the linear term in temperature versus percent Cobalt ; our results below T_o (black circles), Crane's results above T_o triangles) (ref.3) and corresponding theoretical laws : 38 N_1 + 520 N_2 mJ/mole K^2 (solid line) and 5 + 38 N_1 + 520 N_2 mJ/mole K^2 (dashed line).

R E F E R E N C E S

1 G.J. VAN DER BERG, Miss J. VAN HERK and B. KNOOK in Proceedings of the tenth International Conference on Low Temperature Physics, Moscow, 1966, part A p. 272

2 J. LE GUILLERM, R. TOURNIER and L. WEIL in Proceedings of the eigth International Conference on Low Temperature Physics 1962, p. 236 (BUTTERWORTHS, LONDON 1963) and O.S. LUTES and J.L. SCHMIT, Phys. Rev. 134, A 676 (1964).

3 L.T. CRANE , Phys. Rev. 125, 1902 (1962).

4 R. TOURNIER and A. BLANDIN, Submitted for publication to Phys. Rev. Letters.

5 A. BLANDIN and J. FRIEDEL, J. Phys. Radium 20, 160 (1959).

6 P. LEDERER and D.L. MILLS, Phys. Rev. 165, 837 (1968), and Phys. Rev. Letters, 19, 1040 (1968).

7 B. CAROLI, P. LEDERER and D. SAINT-JAMES, Phys. Rev. Letters 23, 700 (1969).

8 N. RIVIER and M.J. ZUCKERMANN, Phys. Rev. Letters 21, 904 (1968).

9 B. CAROLI, J. Phys. Chem. Solids. 28, 1427 (1967).

10 P. LEDERER, Thesis Université de Paris (1967).

11 E. BOUCAI, B. LECOANET, J. PILON and R. TOURNIER, to be published.

12 J.R.G. KEYSTON, A. LACAZE and D. THOULOUZE, Cryogenics 8, 295 (1969).

13 W. PROCTOR, R.G. SCURLOCK and E.M. WRAY, Phys. Letters 20, 621 (1966).

14 D. THOULOUZE, Thesis Université de Grenoble (1968) unpublished, and B. DREYFUS, J.C. MICHEL and D. THOULOUZE J. Appl. Phys. 39, 1320 (1968).

15 G. CHOUTEAU, R. FOURNEAUX and R. TOURNIER and P. LEDERER Phys. Rev. Letters 21, 1082 (1968).

16 J. SOULETIE and R. TOURNIER (and references here included) J. Low Temp. Phys. 1, 95 (1969).

17 C.A. DOMENICALI and E.L. CHRISTENSON, J. Appl. Phys. 32, 2450 (1961).

18 P.J. FORD, T.E. WHALL and J.W. LORAM in Proceedings of the eleventh International Conference on Low Temperature Physics, St. Andrews, 1968, edited by J.F. Allen, D.M. FINLAYSON, D.M. Mc CALL, p. 1246.

NUCLEAR SPECIFIC HEAT AND SUSCEPTIBILITY MEASUREMENTS OF NON MAGNETIC Co ATOMS POLARIZED BY Fe IMPURITIES IN Au-Co-Fe ALLOYS.

P. COSTA-RIBEIRO[+‡], J. SOULETIE, D. THOULOUZE and R. TOURNIER

+ In partial fulfilment of a thesis

‡ C.A.P.E.S. Fellow (Brazil)

A B S T R A C T

We report here nuclear specific heat of 7 samples of Au-Co-Fe alloys with different Co (1.5 to 3 at %) and Fe (0.1 to 3 at %) concentrations, between 0.02 K and 0.5 K. The presence of Fe in Au-Co increases by a large factor the nuclear contribution and evidencies the existence of a large fraction of non magnetic Co atoms in these alloys. The dependence of this nuclear contribution with the impurity concentration is analized using auxiliary susceptibility measurements made around the ordering temperature ($\sim$ 10 K) of 4 samples. Using a crude molecular field model the results are well explained when characteristic temperatures T_{K_1} and T_{K_2} of 200 and 14 K are associated to the configurations of isolated and pairs of Co atoms.

INTRODUCTION

A - DISCUSSION OF PREVIOUS RESULTS ON THE Au-Co SYSTEM

A model has been proposed in the interpretation of low temperature specific heat[1] and magnetization measurements[2] in Au-Co alloys that succeeded to explain the apparently contradictory results obtained previously by electrical resistivity[3], specific heat[4] and magnetic susceptibility[5] measurements. Down to 20 mK, the magnetic atoms are found to be those belonging to groups of at least three nearest-neighbours ; they carry a saturation moment of 1.7 μ_B with an hyperfine field of 190 kOe. The number of magnetic impurities varies then as the cube of the cobalt concentration and decreases drastically with the concentration, which explains the paradoxical magnetic behaviour observed by the above bulk types of measurements (ref. 3 to 5) in different concentration ranges.

Pairs of nearest neighbours and isolated Co atoms have been found to have LSF temperatures around 50 K and 700 K respectively according to ref. 1 when the formula $\gamma_c = \pi R/T_K$ was used or about 16 K and 133 K according to ref. 2[6]. Then magnetic impurities are detected at temperatures about $T_{K_1}/10\ 000$, where T_{K_1} is the characteristic temperature of isolated impurities.

In later nuclear orientation results[7] obtained on very dilute samples (where only isolated impurities should be present) the absolute value of the ratio between internal and applied field was found to be 1.29 ± 0.11 and a value for T_K of 32 K was estimated for isolated Co in Au, which is too small by one order of magnitude.

Nevertheless, another interpretation for this nuclear orientation result was to assume a dominant orbital contribution to the knight shift of isolated Co atoms as have been found by NMR in Cu-Co alloys[8]. The value of $H_{eff}/H_{int} = 1.29 \pm 0.11$ would then lead to a knight shift K of $+ (29 \pm 11)$ %. In recent measurements of ^{59}Co nuclear magnetic resonance, Narath and Barham[9] confirmed this interpretation showing that $K = +(29.2 \pm 0.2)$ % in the temperature range between 1.2 and 4.2 K. The lack of strong temperature dependance of K between 1.2 K and 300 K led the authors to estimate 300 K as a low limit for the T_K of isolated Co.

No information about the presence of an absorption line due to pairs of Co atoms was reported in this paper, despite the existence of 0.1 at % of Co pairs in the more concentrated (1 at %) sample studied by them. Moreover the lack of agreement between the values of T_K for pairs and isolated impurities as determined by the magnetization[2] and specific heat measurements[1] may cast some doubt about the model used to explain those results. Furthermore the value of K determined by the nuclear orientation and NMR measurements leads to increase the discrepancy between the estimation of T_K made in ref. 1 and 2.

In fact, we may write K as the sum of three terms :

$$K = K_s + K_d + K_{orb} \qquad (1)$$

where K_S is an s contact part resulting from the s band parmagnetism, K_d is a core polarization term resulting from the d electron spin paramagnetism and K_{orb} is due to an orbital paramagnetism. K_S is expected to be smaller than 0.2 %[8], and

$$K_d = h_{hf}^{d} \cdot \chi_d / \mu_B$$

$$K_{orb} = h_{hf}^{orb} \cdot \chi_{orb} / \mu_B$$

where h_{hf} and χ are the hyperfine field and static susceptibility and μ_B the bohr magneton. So (1) becomes :

$$K = h^{d}_{hf}\,\chi_d/\mu_B + h^{orb}_{hf}\,\chi_{orb}/\mu_B \qquad (2)$$

Now, using the experimental value of K_1, as determined by Narath, the value of $\chi_d + \chi_{orb}$ of 15×10^{-27} uem/at obtained from ref. 2 for the isolated impurities, and for the parameters h^{d}_{hf} and h^{orb}_{hf} the values - 100 and 600 kOe, as calculated for free Co atoms atoms[10], we found[11] :

$$K_{orb} \simeq +0.39 \qquad \chi_{orb} = 6 \times 10^{-27} \text{ uem/at}$$

and

$$K_d \simeq -0.09 \qquad \chi_d = 8.4 \times 10^{-27} \text{ uem/at}$$

The existence of an orbital contribution to the susceptibility gives origin to the definition of two spin fluctuation temperatures corresponding to the orbital susceptibility and spin susceptibility respectively[12]. Calling T_{K_1} the spin characteristic temperature of isolated impurities, the above value of χ_d yields using the formula $T_{K_1} = \frac{2\mu_B^2(2\ell+1)}{\pi k \chi_d}$

$$T_{K_1} = 240 \text{ K}$$

instead of 133 K as would be determined if the measured susceptibility of 15×10^{-27} uem/at was only of spin in origin.

But now, the existence of a very small Hund's coupling ($J \sim 2.10^{-2}$ eV) deduced from the presence of a large orbital susceptibility leads to use for the specific heat the formula[12]

$$\gamma/c = (2\ell+1)\,\pi R/T_K$$

The measured value of γ yields then $T_{K_1} = 3\,500$ K for the isolated impurities.

For the pairs of Co atoms, the susceptibility being an order of magnitude larger than for the isolated impurities, the orbital contribution may be neglected[13] and the characteristic temperature T_{K_2} of pairs will be :

$$T_{K_2} = 16\ K$$

There is now a factor of about 15 between the estimation of T_{K_1} and of about 3 between the determination of T_{K_2}. Such a large difference may not be explained by experimental errors or by a bad estimation of χ_d from the K value and should be attributed to the inadequacy of the L.S.F. theory to describe the Au-Co alloy, as has been advanced by Narath to explain the complete NMR results.

B - STUDY OF THE Au-Co-Fe ALLOY

To confirm the existence of 3 distinct magnetic behaviour associated with the different configurations of isolated, pairs and groups of at least three Co neighbours. We studied the effect of introducting Fe impurities in Au-Co alloys, completing previous results already reported[14]. The interaction between the Fe and Co impurities will enable to get informations about the magnetic states of the different Co configurations in Au.

The study of interaction effects between impurities of different kind has been already performed in some ternary alloys. By the evolution of the Mössbauer spectra at 4.2 K, Window[15] observed the effect of Mn ions on ^{57}Fe, when the Mn concentration was increased, in a Cu-$Fe_{1\%}$-Mn_x alloy. He concluded that iron atoms with manganese neighbours are not magnetic (in good agreement with Morya's[16] predictions) but may have large polarizations induced by the magnetic ordering of the host (induced moments). Mössbauer[17] and magnetization[18] measurements have also been done with Fe as impurities introduced in Cu-Ni alloys. For less concentrated alloys the T_K of Fe is lowered by

the presence of Ni neighbours and for high concentrations the magnetic Fe polarizes the Ni impurities. In Cu-Co, a system similar to Au-Co[19], the introduction of magnetic Mn impurities has no result, as far as interaction effects are concerned[20]. The susceptibility and the line width at 77 K of Cu-Co-Mn were found to be equal to the simple addition of those of Cu-Mn and Cu-Co alloys, showing that no moment was induced on Co by the Mn ions but the high temperature where these experiments have been performed cast some doubt on this conclusion.

We report here a study of interaction effects between Co and Fe in Au, by specific heat and susceptibility measurements. The specific heat of 7 Au-Co-Fe samples was measured between 20 mK and 0.5 K using a double stage demagnetization apparatus[21], with an automatic system of acquisition and treatment of data[22]. In the temperature range between 20 mK and 100 mK, the specific heat is dominated by the high temperature tail of the nuclear Schottky anomaly due to the Zeeman splitting of the nuclear levels of the impurities which are magnetic or on which a moment has been induced.

The advantage of using Fe instead of another magnetic transition impurity on Mn, to study interaction effects with Co by the nuclear specific heat results from the fact that the nuclear contribution of Fe is negligible (due to the small nuclear moment value and natural isotopic abondance of ^{57}Fe). The nuclear specific heat will then be chiefly sensitive to the moments induced on the Co atoms.

The susceptibility results of 4 samples have been deduced from magnetization measurements, made in fields up to 85 Oe using an extraction method[23] around the ordering temperatures, that is, between 1 and 30 K. The magnetization curves versus field were straight lines up to the maximum field. These measurements will enable a quantitative interpretation of the specific heat results.

The Au-Co-Fe samples have been prepared using the same procedure described in ref. 1 with the addition of 99.999 % Fe, by the metallurgical group of the laboratory.

SPECIFIC HEAT MEASUREMENTS

A - RESULTS

In fig. 1 we have represented the specific heat of four different samples with the same cobalt content (1.5 at %) and iron concentrations 0.1, 0.3, 1 and 3 at %. The result obtained previously[1] with a Au-Co sample 1.5 at % is shown by a continuous line. In fig. 2 we have reported the data for another series of samples with three different Co concentrations (1.5, 2 and 3 at %) and the same amount of iron (0.1 at %). Also shown is the result obtained with a concentrated alloy containing 1 at % Fe and 3 at % Co.

In this temperature range (20 mK to 1 K) the dominant contributions are :

- A linear term in temperature γT (righ side of the figures) which is the sum of the electronic contribution of the host, of the concentration independent term due to the ordering of the magnetic impurities and of the one impurity contribution (Kondo or localized spin fluctuation) due to the impurities with a high T_K.

- A nuclear term (left side) which is the high temperature tail of a Schottky anomaly, that may be represented by a series of T^{-2} :

$$A T^{-2} + B T^{-4} + \cdots \qquad (3)$$

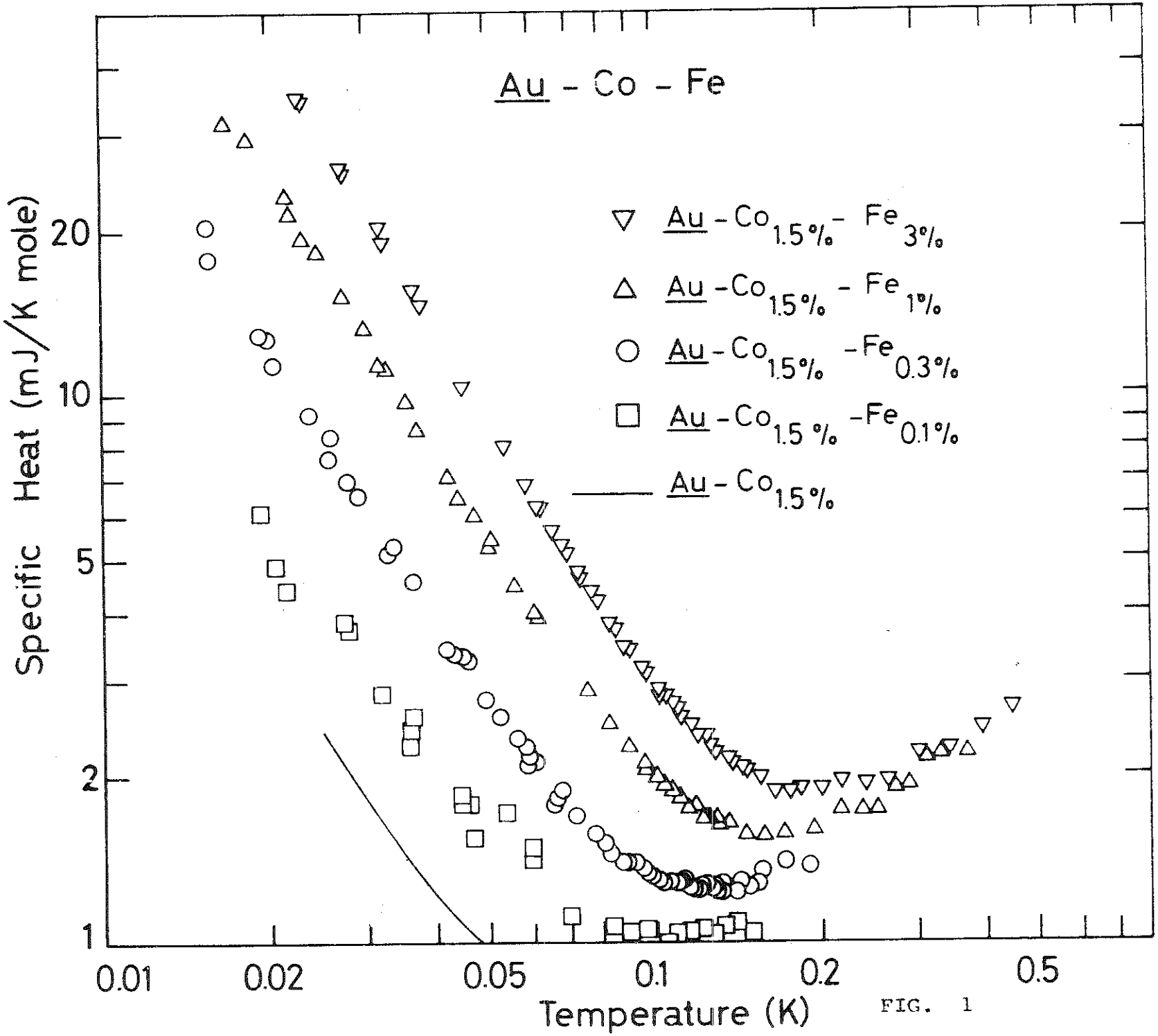
Au - Co - Fe
Au - Co1.5% - Fe3%
Au - Co1.5% - Fe1%
Au - Co1.5% - Fe0.3%
Au - Co1.5% - Fe0.1%
Au - Co1.5%
Specific Heat (mJ/K mole)
20
10
5
2
1
0.01
0.02
0.05
0.1
0.2
0.5
Temperature (K)

FIG. 1

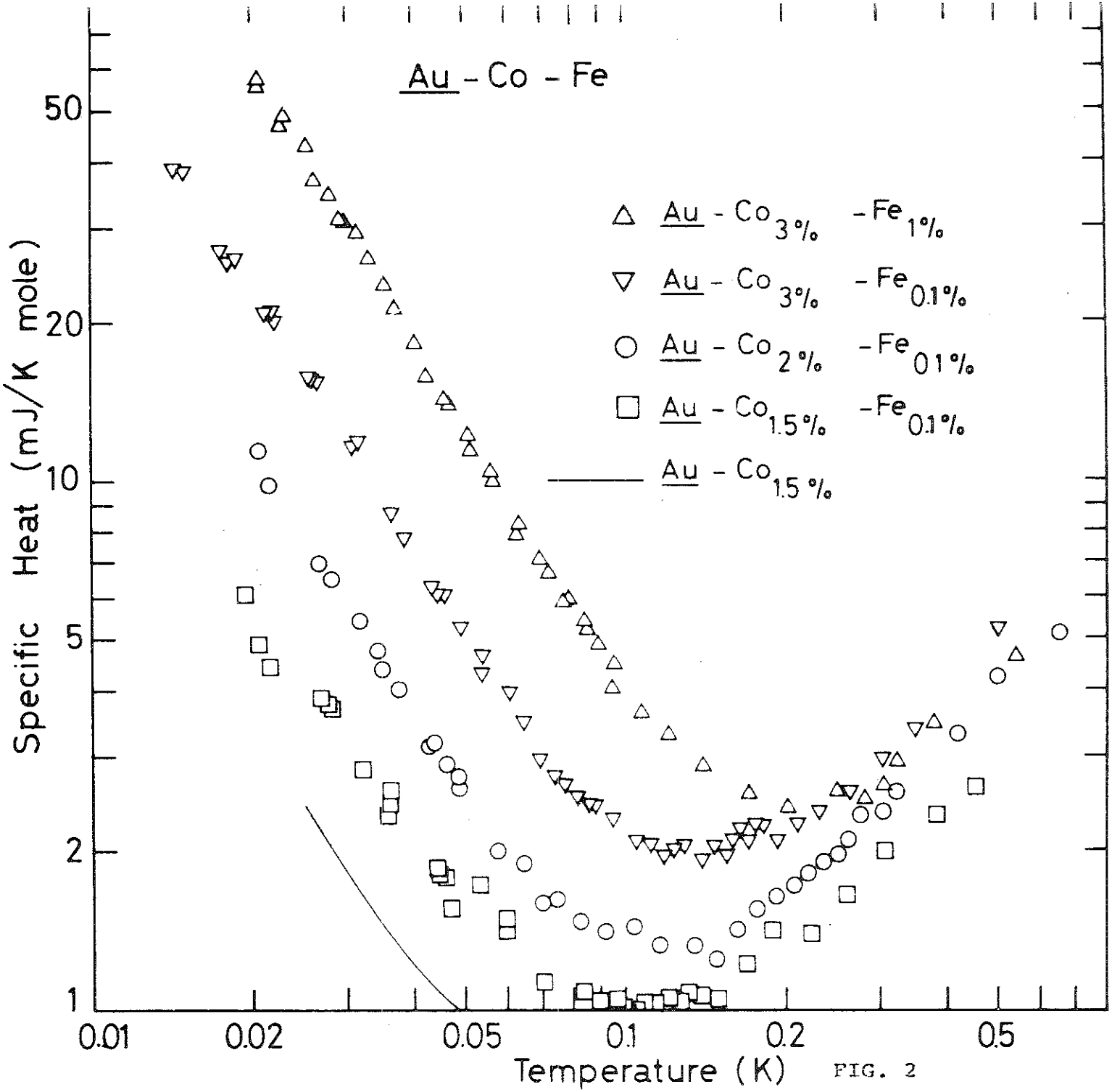
Au - Co - Fe
Au - Co 3% - Fe 1%
Au - Co 3% - Fe 0.1%
Au - Co 2% - Fe 0.1%
Au - Co 1.5% - Fe 0.1%
Au - Co 1.5 %
Specific Heat (mJ/K mole)
50
20
10
5
2
1
0.01
0.02
0.05
0.1
0.2
0.5
Temperature (K)

FIG. 2

due mainly to the Co atoms carrying a magnetic moment.

B - DETERMINATION OF A AND γ

A graphic of $CT^2(T^3)$ seems adequate to determine the coefficients A and γ for a specific heat of the form

$$C = \gamma T + A T^{-2} + \sum \varepsilon_n . T^{-n} \qquad (4)$$

when all the ε_n are negligible ; in our temperature range we see (fig. 3) that more than half the total number of experimental points deviate from the straight line $CT^2 = A + \gamma(T^3)$, thus underlining the relative importance of the higher order terms in the Schottky development below 0.1 K and affecting the accuracy of the determination of A and γ. We then adopted the following proceduce : a first determination of γ is made from the slope of a straight line fitting the points in a $CT^2(T^3)$ plot (fig. 3). Then $C - \gamma T$ is represented in a log-log plot (fig. 4 and 5) and A determined from the T^{-2} tangent on the high temperature side of this graphic. A new straight line is then drawn from this value of A (the intercept in fig. 3) through the high temperature experimental points in the $CT^2(T^3)$ plot, (fig. 3), and so on. A few iterations yield values for γ and A consistent in the two diagrams. These values are reported in table I, together with the corresponding data for the Au-Co system[1].

Although the intrinsic nuclear contribution of the magnetic impurities of Fe is negligible, there is a small nuclear contribution induced by the Fe atoms on the host ^{197}Au

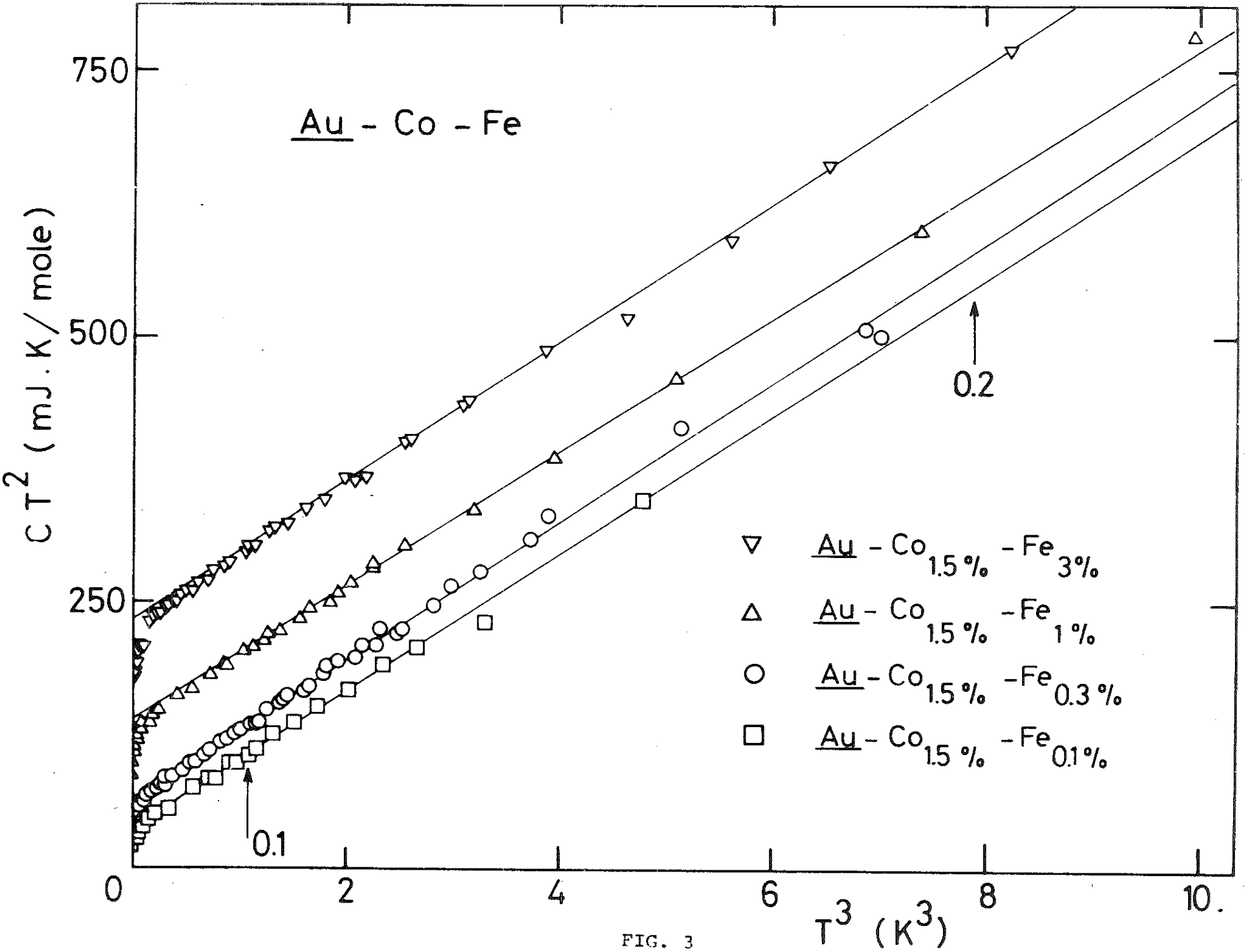
Au - Co - Fe
750
500
250
0
2
4
6
8
10.
$C T^2$ (mJ. K/ mole)
T^3 (K^3)
0.1
0.2
Au - $Co_{1.5\%}$ - $Fe_{3\%}$
Au - $Co_{1.5\%}$ - $Fe_{1\%}$
Au - $Co_{1.5\%}$ - $Fe_{0.3\%}$
Au - $Co_{1.5\%}$ - $Fe_{0.1\%}$

FIG. 3

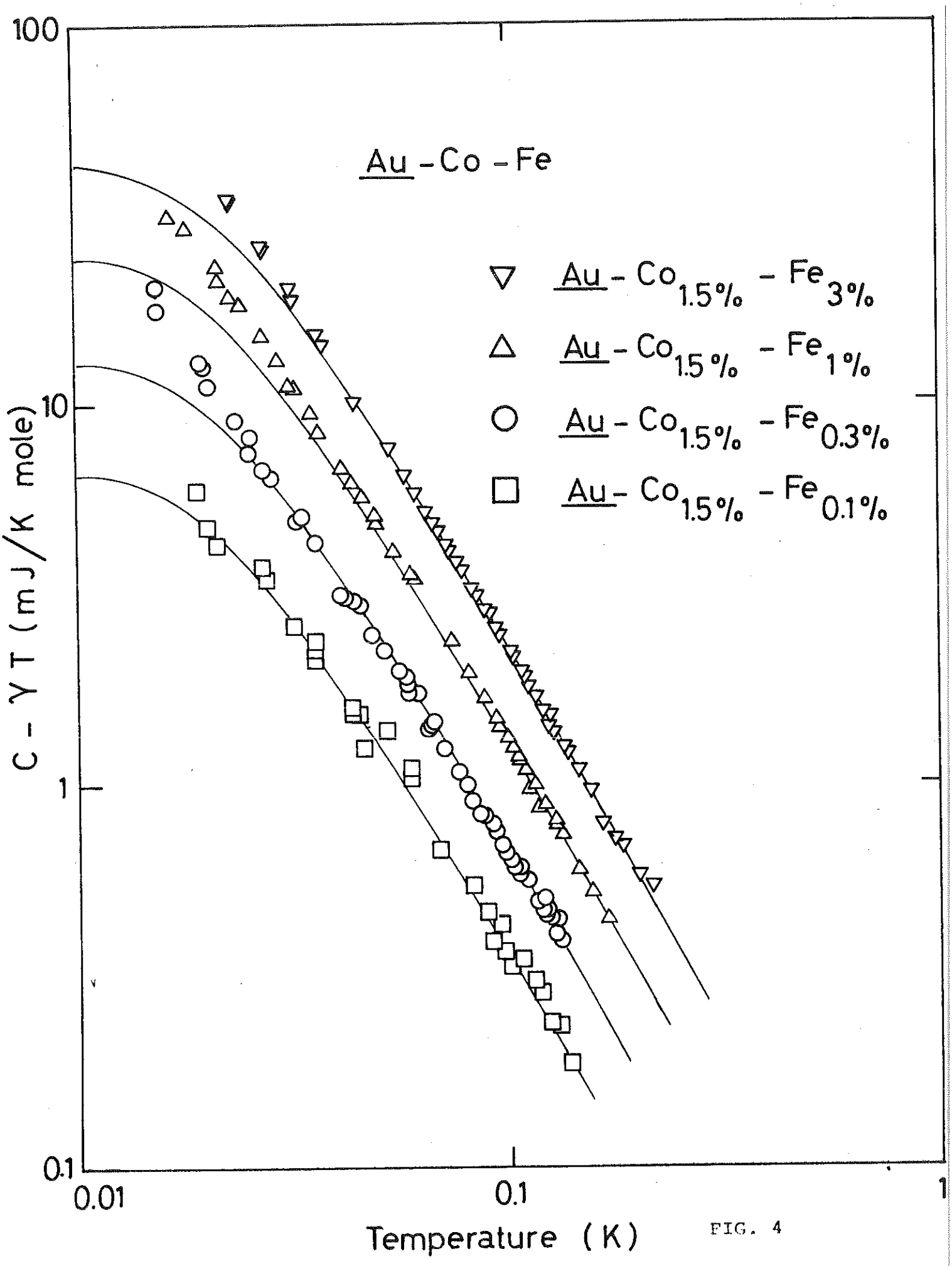
Au - Co - Fe
Au - Co 1.5% - Fe 3%
Au - Co 1.5% - Fe 1%
Au - Co 1.5% - Fe 0.3%
Au - Co 1.5% - Fe 0.1%
C - γT (mJ/K mole)
Temperature (K)
100
10
1
0.1
0.01
0.1
1

FIG. 4

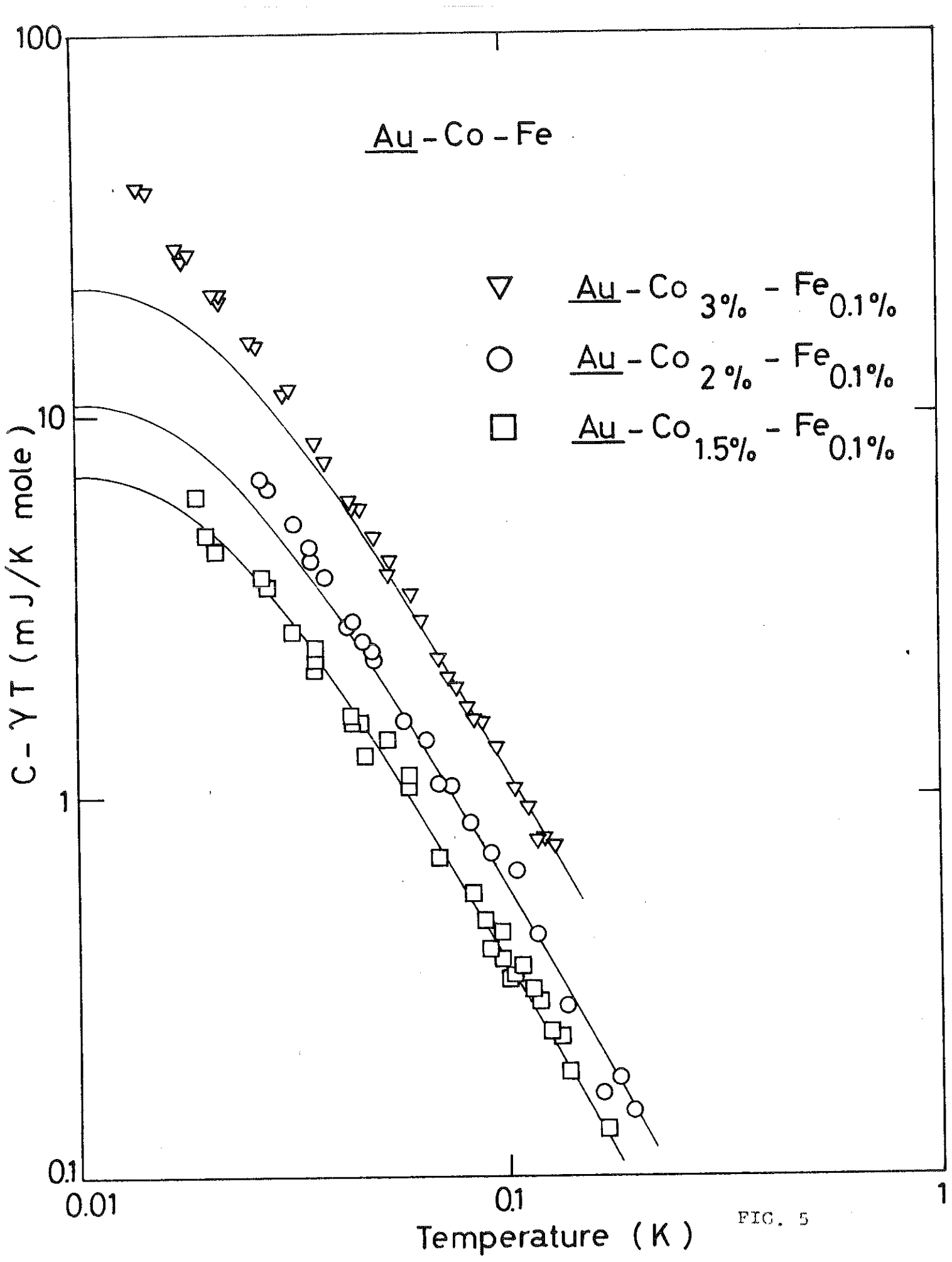
Au - Co - Fe
Au - Co 3% - Fe 0.1%
Au - Co 2% - Fe 0.1%
Au - Co 1.5% - Fe 0.1%
C - γT (m J / K mole)
Temperature (K)
100
10
1
0.1
0.01
0.1
1

FIG. 5

TABLE I

Alloy	γ (mJ/mole K^2)	A (μJ.K/mole)	$A_{exp} - A_{host}$ (μJ.K/mole)
$Au-Co_{1,5\%}$	7.9	1.5	
$Au-Co_{2\%}$	7.7	3.4	
$Au-Co_{3\%}$	10.8	11.0	
$Au-Co_{4\%}$	10.7	23.4	
$Au-Co_{6\%}$	13.5	82.3	
$Au-Co_{1.5\%}-Fe_{0.1\%}$	6.5	3.7	3.5
$Au-Co_{1.5\%}-Fe_{0.3\%}$	6.5	6.3	6.0
$Au-Co_{1.5\%}-Fe_{1\%}$	6.3	13.5	12.5
$Au-Co_{1.5\%}-Fe_{3\%}$	6.6	23.6	20.6
$Au-Fe_{0.1\%}-Co_{1.5\%}$	6.5	3.7	3.6
$Au-Fe_{0.1\%}-Co_{2\%}$	7.7	5.5	5.4
$Au-Fe_{0.1\%}-Co_{3\%}$	10	11.5	11.4
$Au-Co_{3\%}-Fe_{1\%}$	8.5	33.0	32.0

nuclei via the conduction electrons ; this host contribution amounts to about 1 μJ/mole per at. % Fe[24] and has been substracted in table 1 ($\Delta_{exp} - \Delta_{host}$).

C - QUALITATIVE CONCLUSIONS

The addition of Fe results (fig. 1 and table 1) in a very large increase of the nuclear specific heat ; for example 3 at % of Fe atoms increase the coefficient A of the Au-Co 1.5 at % Co sample by a factor 14. This has the following important implications :

1°) There are large interactions between the impurities of Cobalt and Iron in gold, since the total nuclear specific heat of Au-Co-Fe is far from being just the sum of Au-Co plus Au-Fe contributions.

2°) It is shown that only a small amount of the Co was magnetic in pure Au-Co, in agreement with our model where the magnetic impurities are those belonging to the groups of 3 or more Co atoms. Indeed, the nuclear specific being mainly sensitive to the Co nuclei contribution acts as a probe for the electronic magnetism of those Co atoms ; due to the interactions with the iron atoms a large fraction of Co impurities, that does not contribute to the nuclear specific heat in Au-Co alloys is now polarized and sensing hyperfine fields.

As shown in fig. 4 and 5, the experimental points for a given sample are not described by a single nuclear magnetic Schottky curve. The low temperature points are situated above the Schottky curve (corresponding to the Co hyperfine field of 190 kOe) that fits the high temperature points. This means that there are Co nuclei with hyperfine fields which values are less than 190 kOe, suggesting the existence of a distribution of hyperfine fields and moments on the cobalt atoms.

SUSCEPTIBILITY MEASUREMENTS

A - RESULTS

We have reported in fig. 6 the magnetic susceptibility versus temperature for the Au-$Co_{1.5\ \%}$-$Fe_{1\ \%}$ and Au-$Co_{3\ \%}$-$Fe_{1\ \%}$ samples. Also shown are the curves corresponding to the susceptibility of the binary alloys[25][26] : Au-$Fe_{1\ \%}$, Au-$Co_{1.5\ \%}$ and Au-$Co_{3\ \%}$.

The temperature of the maximum (T_{max}) of the two Au-Co-Fe samples containing 1 at % Fe is within the experimental error, the same than that observed for the pure Au-$Fe_{1\ \%}$. The same thing is true for the two other samples measured (not reported in fig. 6), Au-$Co_{1.5}$-$Fe_{3\ \%}$ and Au-$Co_{1.5}$-$Fe_{0.3}$, where the T_{max} are respectively around 16 and 3.5 K, in good agreement with the general feature of the concentration dependence of T_{max} in the Au-Fe system, as shown in fig. 7.

B - ANALYSIS OF THE RESULTS

The susceptibility of the Au-Co-Fe is obviously not the simple addition of those the corresponding Au-Co and Au-Fe alloys (see fig. 6). This implies the existence of interactions between Fe and Co impurities in Au and confirms that the detection of hyperfine fields on Co nuclei are really correlated to the electronic moments on Co atoms (such would be not the case if K_S was not negligible). The similarity between $\chi_{Au\text{-}Co\text{-}Fe_x}$ and $\chi_{Au\text{-}Fe_x}$ is not only in the observation of the same T_{max}. Indeed, the excess susceptibility $\Delta\chi = \chi_{Au\text{-}Co\text{-}Fe} - \chi_{Au\text{-}Co}$ produced by the addition of Fe in the Au-Co sample is found to be proportional to $\chi_{Au\text{-}Fe}$ around T_{max}, as may be seen in fig. 8 where we reported

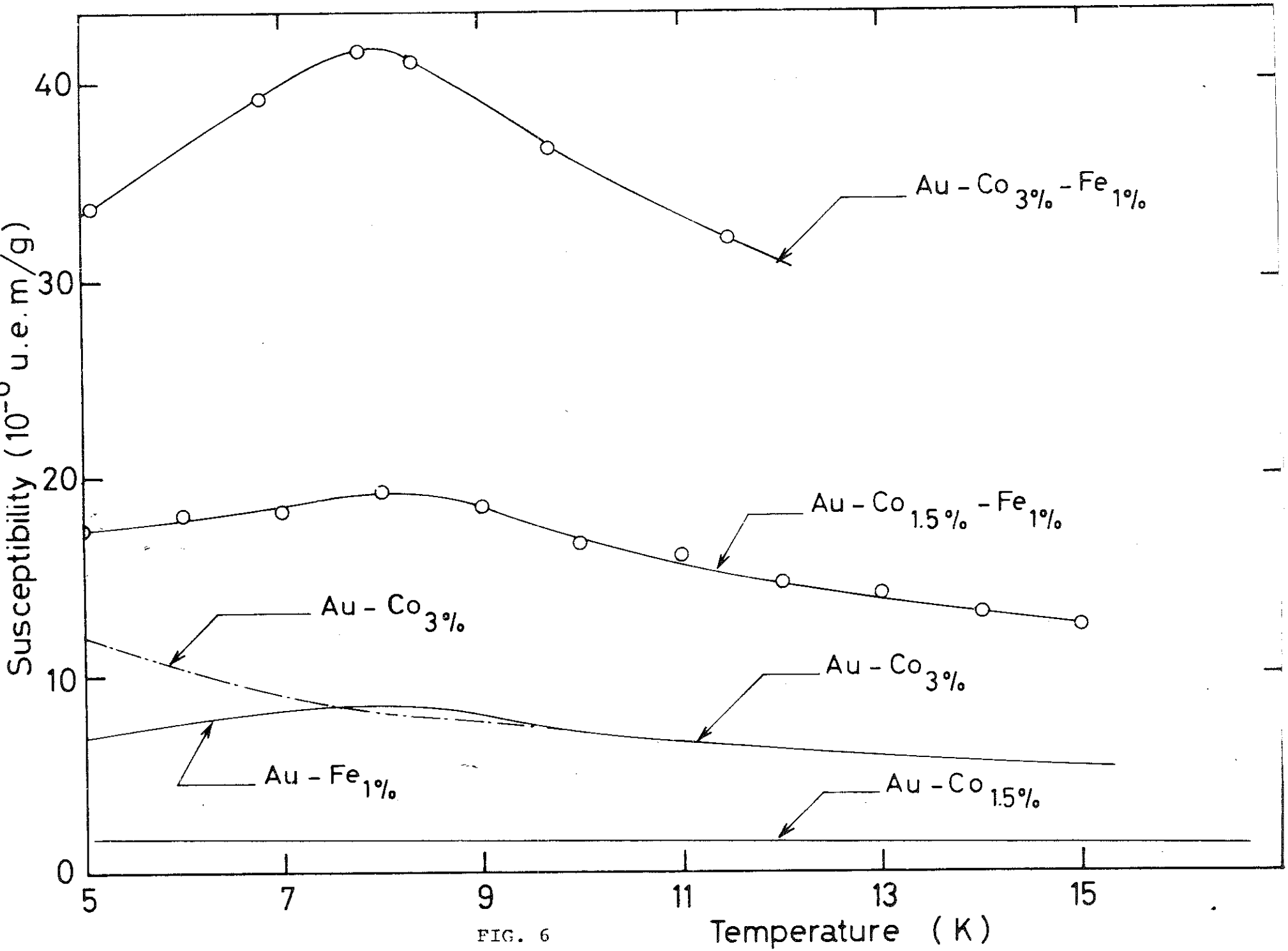
Susceptibility (10^{-6} u.e.m/g)
40
30
20
10
0
5
7
9
11
13
15
Temperature (K)
Au - Co 3% - Fe 1%
Au - Co 1.5% - Fe 1%
Au - Co 3%
Au - Co 3%
Au - Fe 1%
Au - Co 1.5%

FIG. 6

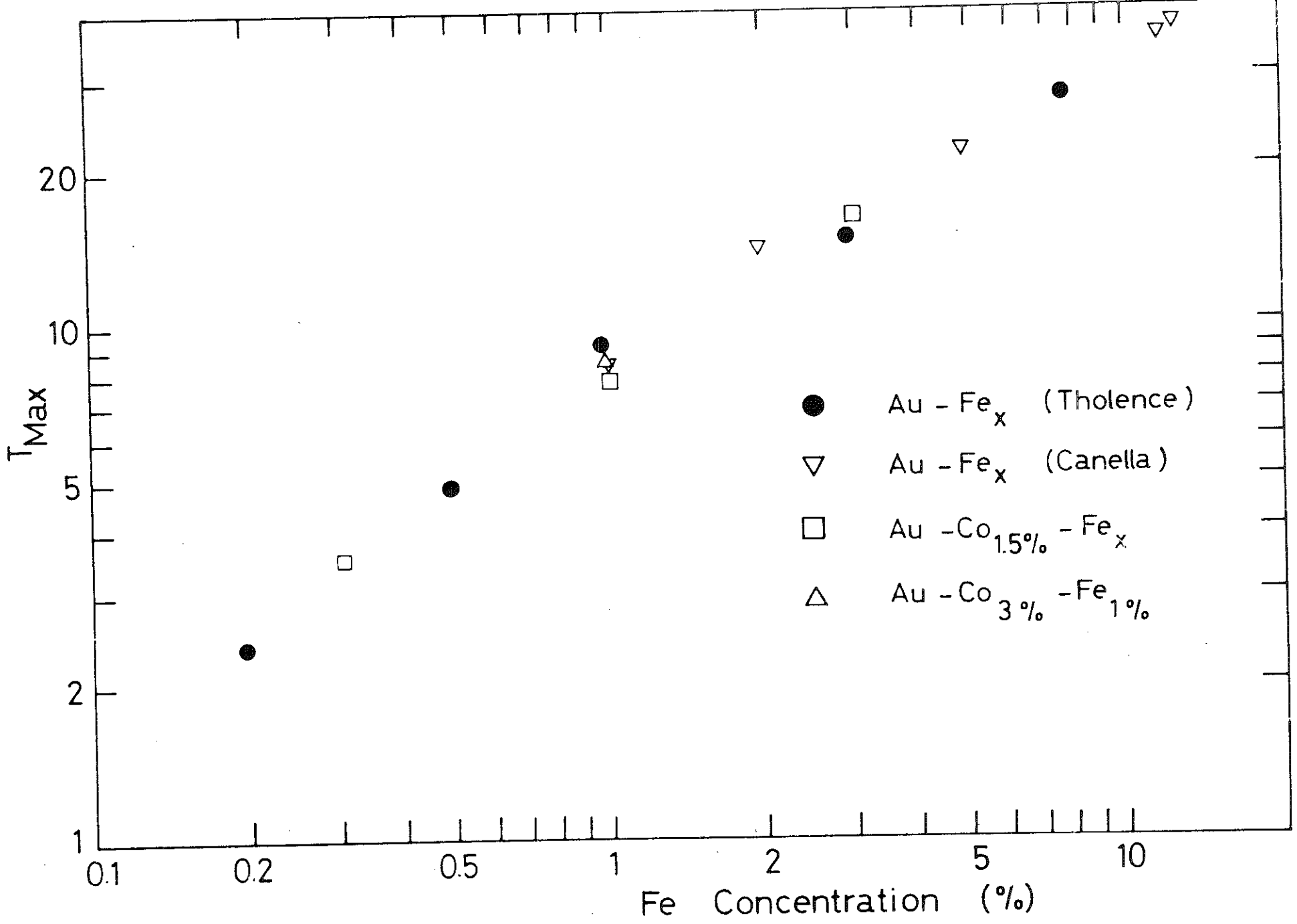
20
10
5
2
1
T_{Max}
0.1
0.2
0.5
1
2
5
10
Fe Concentration (%)
Au - Fe_x (Tholence)
Au - Fe_x (Canella)
Au - $Co_{1.5\%}$ - Fe_x
Au - $Co_{3\%}$ - $Fe_{1\%}$

FIG. 7

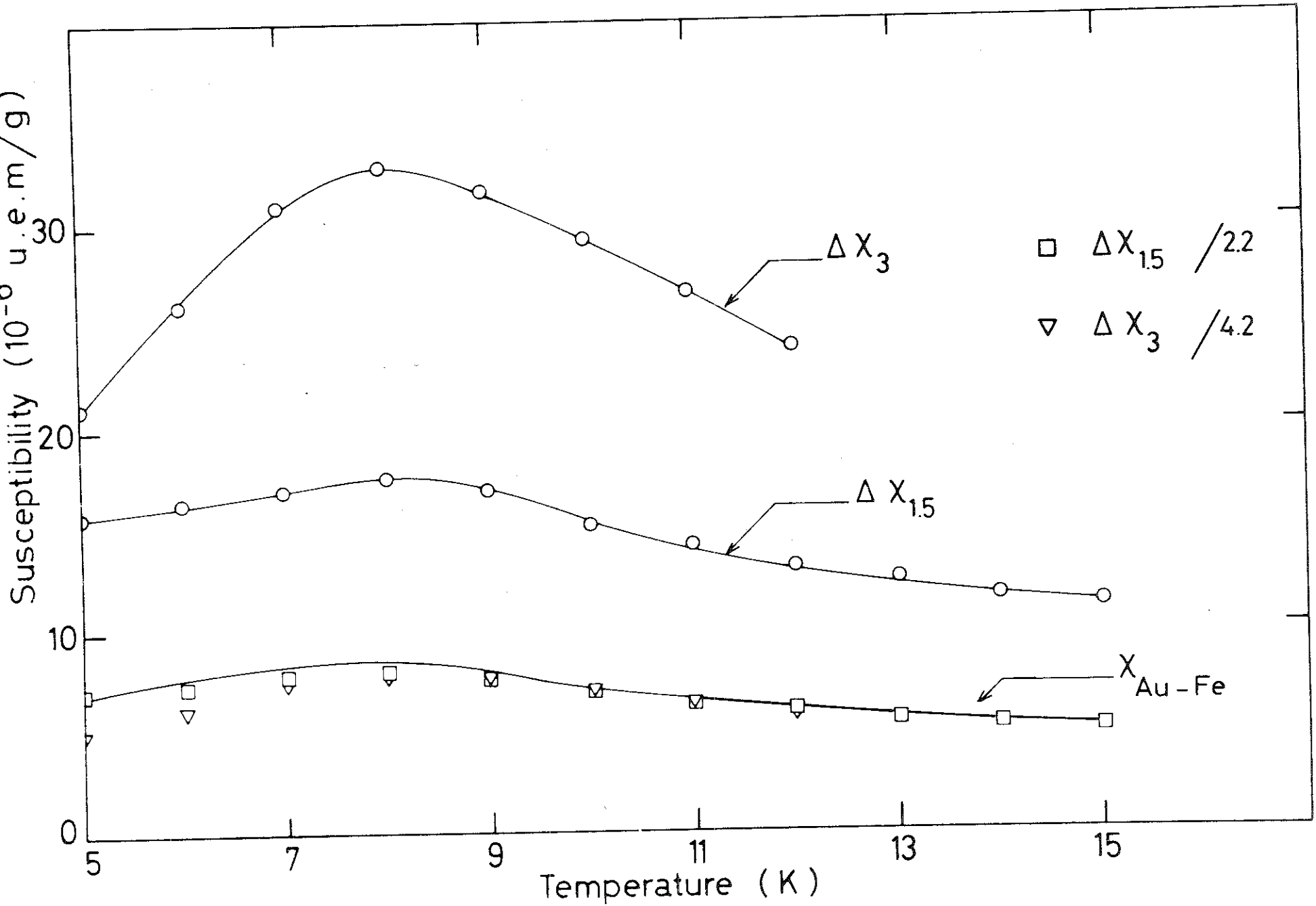
Susceptibility (10^{-6} u.e.m/g)
30
20
10
0
5
7
9
11
13
15
Temperature (K)
ΔX_3
$\Delta X_{1.5}$
$\Delta X_{1.5}$ /2.2
ΔX_3 /4.2
X_{Au-Fe}

FIG. 8

$\Delta\chi_3 = \chi_{\underline{Au}\text{-}Co_{3\,\%}\text{-}Fe_{1\,\%}} - \chi_{\underline{Au}\text{-}Co_{3\,\%}}$ and $\Delta\chi_{1.5} = \chi_{\underline{Au}\text{-}Co_{1.5\,\%}\text{-}Fe_{1\,\%}} - \chi_{\underline{Au}\text{-}Co_{1.5\,\%}}$: the points obtained by dividing $\Delta\chi_3$ and $\Delta\chi_{1.5}$ by the factors 4.2 and 2.2 respectively are roughly confounded with $\chi_{\underline{Au}\text{-}Fe_{1\,\%}}$. In other words, within a factor, the excess susceptibility $\Delta\chi$ may be described by the same law followed by $\chi_{\underline{Au}\text{-}Fe}$.

Now, using a "mean-random molecular field approximation", Klein[27] obtain an expression for the high temperature susceptibility of dilute alloys valid between T_{max} and $2T_{max}$, that seems to be verified by different systems including Au-Fe :

$$\chi(T) = \frac{N \cdot c \cdot P_{eff}^2 \cdot \mu_B}{3k(T-\theta)} \left[1 - \left(\frac{2}{\pi}\right)^3 \frac{\Delta}{kT} \right] \qquad (5)$$

Here the symbols have their usual meaning, 0 comes from the mesured high temperature susceptibility $\chi \alpha (T - 0)^{-1}$ of the alloy, and Δ gives the width in energy of the lorentzian function obtained in this model for the probability distribution of molecular field.

Then if (5) describes $\chi_{\underline{Au}\text{-}Fe}$, it will also describe $\Delta\chi$, but with a different value of p_{eff}^2 depending on the Co concentration. The addition of Co in Au-Fe alloy results then in an increase of the apparent moment of each Fe atom which is now "dressed" with all the moments induced on the Co atoms of the vicinity. But according to the above model $\Delta/k\ T_{max}$ is independent of the moment carried by the impurity, and amounts to 2.5, as is well verified experimentaly[27]. It follows that we may characterize the molecular field distribution created by the Fe in the Au-Co matrix by the same lorentzian function used to describe this molecular field in Au-Fe. A quantitative interpretation for the nuclear specific heat is now possible, using a simplified model to characterize the response of the non magnetic Co atoms.

ANALYSIS OF THE SPECIFIC HEAT RESULTS

The distribution P(H) of molecular field created by the iron atoms produces a distribution of induced moments on the pairs and the isolated Co atoms, and a corresponding distribution of hyperfine fields. However, according to magnetization measurements of Au-Co alloys[2], the pairs of Co atoms respond to an external field with a susceptibility χ_2 much larger than the susceptibility χ_1 of isolated Co. It is then expected that the moments induced on the pairs and isolated Co atoms will be different for the same value of the molecular field.

The coefficient A of the T^{-2} term will be the result of three contributions :

1°) The contribution of the atoms belonging to groups of at least three Co neighbours. They are magnetic and contribute with the same saturated hyperfine field H_{eff_o} = 190 kOe. They are responsible for the value of A in the pure Au-Co alloy which has been yet measured[1]. The value of H_{eff_o} have been deduced from the expression :

$$A_3 = \chi_3 R \frac{I(I+1)}{3} \gamma^2 \hbar^2 H_{eff_o}^2 / k^2 \qquad (6)$$

where I and γ are the nuclear spin and gyromagnetic ratio, χ_3 is the concentration of group of at least three Co neighbours given in fonction of the total concentration c by :

$$\chi_3 = c\left[1 - (1-c)^{12} - 12c(1-c)^{18}\right]$$

and the other constants have their usual meaning.

2°) The contribution of the atoms belonging to pairs of Co, in concentration $X_2 = 12\ c^2\ (1 - c)^{18}$. They are polarized and their nuclei experience a distribution of hyperfine fields H_{eff} ranging from zero to the saturation value of 190 kOe.

3°) The contribution of the isolated Co atoms, in concentration $X_1 = c(1 - c)^{12}$. They also probe a distribution of H_{eff} of the same nature but where a molecular field larger will be needed to produce the same effect as for the pairs.

The total predicted value of A will then be

$$A = A_3 + \frac{A_3}{X_3}\left[\alpha_1 X_1 + \alpha_2 X_2\right] \qquad (7)$$

where A_3/X_3 gives the contribution to A per magnetic impurity having the saturated value of the hyperfine field and α_1 and α_2, are the mean value of the square of the hyperfine field H_{eff} divided by the saturation value H_{eff_o}, for isolated and pairs of Co atoms :

$$\alpha_i = \frac{\overline{H^2_{eff_i}}}{H^2_{eff_o}} \qquad (8)$$

As far as hyperfine fields are concerned, the important parameter to know in order to characterize the response of the Co nuclei is not the magnetic susceptibility determined in ref. 2 but the knight shift K_1 and K_2 of isolated and paired atoms. The coupling between the conduction electrons and the impurities described by the molecular field is of the type $J.\vec{S}.\vec{s}$, and assuming no spin-orbit term, involves only the spin part of the impurity susceptibility. Then, just the value of K_d is concerned here. The pairs and isolated Co response to the same molecular field will then differ by the factor :

$$K_2/K_{d_1} = \chi_2/\chi_{d_1} = 14$$

The polarization of a non magnetic impurity ($T << T_K$) by an external field H is a linear function of this field for the low values and approaches the saturation for $H \sim H_K \sim T_K$ with a value close to that of the moment carried by the impurity for $T >> T_K$ or when the moment is restituted by interaction[28]. For simplicity we will assume that the K_i values (d knight shift of isolated Co or knight shift of pairs) remain constant up to the molecular field H_{Ki}, for which the moment and the consequent hyperfine field attain their saturated value H_{eff_o}. With this assumption and using the lorentzian molecular field distribution P(H) created by the iron impurities:

$$\alpha_i = \frac{2}{H_{eff_o}^2} \int_0^{H_{K_i}} K_i^2 \cdot H^2 \, P(H) \, dH + 2 \int_{H_{K_i}}^{\infty} P(H) \cdot dH \qquad (9)$$

with $P(H) = \frac{\Delta}{\Delta^2 + H^2}$

and $\Delta \sim 2.5 \times T_{MAX}$ as given by Klein's model

Calling $x_i = \Delta / H_{K_i}$

$$\alpha_i = 1 + 2/\pi \left\{ x_i - [x_i^2 + 1] \, tg^{-1} 1/x_i \right\} \qquad (10)$$

Since $K_2/K_{d_1} = 14$, the expresion (4), may be written as a function of an unique parameter Δ/H_{K_2} or $2.5 \times T_{max}/T_{K_2}$.

Fig. 9, shows the experimental results for A and the three curves determined with the above crude model for 3 distinct values of T_{K_2}. The best value for T_{K_2}, with $T_{max} = 8$ K per % Fe (fig. 7), is obtained for $T_{K_2} = 14$ K and consequently $T_{K_1} = 200$ K in very good agreement with the T_K values determined from the susceptibility. Using these values of T_{K_2}, a good fit is also observed for the second series of samples containing 0.1 at % Fe and the sample with 3 at % and 1 at % Fe, as shown in fig. 10.

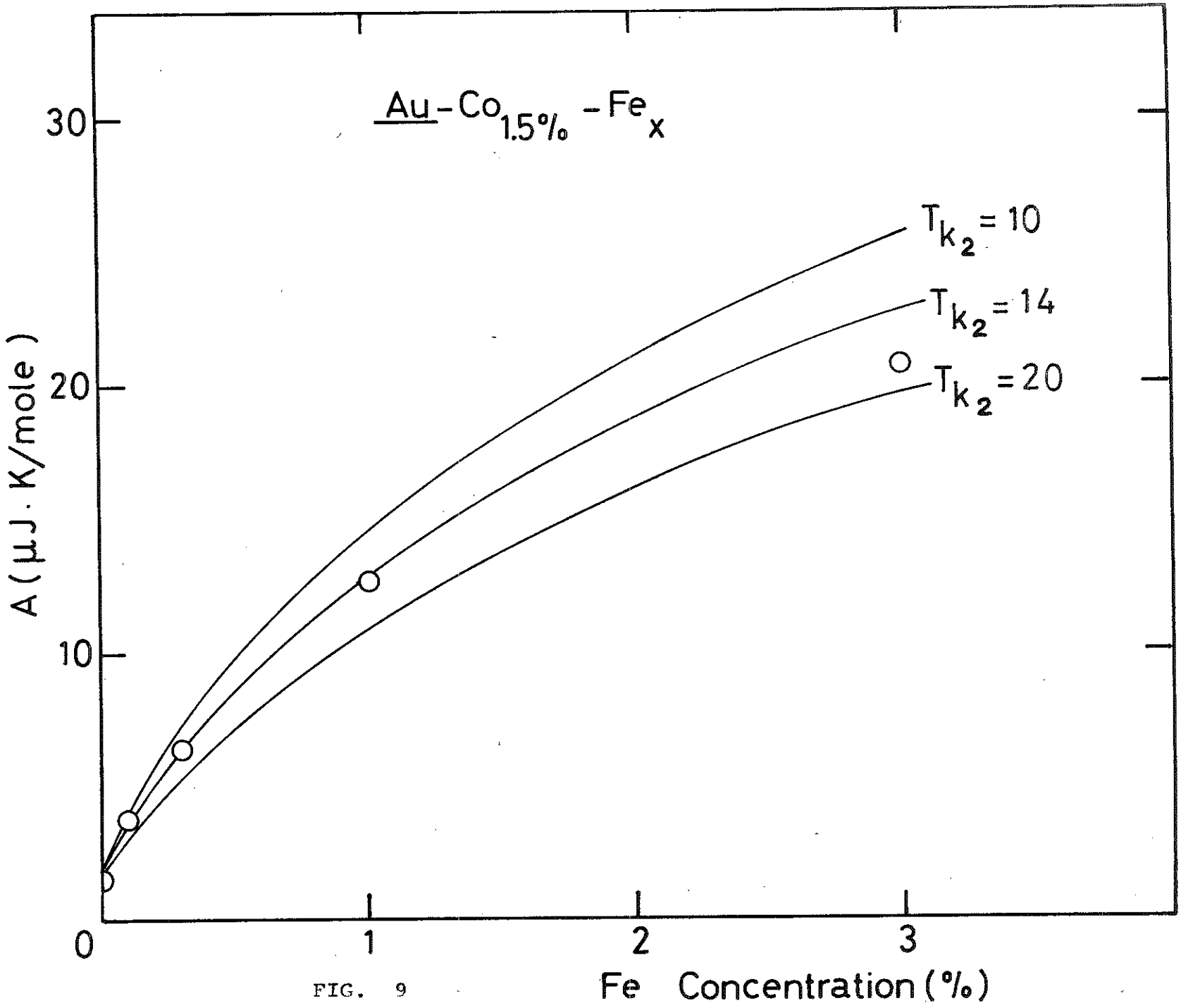
Au - Co1.5% - Fex
30
20
10
0
A (μJ. K/mole)
Tk2 = 10
Tk2 = 14
Tk2 = 20
1
2
3
Fe Concentration (%)

FIG. 9

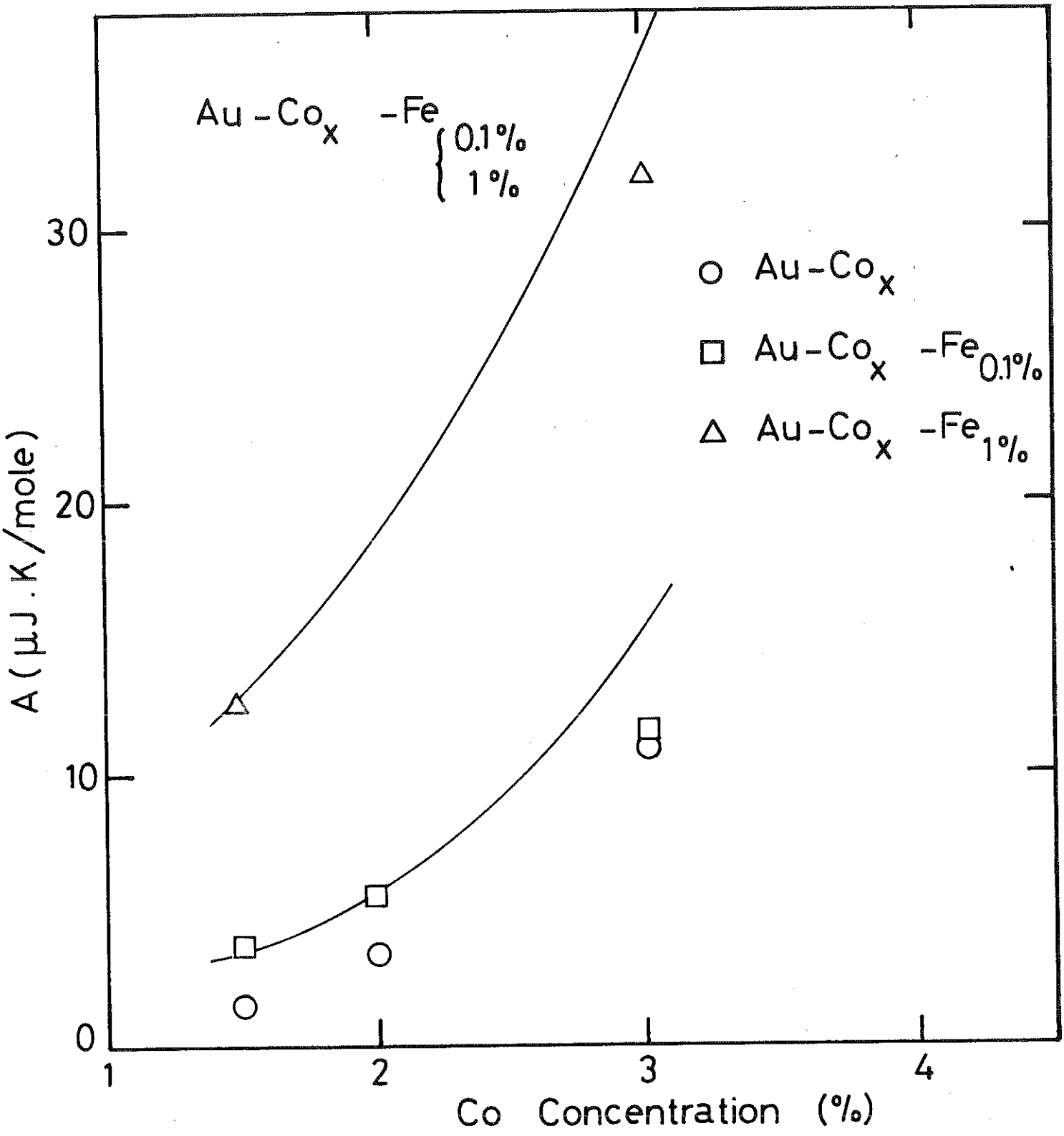
Au - Co$_x$ - Fe { 0.1% 1%
Au - Co$_x$
Au - Co$_x$ - Fe$_{0.1\%}$
Au - Co$_x$ - Fe$_{1\%}$
A (μJ . K / mole)
30
20
10
0
1
2
3
4
Co Concentration (%)

FIG. 10

In spite of the crudeness of the model, the above results enable to confirm not only the existence of both configurations of isolated and pairs of Cobalt, but also the good choice of 240 and 16 K for the corresponding values of T_{K_S}, as determined by the susceptibility measurements.

CONCLUSION

The introduction of magnetic Fe impurities in Au-Co increases largely the nuclear contribution of the Co atoms to the specific heat, evidencing the existence of a large fraction of non magnetic atoms in Au-Co that becomes polarized by the Fe impurities. This is in qualitative agreement with the model proposed to explain previous results on Au-Co system, where at low temperatures the magnetic atoms are only the small fraction belonging to groups of at least three Co neighbours.

The Au-Co-Fe nuclear specific heat are not described by a single Schottky anomaly ; this suggests that the polarized Co atoms carry distribution moments ranging from zero to the saturation value, corresponding to the hyperfine field of 190 kOe. The susceptibility results confirms this analysis, showing that the magnetic Fe atoms are "dressed" by polarized neighbouring Co atoms.

A simplified assumption for the response of pairs and isolated Co atoms to the molecular field created by the Fe atoms, enable to describes reasonably well the measured concentration dependence of the nuclear specific heat coefficient A for the seven Au-Co-Fe samples containing different amounts of Fe and Co. Values of 14 and 200 K are then found for the T_K of pairs and isolated Co, in good agreement with the susceptibility results of Au-Co.

The lack of agreement between the values of T_K for isolated and paired Co atoms deduced from the susceptibility and specific heat results using the formulas given by the LSF theory makes questionable the application of this theory to Au-Co system, as have been also suggested by Narath.

A K N O W L E D G M E N T S

We thank B. PICOT and J. PILON for their assistance in performing experiments and the metallurgical group of the laboratory for the preparation of the samples.

-- FIGURE CAPTIONS --

-:-:-:-:-:-:-:-:-

Figure 1 - The specific heat of 4 samples containing the same amount of Co (1.5 at.%), as measured between 0.02 and 0.5K. The continuous line represent the result of pure $Au\text{-}Co_{1.5\%}$ sample.

Figure 2 - The specific heat of 3 samples containing the same amount of Fe (0.1 at.%) and a concentrated $Au\text{-}Co_{3\%}\text{-}Fe_{1\%}$ alloy.

Figure 3 - The product CT^2 of the measured specific heat by the square of the temperature as a function of T^3 below 0.2K for 4 samples.

Figures 4 and 5 - The nuclear anomalies versus temperature for the samples appearing in figures 1 and 2. The term linear in temperature have been substracted from the total specific heat. The full lines represent the calculated Co nuclear Schottky anomalies with H_{eff}=190KOe.

Figure 6 - The susceptibility versus temperature for two Au-Co-Fe samples with the same iron content. Also shown are the susceptibility of the bynary alloys of Au-Co and Au-Fe obtained in references 25 and 26.

Figure 7 - The temperature T_{Max} of the maximum of the thermal variation of the susceptibility obtaine for the four Au-Co-Fe samples measured. Also shown the T_{Max} for pure Au-Fe in ref.25.

Figure 8 - The excess susceptibility $\Delta\chi$ of $\underline{Au}$-Co_x-$Fe_{1\%}$ above that of pure $\underline{Au}$-Co_x. The squares and triangles show this excess susceptibility divided by factors (2.2 and 4.2). The susceptibility of $\underline{Au}$-$Fe_{1\%}$ of ref. 25 is represented in the lower part of the diagram.

Figure 9 - The coefficient A of the $1/T^2$ term of the nuclear Schottky anomaly as a function of the iron concentration for 5 samples containing 1.5 at% Co. The continuous lines are the calculated dependence of A for three different values of T_{K2}.

Figure 10 -The coefficient A as a function of the Cobalt concentration for 5 samples containing two different amounts of Fe (squares and triangles). The values for pure $\underline{Au}$-Co are also shown (circles). The full lines represent the calculated dependence of A using $T_{K_2}=14K$.

--- R E F E R E N C E S ---

-:-:-:-:-:-:-:-:-

(1) P. COSTA-RIBEIRO, J. SOULETIE and D. THOULOUZE, Phys. Rev. Letters 24, 900 (1970)

(2) E. BOUCAI et al. Phys. Rev. B3, 3834 (1971)

(3) G.J. VAN DER BERG, J. VAN HERK, and B. KNOOK, Proc. 10th Int. Conf. Low Temp. Phys. p.272

(4) L.T. CRANE, Phys. Rev. 125, 1902 (1962)

(5) J. Le GUILLERM, R. TOURNIER and L. WEIL, Proc. 8th Int. Conf. Low Temp. Phys. p.236

(6) An error in the determination of T_K have been made in Ref. 2 from the experimental result reported there for the susceptibility of pairs and isolated impurities.

(7) R.J. HOLLIDAY and W. WEYHMANN, Phys. Rev. Letters, 25, 243 (1970)

(8) S. WADA and K. ASAYAMA, J. Phys. Soc. Japan 30, 1337 (1971)

(9) A. NARATH and D.C. BARHAM, to appear in Phys. Rev. B.

(10) A.J. FREEMAN and R.E. WATSON, in Magnetism, Vol.IIA, edited by G.T. Rado and H.Suhl (Academic Press Inc, N.Y. 1965)

(11) Such a separation between K_{orb} and K_d have been done recently by J. BOYSEN, W.D. BREWER and J. FLOUQUET (to appear). The desagreement between our results come from 6.

(12) B. CAROLI, P. LEDERER and D. SAINT-JAMES, Phys. Rev. Letters 21, 904 (1968)

(13) L. DWORIN and A. NARATH, Phys. Rev. Letters 25, 1287 (1970)

(14) P. COSTA RIBEIRO, J. SOULETIE, D. THOULOUZE and R. TOURNIER Suppl. J. Physique 32, C1 - 753 (1971)

(15) B. WINDOW, J. Phys. C.3, 922 (1970)

(16) T. MORYA, Proceeding of International School of Physics Enrico Fermi Course 37, Academic Press (1968)

(17) B. WINDOW et al, J. Phys. C. 2, 5218 (1970)

(18) J.L. THOLENCE, B. TISSIER, R. TOURNIER and R. VERGNE Solid State Comm. 8, 201 (1970)

(19) R. TOURNIER and A. BLANDIN, Phys. Rev. Letters 24, 397 (1970)

(20) S. ODA and K. ASAYAMA, to appear

(21) J.R.G. KEYSTON, A. LACAZE and D. THOULOUZE, Cryogen. 8, 295 (1968)

(22) P. COSTA RIBEIRO, B. PICOT, J. SOULETIE and D. THOULOUZE, to appear.

(23) J.A. CAREAGA et al, Proc. 10th Int. Conf. Low Temp. Phys. (1966)

(24) B. DREYFUS, J.C. MICHEL and D. THOULOUZE, J. Applied Phys. 39, 1320 (1968)

(25) J. THOLENCE and R. TOURNIER, to appear
V. CANNELA and J.A. MYDOSH, Phys. Rev. B., 6, 4220 (1972)

(26) B. LECOANET, thesis Université de Grenoble (1971)

(27) M.W. KLEIN, L. SHEN, Phys. Rev. B 5, 1174 (1972)

(28) J.C. GALLOP, thesis, Oxford Clarendon (1969).

ABSENCE D'EFFET DES INTERACTIONS IMPORTANTES ENTRE Co ET Ni DANS L'Au

La température caractéristique de la paire de Co dans l'Au ayant été évaluée à 50K ou 16K, selon que l'on considère les mesures de chaleur spécifique ou de susceptibilité magnétique, on pourrait s'attendre à ce que la présence d'une ou plusieurs impuretés de Ni près d'une paire de Co puisse permettre à cette dernière de remplir le critère de Stoner et devenir magnétique. En effet, d'après MORYA, le terme de mélange H_{d-d} entre les électrons d d'un site de Co et deux d'un site voisin de Ni pourrait faciliter l'apparition d'un moment magnétique sur le Cobalt même si le Ni n'est pas magnétique dans l'Au (pour l'Au-Ni $T_K \sim 10^3$K). En supposant que la présence d'un ou 2 atomes de Ni proches voisins de la paire de Co la rendrait magnétique, un simple calcul de probabilité montre que le coefficient A de la chaleur spécifique nucléaire d'un alliage Au-$Co_{1,5\%}$ serait multiplié par 3 ou 2 avec 5% de Ni.

Un échantillon d'Au-$Co_{1,5\%}$-$Ni_{5\%}$ et un autre d'Au-$Ni_{5\%}$ ont été préparés par le groupe de Métallurgie du laboratoire, à partir de l'Au, Ni et Fe 99,999% dans un four à induction.

L'Au-Ni présente une remontée hyperfine dont l'amplitude correspond bien à la contribution quadrupolaire électrique induite sur les noyaux d'or par les impuretés de Nickel (A=0.8 µJ.K/mole). L'Au-$Co_{1,5\%}$-$Ni_{5\%}$ présente une contribution nucléaire plus importante, mais à l'erreur expérimentale près, la chaleur spécifique de l'Au-$Co_{1,5}$-$Ni_{5\%}$ est la simple

addition de celle mesurée pour l'Au-$Ni_{5\%}$ et Au-$Co_{1,5\%}$ (courbe continue sur la figure). Aucun effet d'interaction sur l'apparition d'un moment nucléaire sur les atomes de Co n'a donc été observé.

La limitation dans la précision de nos estimations de la valeur de γ, nous empêche de détecter un éventuel changement des T_K de certaines paires de Co. Nous pouvons néanmoins affirmer que le nombre d'impuretés magnétiques dans l'Au-Co n'a pas changé avec l'introduction de 5% de Ni, contrairement à ce qui pourrait être déduit du modèle de MORYA.

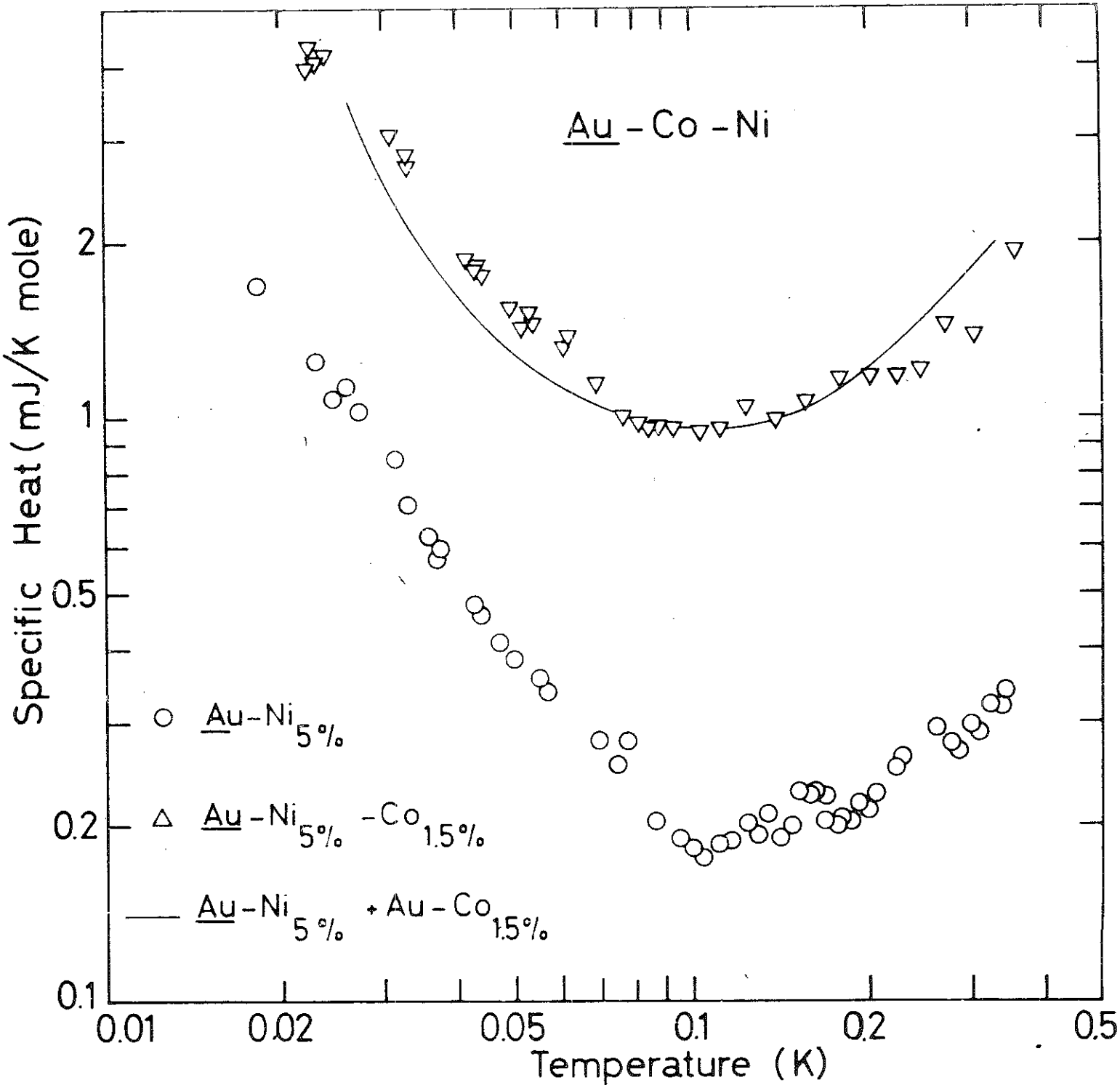
Au - Co - Ni
Specific Heat (mJ/K mole)
2
1
0.5
0.2
0.1
0.01
0.02
0.05
0.1
0.2
0.5
Temperature (K)
Au-Ni 5%
Au-Ni 5% -Co 1.5%
Au-Ni 5% + Au-Co 1.5%

C H A P I T R E V

ALLIAGES AVEC $10^{-2} < T_K < 1$ K : Pt-Co et Zn-Mn

A - ANOMALIE ASSOCIEE A L'EFFET A UNE IMPURETE ET MAGNETISME RESIDUEL DANS LES ALLIAGES DILUES DE Pt-Co.

(à paraître)

B - EFFET DES INTERACTIONS DANS LE Zn-Mn ET VALEUR DU CHAMP HYPERFIN SUR LE Mn.

ONE IMPURITY EFFECT ANOMALY AND RESIDUAL MAGNETISM IN DILUTE Pt-Co ALLOYS BY SPECIFIC HEAT MEASUREMENTS

P. COSTA RIBEIRO †‡, M. SAINT-PAUL ‡, D. THOULOUZE and R.TOURNIER

Centre de Recherches sur les Très Basses Températures
Centre National de la Recherche Scientifique
38. GRENOBLE Gare - France

† In partial fulfilment of a thesis

‡ C.A.P.E.S. Fellow

ABSTRACT

Specific heat measurements on dilute alloys of Pt-Co ($0.08 \leq c \leq 2.6$ at.%) between 0.02 K and 4 K are reported here. For the less concentrated samples, a one impurity effect anomaly, due to the Kondo state or localized spin fluctuation effect, is identified near the characteristic temperature T_K = I.6 K, previously determined by nuclear orientation and magnetization measurements. As shown by the presence of nuclear Schottky contributions, a fraction of the impurities remains magnetic even much below T_K, probing an hyperfine field of 2I0 kOe, corresponding to the maximum moment of I.7 μ_B for the Co. This nuclear contribution allows to study the concentration dependence of the magnetic fraction which is found to vary as the square of the total concentration, for the lowest concentrations. In this limit, the magnetic impurities are "pairs" of Co atoms, that are less than about 8 Å apart. This quadratic concentration dependence seems to be a general trend in the appearance of the magnetism in dilute alloys. A comparison with magnetic measurements shows that the impurities in a "pair" are ferromagnetically coupled.

I - INTRODUCTION

There has been already a number of experimental studies on the dilute Pt-Co system, each presenting different partial aspects of its magnetic behaviour. For concentrations higher than 2 at.% Co, magnetization measurements show the presence of giant moments of $3.6\mu_B$ per solute atom [1]. The existence of ordering temperatures persisting at very low concentrations was explained by ferromagnetic coupling. However, no net long range ferromagnetic polarization of the host was found by N.M.R. measurements in the paramagnetic state for concentrations lower than 0.1 at.% Co [2]. On the contrary, the fact that the platinum line width was growing with the Co concentration and was a function of H and T, as in Cu-Mn, has been attributed to an oscillatory RKKY polarization. Even more, below 5K, this line width being no more a function of H/T, the existence of a Kondo state was suggested [3].

In a 1 ppm alloy, the hyperfine field acting on the Co nuclei, as measured by nuclear orientation [5], was found proportional to the externally applied field up to 4 kOe. From the value of this susceptibility, a characteristic or Kondo temperature, T_K, of 1.6K was determined. For 2 at % Co, the saturation hyperfine field of -180 kOe obtained in 4kOe was attributed to the destruction of the Kondo state by interactions between impurities. The resistivity [3] finally has the same type of variation than that of nickel in palladium, which is explained by the local spin fluctuation model.[4]

Thus, this system appears to vary from a non magnetic state (Kondo or local spin fluctuations) at the lowest concentrations to a magnetic state with giant moment and

ferro-magnetic order for high concentrations, via the progressive apparition of localized moments coupled by RKKY interactions near a critical concentration.

The point to be cleared here concerns the appearance of those magnetic moments on the impurity due to interactions between them below the observed characteristic temperature T_K and also the way in which they appear near the critical concentration : smoothly, all the impurities carrying the same moment increasing with the concentration, or abruptly, some impurities being magnetic with their total moment and others being non magnetic, depending on their environment (1 - 0 model). In that case, just the fraction of magnetic atoms would increase with the concentration.

This second kind of model has already explained successfully the results on other systems with noble metal hosts : Cu-Fe [6], Au-Fe [7], Cu-Co [8], Au-Co [9-10] and the magnetization of the same Pt-Co system [11].

We have made a systematic study of the specific heat of this Pt-Co system as a function of the Co concentration in a large range of temperature, from 20mK to 4K, that is to say from well below to above T_K.

The contributions to the specific heat are mainly from nuclear and electronic origin, apart from the lattice contribution which will be substracted.

From the contribution of the electrons for the low concentrations, we specially expect to get the anomaly associated with the Kondo effect or localized spin fluctuations around 1.6K and clarify previous results obtained at higher temperatures.

Effectively, specific heat measurements made by Wheeler [12] between 1.4K and 20K show, for concentrated alloys (c>1at.%), a peak in the excess specific heat, rising with the concentration, that he attributed to magnetic ordering.

For lower concentrations (c<1 at.%), the nearly flat excess specific heat was explained by a broadening in the magnetic anomaly due to inhomogeneities in the Co concentration. Boerstoel and Van Baarle [13-14] also observed for concentrations down to 0.067 at.% the tail of a specific heat anomaly, which was shifted to higher temperatures by application of an external field and also attributed to ordering effects.

From the contribution of the nuclei, we intend to study the effect of interactions between impurities on the appearance of localized moments below T_K, using the hyperfine field as a probe for the existence of electronic magnetism. Such concentration effects could already be guessed from the nuclear orientation results [5] and also from polarized Mossbauer experiments at very low temperature[15], which yield a mean hyperfine field of -112 kOe on the ^{57}Co parent nuclei for a nominal concentration of 0.1 at.%, instead of - 180 kOe in a 2 at.% sample by Nuclear Orientation.

The nuclear specific heat has been used since a long time in the dilute alloy problem as a probe to answer the "Yes or No type of question" to fill the Friedel's table [16] or to measure the r.m.s amplitude of spin oscillations produced in the host by magnetic impurities [17]. More recently, it appeared as an interesting tool to count the number of magnetic impurities, for the study of interaction effects in the appearance of localized moments in Au-Co [9] and Au-Co Fe [18]. Its advantage, compared to N.M.R., Mössbauer or nuclear orientation, is that of measuring a parameter directly proportional to the concentration of magnetic impurities ; compared to magnetization, it is only sensitive to the magnetic impurities (since the electric quadrupole contribution is generally small) but as well to the anti-ferromagnetically than to the ferromagnetically coupled impurities. Furthermore, the experiments are performed in zero external field, and the results are

mainly sensitive to the highest hyperfine fields, since they are proportional to the square of the hyperfine field. This insures that the main contribution comes from the magnetic impurities and that the influence of the small induced moments or of the s contact term may be neglected.

Finally the Pt-Co system is very adequate for specific heat measurements in the range 20 mK to 4K. In fact, up to now the one impurity effect anomaly has only been observed in two systems namely Cu-Fe and Cu-Cr. As for Cu-Cr, the low value of T_K enables the one impurity anomaly to be easily observed, since the lattice contribution will be small. Furthermore the nuclear moment of Co being much bigger than the Fe or Cr ones, the nuclear Schottky anomalies will be large and therefore easily measured.

II - EXPERIMENTAL DETAILS

1) Alloys

The specimens were induction melted by a semi levitation technique on a water cooled base plate and cast in a water-cooled copper mold under wacuum by the metallurgy section of our laboratory.[19]. The first serie of samples with nominal concentrations of 0.1, 0.2, 0.4 and 2.6 at.% were prepared from 99.999 % platinum wire and 99.999 % cobalt sponge (both supplied by Johnson Matthey and Co.). The other samples with nominal concentrations of 0.3, 0.75 and 1 at.% were prepared from 99.999 % Leico platinum wire and Johnson Matthey cobalt sponge. The absorption spectroscopy analysis used to determine the actual concentrations of the samples gives respectively 0.08, 0.16, 0.31, 2.6, 0.27, 0.66 and 0.88at.%. The differences between nominal and measured concentrations can be accounted for by the losses of cobalt during melting due to the high cobalt vapor pressure above the platinium melting temperature.

A sample of pure platinum has been also prepared from Johnson Matthey platinum wire in the same manner than the alloys.

The concentration of magnetic impurities detected by magnetization measurements is equivalent to less than 6 ppm of iron[11].

The weights of the samples were about 11 g for the two less concentrated alloys and 15 g for the others.

2) Measurements between 0.3 and 4K

The measurements between 0.3K and 4K were made in a He^3 cryostat [20]. A pulse technique was used, with the sample in partial contact with the cold source. The experimental details of the measurements have been discussed previously[21] and only a brief description is given here.

The specimen was thermally attached to the ^3He pot via a stainless steel tube. The ratio of the length to the area of the stainless steel tube was chosen so that the time constant (τ_1 = R.C, where R is the thermal impedance and C is the heat capacity of the sample and sample holder) was large compared to the internal thermal relaxation times of the sample and sample holder. τ_1 varies from 250 s to 800 s between 0.3 and 4K for the different Pt-Co samples. The total time constant of the measuring system was about 2 seconds.

The specimen temperature was monitored by germanium resistors calibrated against the susceptibility of C.M.N, ^3He and ^4He pressures. The voltage drop across the germanium resistor was compared to a constant DC voltage source ($\simeq$ 200μV). The heater was a constantan wire($\sim$200Ω) wound

non inductively around the sample holder and attached with a thin layer of GE 7031. The ^{3}He pot was stabilized at the desired temperature by an electronic regulator and the specimen temperature kept constant. A small heat pulse was supplied then to the specimen. The specific heat was deduced from the exponential decay of the temperature rise due to the pulse. This procedure was repeated with various heating currents at various temperatures. The heat capacity of the sample holder was equivalent to 15 g of copper.

3) Measurements between 0.02K and 0.3K.

The measurements between 0.02K and 0.3K were made on a double stage demagnetization apparatus described previously [22]. An adiabatic method was used. The temperature was given by the magnetic susceptibility of a small sphere constituted by 5 C.M.N slabs glued to the sample holder with Apiezon N grease. The correction due to the demagnetization factor was found to be negligibly small (<0.5mK). The heater was pressed between the sample and the sample holder.

The equilibrium time constant of the system was rather long and approximately given by

$$\tau = 3.10^3 \, T^{-3} \ \mu s$$

for temperatures lower than 0.07K. At temperature around 20mK, 20 minutes were sometimes necessary to reach an internal equilibrium after heating. To have a good precision in the extrapolation after each heat pulse, the temperature drifts had to be recorded during an equal time period after equilibrium was reached. But the heat capacity of some samples being small, the usual linear graphical extrapolation introduces large systematic error in the determination of the temperature rise ΔT.

A systematic analysis of the equilibrium heat leak has been made and the extrapolation of the temperature drifts was performed by a computer from the data punched in a paper tape during the experiment. The recording of the time derivative of the mutual inductance bridge signal was used to determine when the system was in internal equilibrium after heating. The precise description of all the system will be published later[23].

III - RESULTS ABOVE 0.3K

The "high temperature" results obtained for the pure Platinum and Pt-Co samples are reported in fig.1. The specific heat of all the alloys presents a net excess with respect to that of pure Platinum.

In this temperature range, the specific heat of platinum may be written

$$C = \gamma T + \beta T^3 \qquad (1)$$

where γT and βT^3 are the electronic and lattice contributions. The experimental results plotted in a c/T versus T^2 diagram in fig.2 were analyzed by a least square method using eq. (1) and yield to

$$\gamma = 6.6 \text{ mJ/K}^2 \text{ mole}$$
$$\beta = 0.152 \text{ mJ/K}^4 \text{ mole} \qquad (2)$$

which corresponds to a Debye temperature of 234K. Those values are in good agreement with the other available data [24].

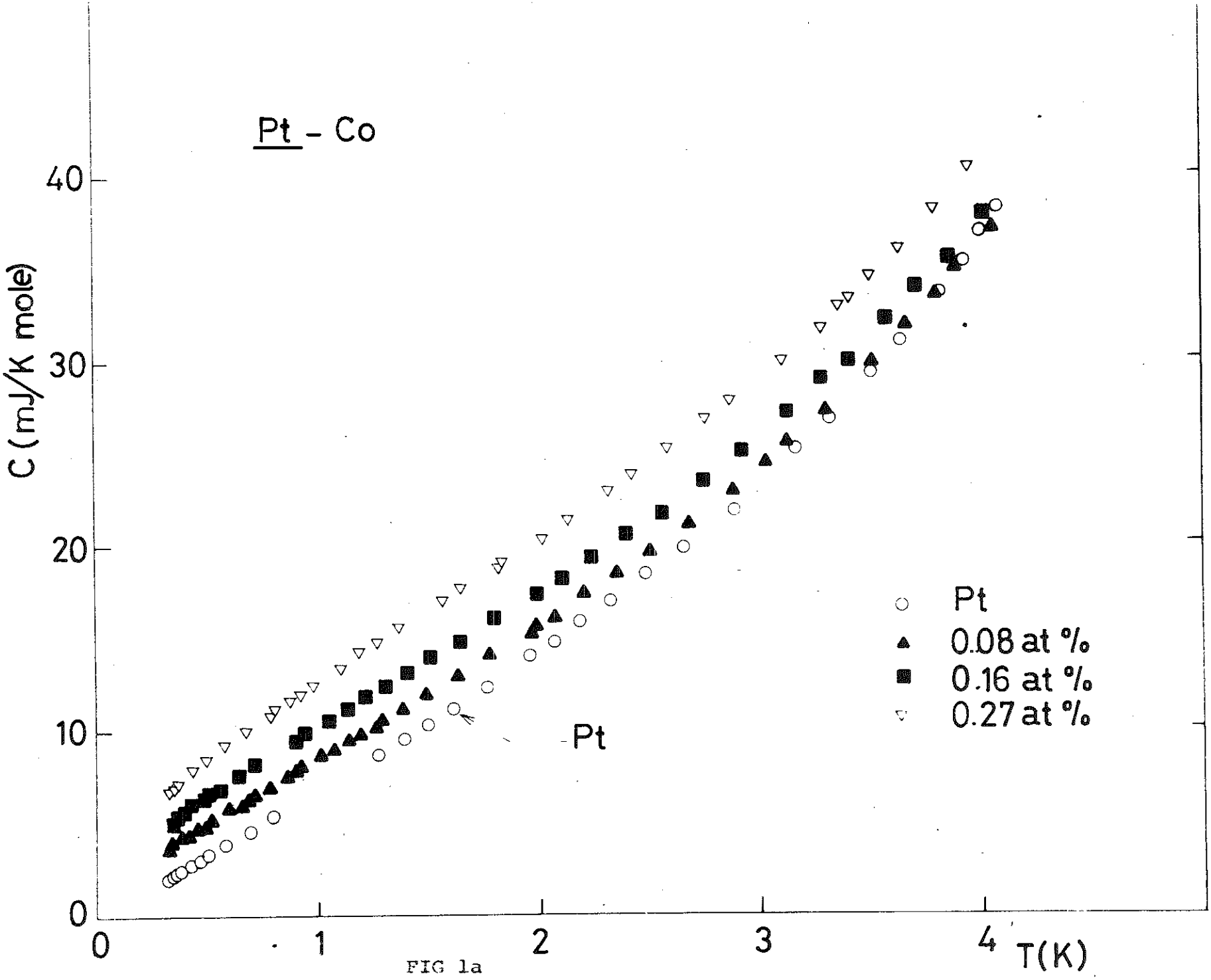

FIG 1a

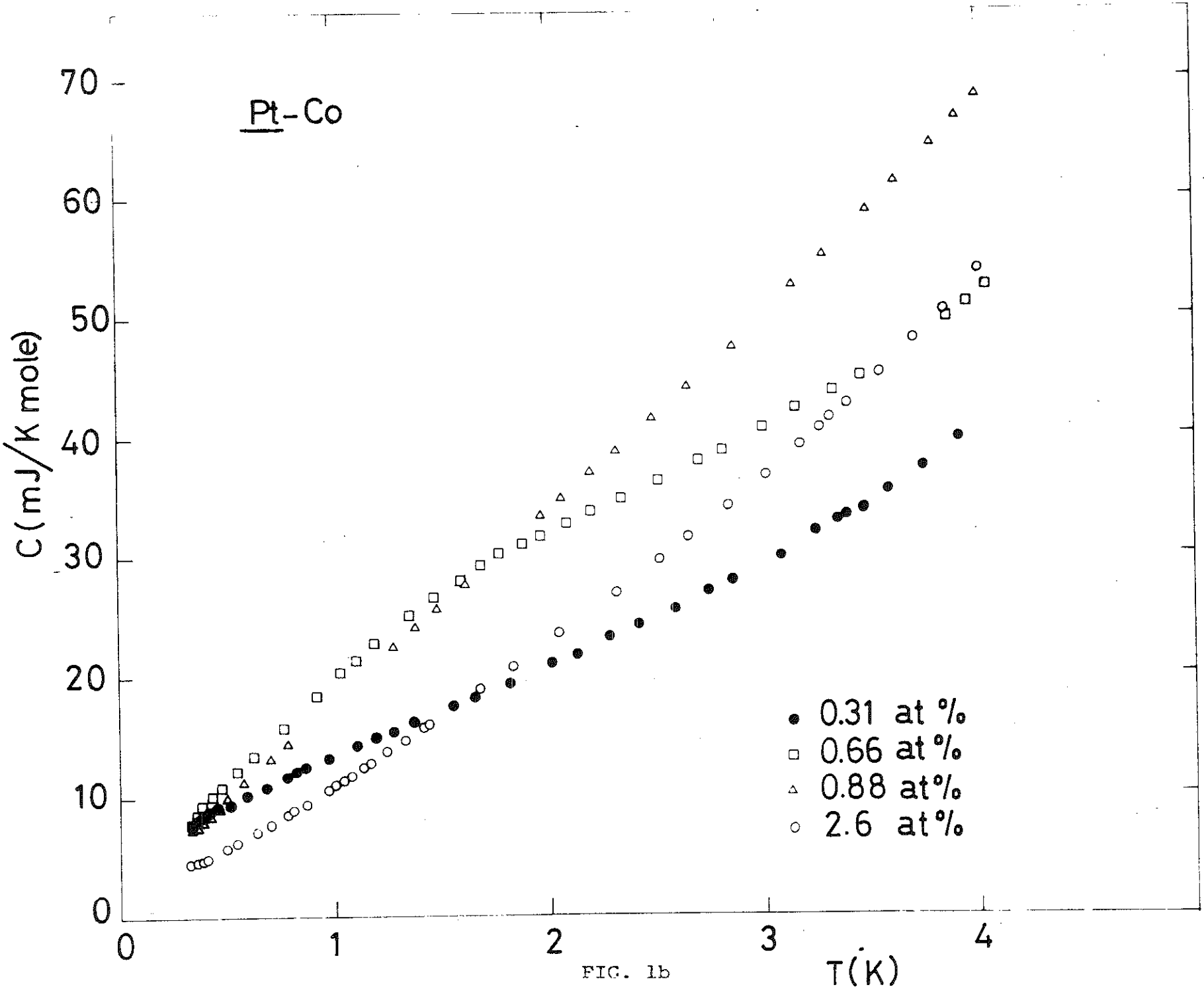
Pt-Co
C(mJ/K mole)
T(K)
0
10
20
30
40
50
60
70
0
1
2
3
4
0.31 at %
0.66 at %
0.88 at %
2.6 at %

FIG. 1b

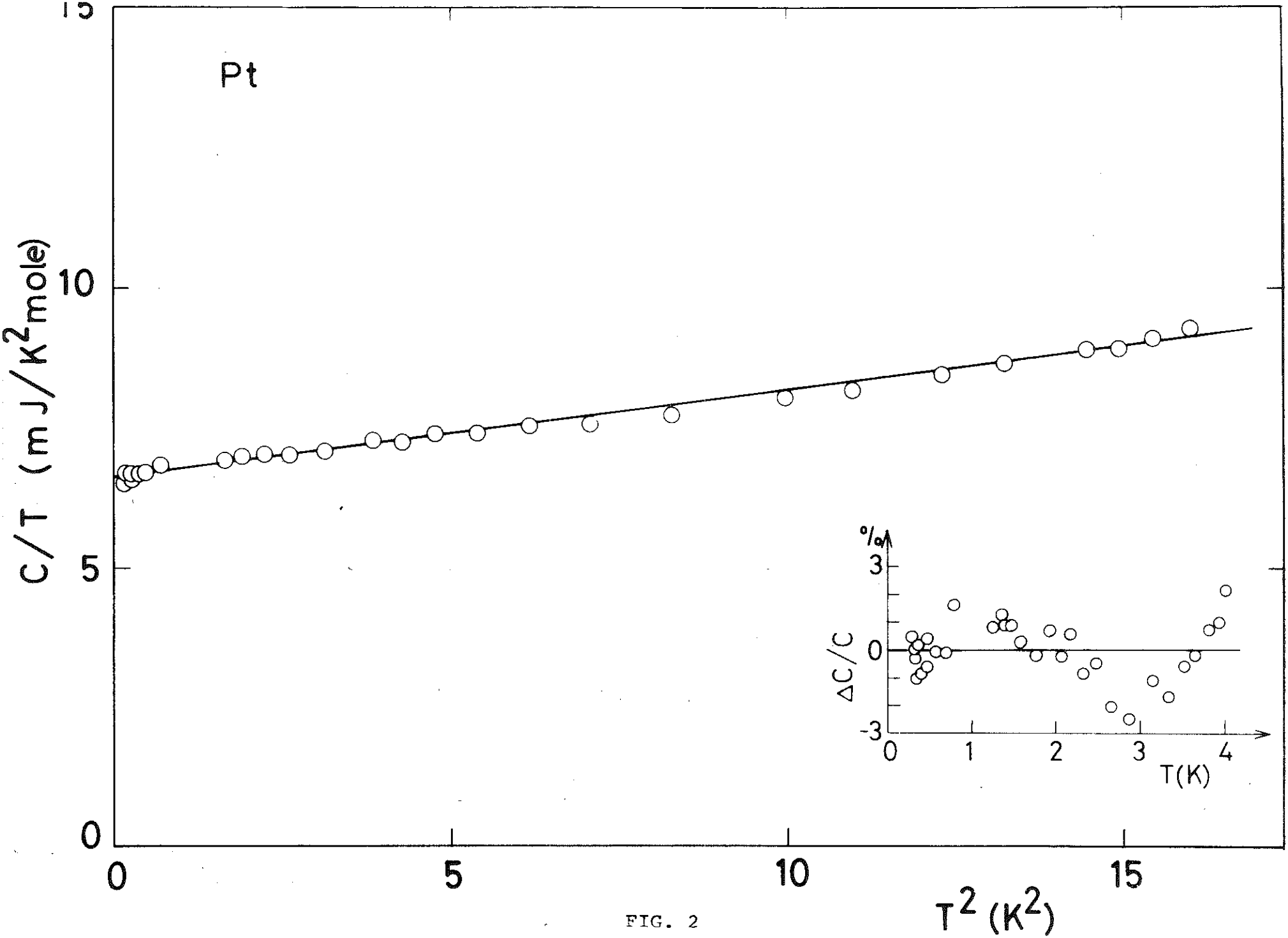

FIG. 2

The experimental points scatter between +2% and - 3% around the calculated curve, with γ and β given in (2), as may be seen in the insert of fig. 2.

The excess specific heat of the various alloys $\Delta C = C_{alloy} - C_{pt}$ is reported in fig.3. The presence of Co atoms produces only a very small modification of the lattice contribution, so that ΔC represents the electronic and magnetic behaviour of the alloys.
Indeed, assuming a linear variation of the Debye temperature with the concentration, given by the isotopic formula[25] :

$$d\,\Theta_D(c) = -\frac{1}{2}\,\Theta_{Pt}\,\frac{dm}{m}\,c \qquad (3)$$

where m is the atomic mass of Pt, the effect upon ΔC in the less favorable case of 2.6 at.% corresponds to about 1% of ΔC at 4K.

The excess specific heat of the 4 less concentrated samples, $0.08 \leqslant c \leqslant 0{,}31$ at.%, has very similar variations ; the different curves exhibit a flat maximum between 1 and 2K. The amplitude of this maximum is proportional to the concentration, as may be seen from the rough superposition observed in the $\Delta C/c$ versus T diagram of fig. 4. This is the evidence for the existence of a one impurity effect in the Pt-Co system, that can be attributed to the formation of the Kondo state or to the anomaly due to the localized spin fluctuations. The maximum is almost independant of the temperature, around $T_M = 1.2K$, not very different from the value of $T_K = 1.6K$ obtained by nuclear orientation and magnetic susceptibility measurements.

For larger concentrations, c >0.3lat.%, the maximum shifts to much higher temperatures (2K for 0.66 at.% and more than 4K for 2.6 at.%). This departure from the one impurity effect results from the existence of a dominant magnetic ordering effect which will be discussed later.

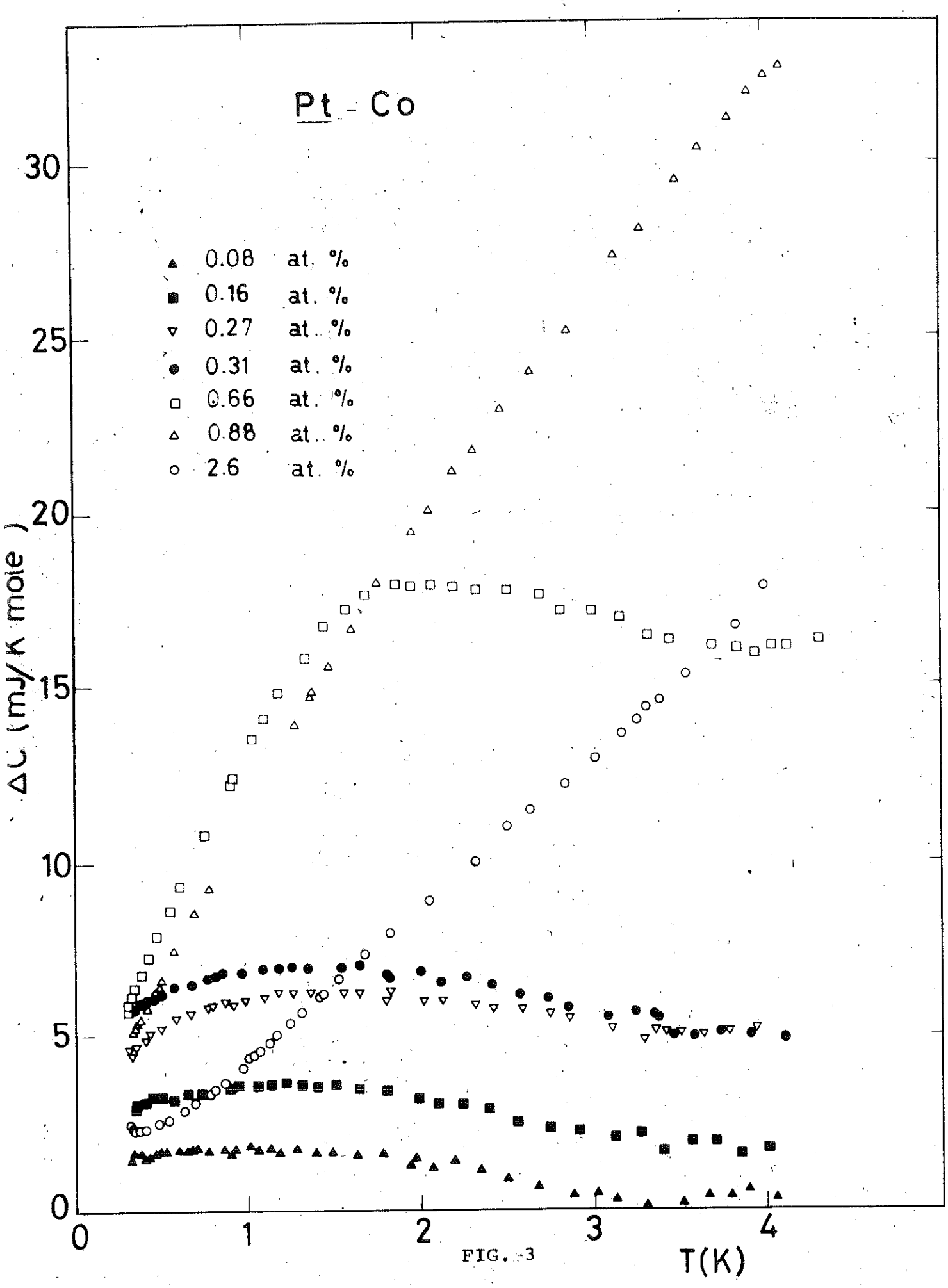
Pt - Co
0.08 at. %
0.16 at. %
0.27 at. %
0.31 at. %
0.66 at. %
0.88 at. %
2.6 at. %
ΔC (mJ/K mole)
T(K)
0
5
10
15
20
25
30
0
1
2
3
4

FIG. 3

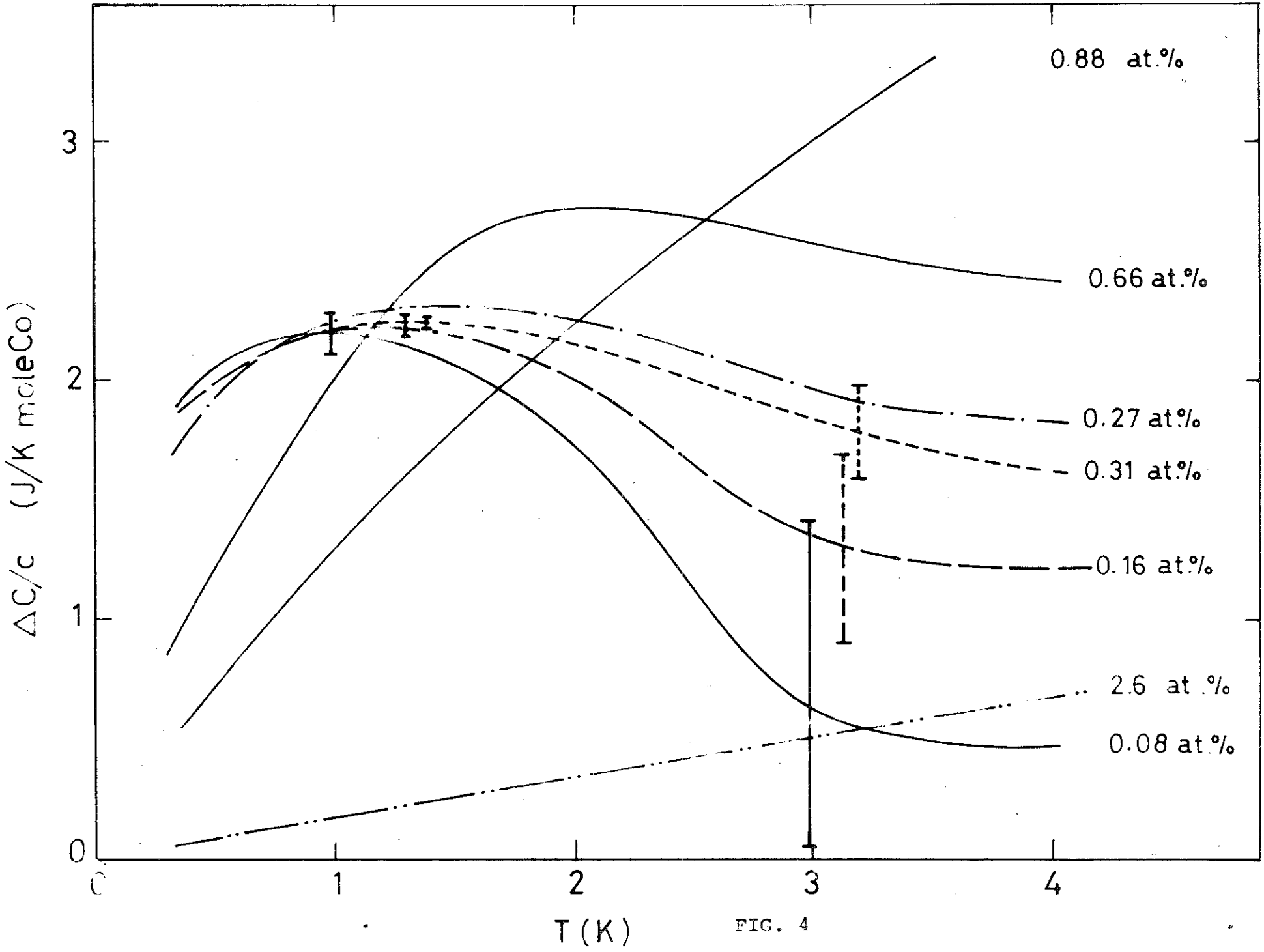
0.88 at.%
0.66 at.%
0.27 at.%
0.31 at.%
0.16 at.%
2.6 at.%
0.08 at.%
ΔC/c (J/K mole Co)
T (K)
0
1
2
3
4

FIG. 4

IV - RESULTS BELOW 0.5K AND NUCLEAR CONTRIBUTION

A - RESULTS

The specific heats obtained below 0.5K for the five more concentrated samples are plotted against the temperature in fig. 5. On the low temperature side, for all the samples measured, an upturn corresponding to the high temperature tail of a nuclear Schottky anomaly is observed. As will be discussed later, such a nuclear contributions is produced by the magnetic cobalt atoms frozen in their molecular field. Therefore, there are impurities which remain magnetic far below T_K, even in samples for which a one impurity effect is observed at higher temperature. On the high temperature side, the lattice contribution is negligibly small and the specific heat varies almost linearly in temperature. The total specific heat may be written

$$C = \gamma T + A\,T^{-2} + \text{higher order terms of } \frac{1}{T} \qquad (4)$$

where $A\,T^{-2}$ is the main nuclear Schottky term.

The graphic of $C\,T^2$ against T^3 is a straight line, as observed in fig. 6. The values of γ are obtained from the slope of this line and those of A from the intercept (see table 1). The deviations from the straight line at the lowest temperatures are due to the higher order terms of $\frac{1}{T}$. The departure also observed at higher temperatures for the less concentrated alloy (0.27 at.% Co) is attributed to the proximity of the ordering temperature. Effectively, the ordering

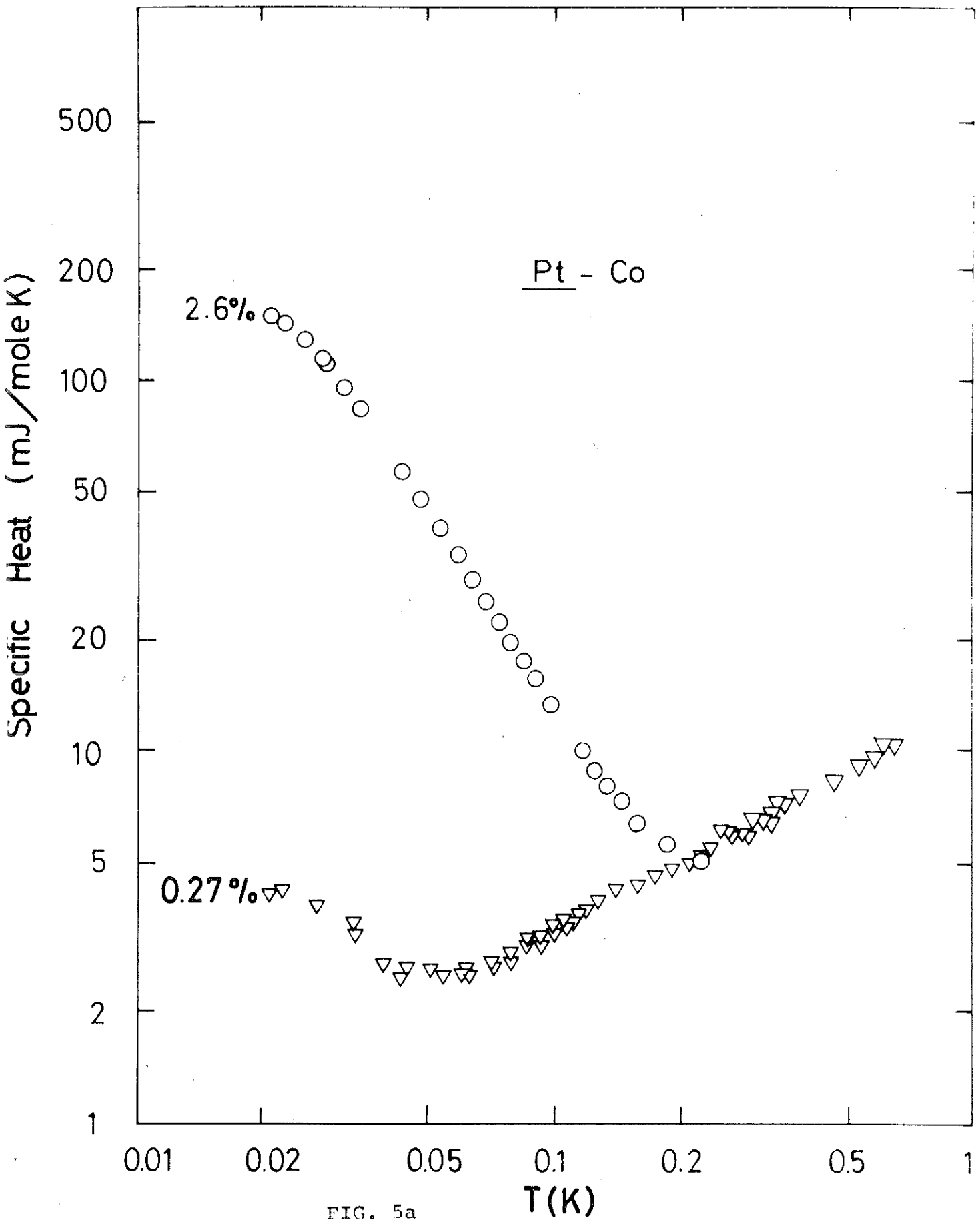
Pt - Co
2.6%
0.27%
Specific Heat (mJ/mole K)
T(K)
500
200
100
50
20
10
5
2
1
0.01
0.02
0.05
0.1
0.2
0.5
1

FIG. 5a

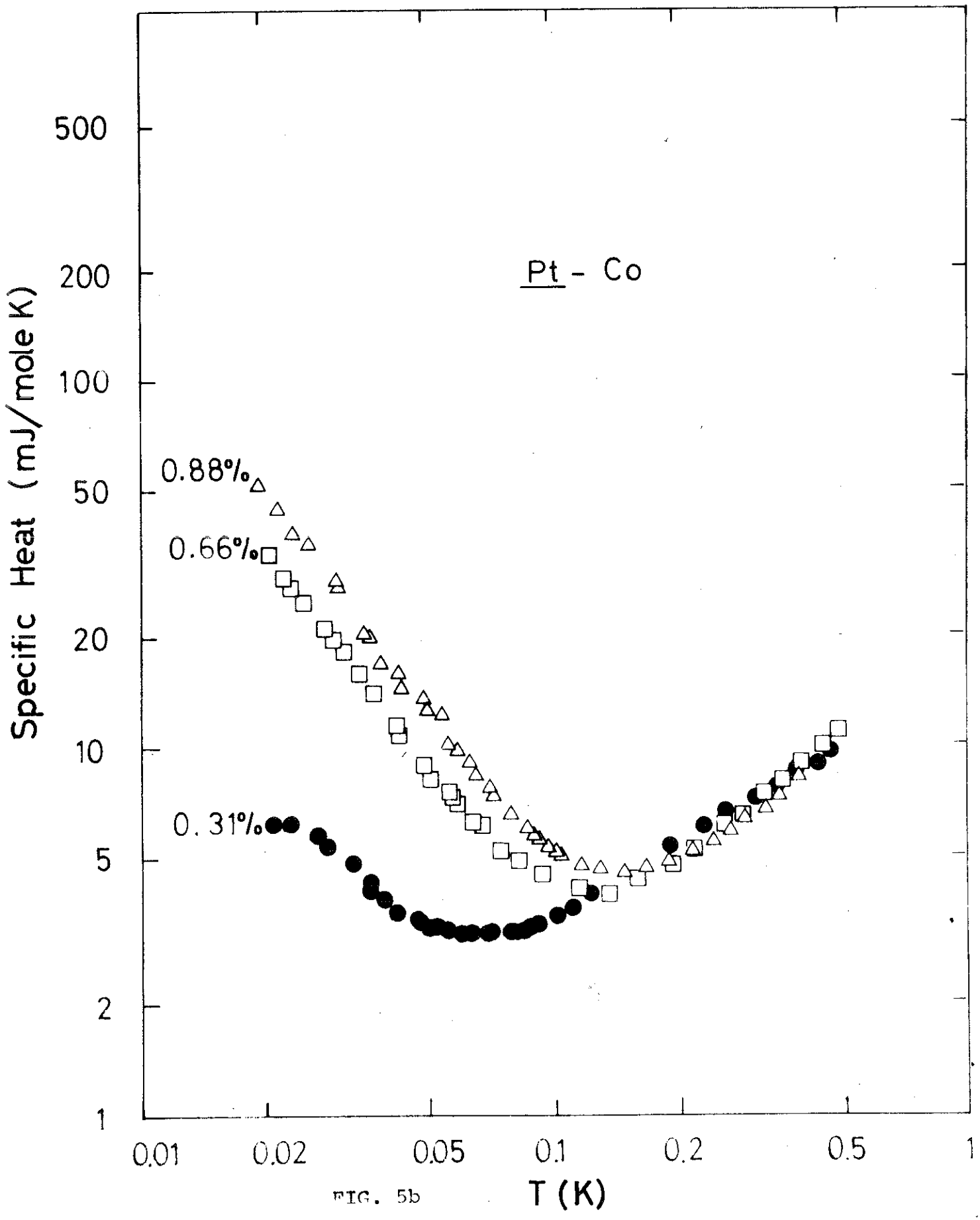
Pt - Co
0.88%
0.66%
0.31%
Specific Heat (mJ/mole K)
500
200
100
50
20
10
5
2
1
0.01
0.02
0.05
0.1
0.2
0.5
1
T (K)

FIG. 5b

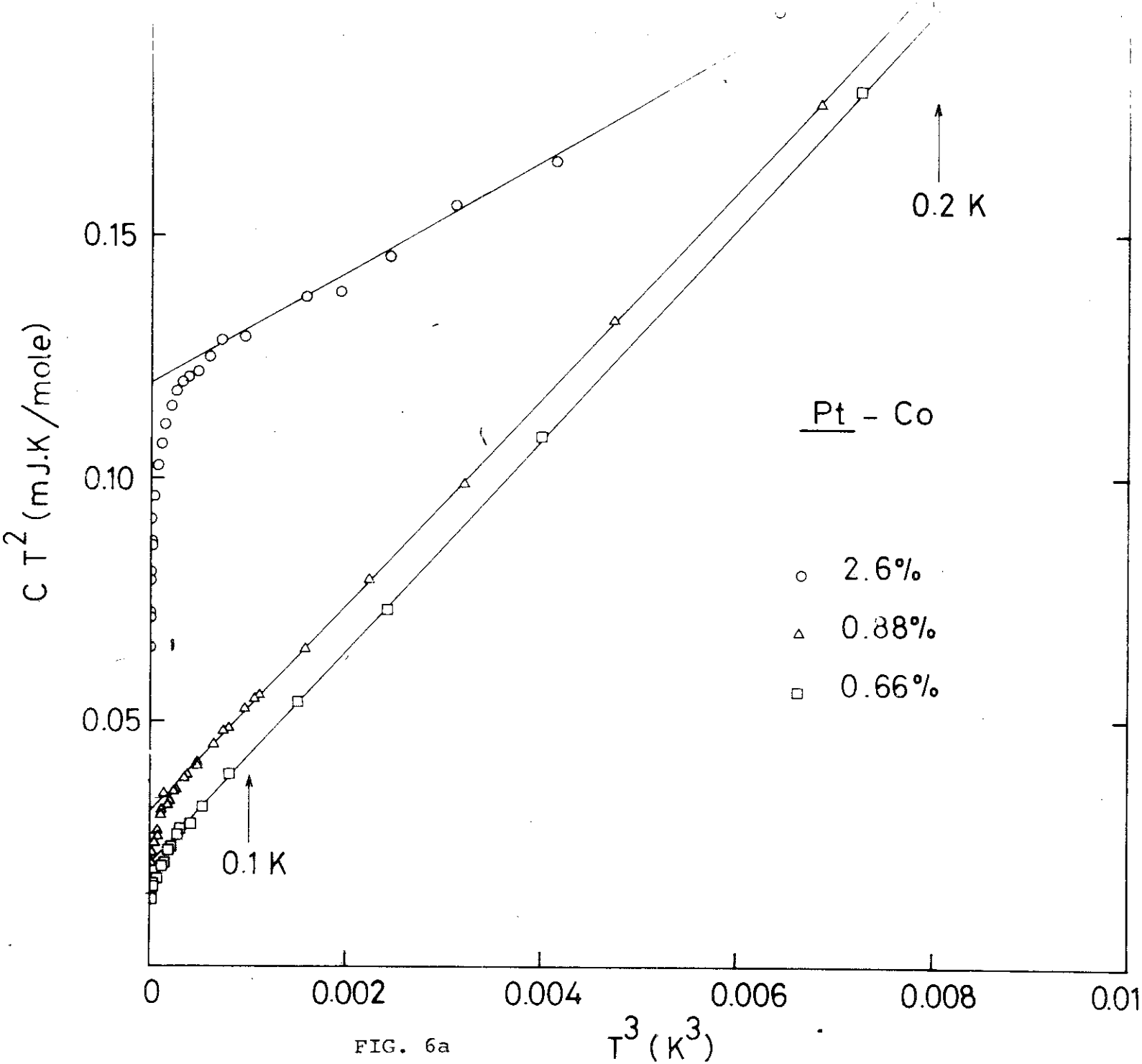
0.15
0.10
0.05
C T^2 (mJ.K/mole)
0.2 K
Pt - Co
2.6%
0.88%
0.66%
0.1 K
0
0.002
0.004
0.006
0.008
0.01
T^3 (K^3)

FIG. 6a

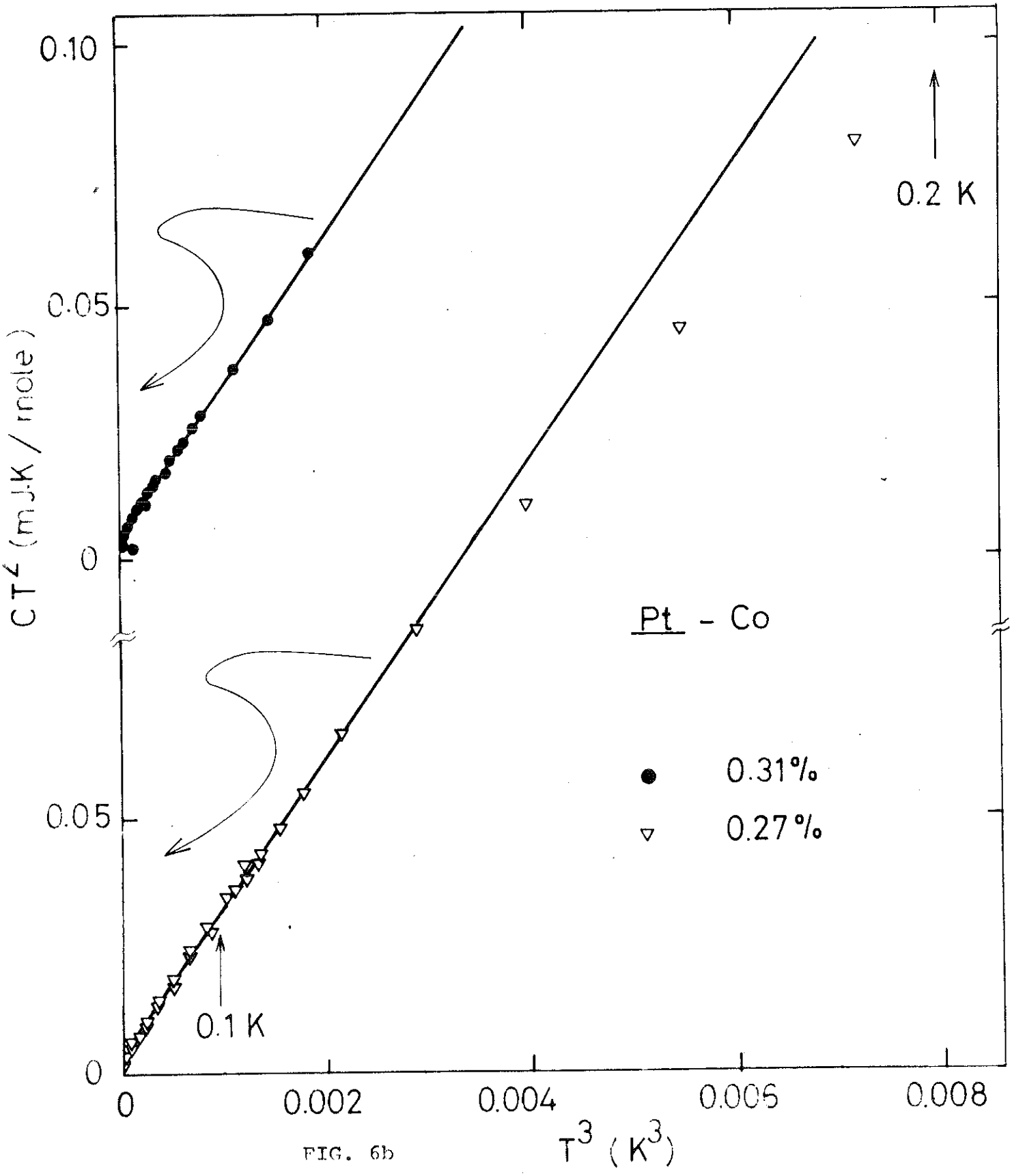
0.10
0.05
0
0.05
0
0
0.002
0.004
0.006
0.008
CT^2 (mJ.K / mole)
T^3 (K^3)
0.2 K
0.1 K
Pt - Co
0.31%
0.27%

FIG. 6b

TABLE 1

Cobalt concentration (at.%)	γ ($mJ/K^2.mol$) of alloy	A ($\mu J.K/mol$) of alloy	c_m/c (specific heat)	c_m/c (magnetization)
2.6	11.5	123.0	1	1
0.88	21	33.4	0.80	0.79
0.66	22	21.0	0.70	0.70
0.31	30	5.4	0.35	0.43
0.27	30	3.3	0.24	0.39
Iron concentration				
1		3.5	1	

temperature associated to the maximum of low field susceptibility is found to be 0.14K for this concentration. For the two less concentrated samples (0.08 and 0.16 at.% Co), the ordering temperatures are lower than 0.1K. Those samples have not been measured below 0.3K, since it is important that the magnetic impurities be in a frozen state to obtain the saturated hyperfine field (see appendix) and also because the sensitivity of our apparatus was not sufficient.

B - ANALYSIS OF THE NUCLEAR CONTRIBUTION

The values of A appears in fig.7 as a function of the Cobalt concentration c. A is not a linear fonction of c, but varies roughly as the square of this concentration for the low values of c.

Using a 1-0 local model, the alloy may be considered as a mixture of magnetic cobalt atoms, in concentration c_m, with a unique value of the magnetic moment and of the hyperfine field and of non magnetic impurities with zero hyperfine field, in concentration $c - c_m$

In that case, the nuclear term is directly proportional to the concentration of magnetic carriers and neglecting the matrix contribution :

$$A = c_m \, R \, \frac{I(I+1)}{3} \, \gamma^2 . \, \hbar^2 \, H^2_{eff}/k^2 \qquad (5)$$

where I and γ are respectively the nuclear spin and gyromagnetic ratio of the Co nuclei and H_{eff} the hyperfine field of the magnetic Co atoms ; the other constants have the usual meaning.

The dependance of A with the total cobalt concentration directly reproduces the variation of the magnetic

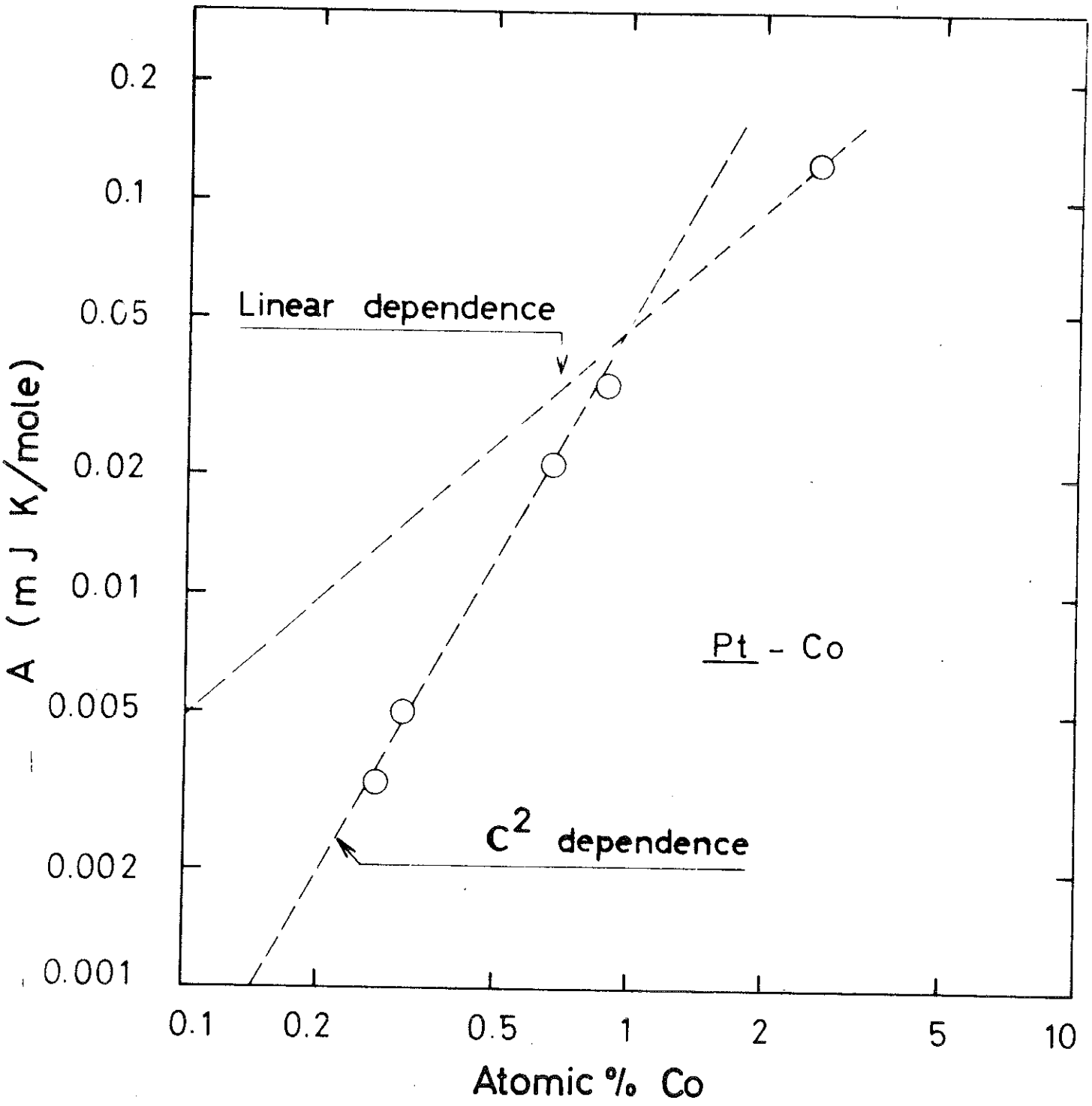
0.2
0.1
0.05
0.02
0.01
0.005
0.002
0.001
A (m J K/mole)
Linear dependence
Pt - Co
C^2 dependence
0.1
0.2
0.5
1
2
5
10
Atomic % Co

FIG. 7

cobalt concentration c_m with the total concentration. Therefore c_m varies with the square of c for the low concentrations

$$c_m \alpha c^2 \qquad (6)$$

This quadratic dependance suggests that for low concentrations the magnetic atoms are "pairs" of Co atoms.

This behaviour has been already observed in Cu-Fe [6] alloys and seems to be a general feature for the appearance of magnetism in dilute alloys, due to interactions between impurities.

Quantitative informations may be obtained from a more detailed analysis. The nuclear anomalies found by substracting from the total specific heat the linear contribution γT and the nuclear host contribution (as will be estimated later) are reported in fig. 8.

The saturation magnetization per impurity being already maximum for 2.6 at.% Co [1], all the impurities are considered magnetic for this concentration, that is $c = c_m$. According to eq.(5), the A/T^2 term (straight line in fig.8) corresponds to an hyperfine field of 210 kOe. The curve representing the Schottky anomaly associated to this field and this concentration fits very well the curvature observed for the experimental points. The results obtained for the other concentrations have been fitted with Schottky anomalies corresponding to this same hyperfine field of 210 kOe. The scaling factor provides the concentration c_m of magnetic carriers. The determination of A obtained in that way from the high temperature part of this anomaly is more precise than from the CT^2 (T^3) diagram, and in fact the values of A and γ presented in table I have been obtained by iterations between these two types of diagrams.

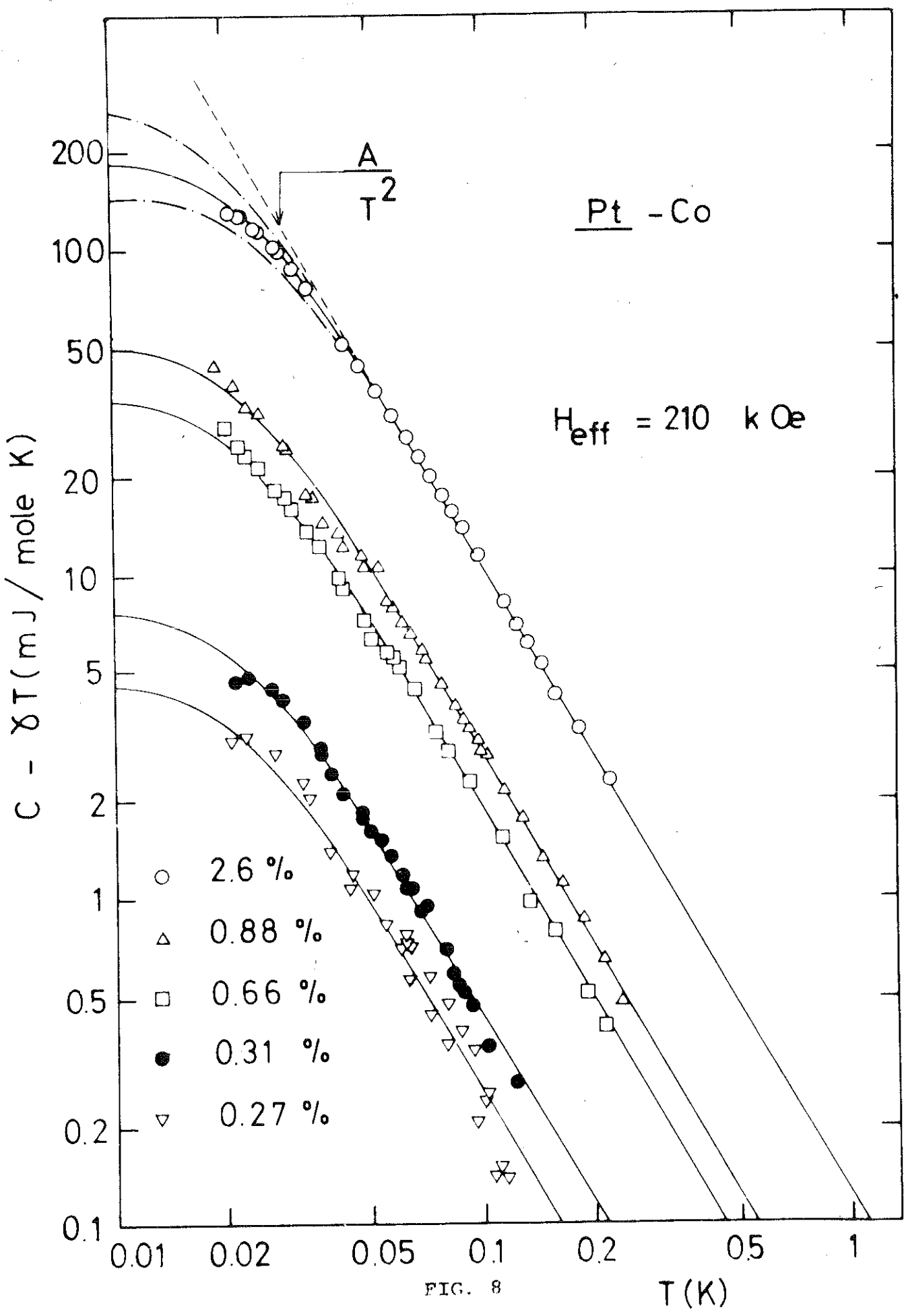
A/T²
Pt - Co
H_eff = 210 k Oe
C - γT (mJ / mole K)
T (K)
2.6 %
0.88 %
0.66 %
0.31 %
0.27 %
200
100
50
20
10
5
2
1
0.5
0.2
0.1
0.01
0.02
0.05
0.1
0.2
0.5
1

FIG. 8

This field of 210 kOe is in very good agreement with the value of 215 kOe found for pure cubic Co [26] and with the 213 kOe observed for Co diluted in Pd [27]. As in the last case, it is natural to believe that the magnetic Co in Pt has the same magnetic moment than the ferromagnetic fcc cobalt, that is 1.7 μ_B. One may conclude that the magnetic impurities carry their maximum magnetic moment.

The fraction c_m/c of magnetic impurities obtained in that way and from the magnetization measurements [11] is reported in table I and plotted in fig.9 as a function of the total concentration. A good agreement is observed for the more concentrated samples. When the concentration decreases a deviation appears between the two determinations.

The fact that the nuclear specific heat never provides values of c_m/c larger than those deduced from the magnetization shows that the magnetic impurities forming the "pairs" are coupled ferromagneticaly, since the magnetization is mainly sensitive to the "ferromagnetic pairs" while the nuclear specific heat is sensitive to both "ferro" and "antiferromagnetic pairs".

For the less concentrated samples the low values of the ordering temperature may lead to an incertitude in the graphical estimation of A, and may explain the different determinations of c_m/c. However, there are also physical reasons to these differences. The magnetic measurements have been performed in a field of 2kOe, while the specific heat measurements were performed in zero external field.As a consequence, some moments will be induced and counted as magnetic impurities in the magnetization measurements. For the concentrated samples (c>0.31 at.%), the molecular field produced by the magnetic Co atoms will take the place of the external field and both types of measurements will give the same values

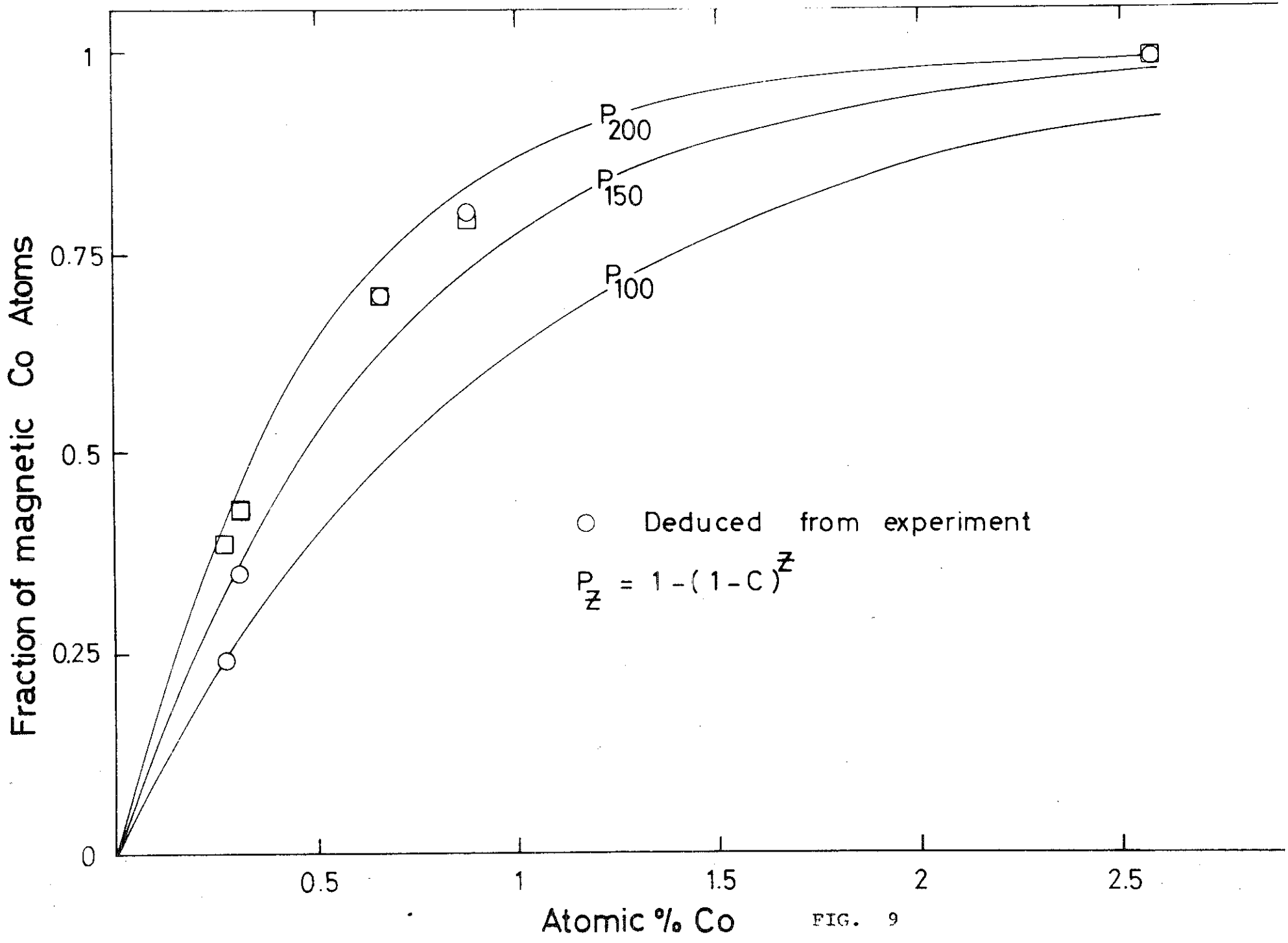
Fraction of magnetic Co Atoms
1
0.75
0.5
0.25
0
0.5
1
1.5
2
2.5
Atomic % Co
P200
P150
P100
Deduced from experiment
$P_Z = 1-(1-C)^Z$

FIG. 9

for c_m/c. The existence of such "nearly magnetic impurities" on which a magnetic moment is easily induced by an external field has already been pointed out in the Cu-Fe system [6]. In that case, fields up to 50kOe are necessary to saturate these "nearly magnetic impurities" instead of 2kOe in our case, which corresponds roughly to the ratio of the respective characteristic temperature T_K (30K instead of 1.6K). In the case of Cu-Fe, an equal number of magnetic and "nearly magnetic impurities" has been experimentally found [6] and explained by considerations of density of charge oscillations [28].

In the rough statistical model already used for the interpretation of the magnetization measurements of the Cu-Fe [6] alloys, the non magnetic atoms are assumed to be the isolated ones, which have no other atom of same kind among their Z neighbours. Their probability will be

$$c\ (1 - c)^z \qquad (7)$$

the probability of the "pairs" will then be the complementary one

$$c_m = c - c\ (1 - c)^z . \qquad (8)$$

The functions

$$P_z = c_m/c = 1 - (1 - c)^z \qquad (9)$$

are the full curves on fig.9 for 3 different values of z, z = 100, 150 and 200. A good estimation of z will be situated between 100 and 200, which means that the characteristic distance between the Co atoms forming the magnetic pairs, in the limit of low concentrations, will be around 8 Å .

C - DISCUSSION

In those analysis some hypothesis have been made, that need to be precised now.

The nuclear term measured is the sum of two contributions : that produced by the impurities on their own nuclei, which is the most important, and that produced by the impurities on the host nuclei. Both of them are from magnetic and electric origin.

- The electric quadrupolar term is zero for the host nuclei since I=1/2 for ^{195}Pt and assumed to be negligibly small for the impurities, as in the case of other dilute alloys in a cubic host [17]. Anyway this term would yield a contribution linear in c (the total impurity concentration) that has not been observed.

- The magnetic contribution of the matrix nuclei may be estimated from the nuclear specific heat measurement of a Pt-Fe alloy. Indeed, for this alloy, the intrinsic contribution of the ^{57}Fe atoms to the nuclear specific heat is negligible due to the small value of the nuclear moment (less than 0.1 nuclear magnetons) and its small isotopic abundance (2 at.%). There only remains the magnetic contribution of the matrix. Furthermore, the value of the giant moment and of the ordering temperature being rather similar in Pt-Fe and Pt-Co, the spin density oscillations amplitude in the host, and thus the contribution of its nuclei, should be comparable for equivalent concentrations of magnetic impurities. This is the case for noble metal hosts, in which the matrix contribution is nearly independant of the nature of the transition impurities, provided they are magnetic [17].

The specific heat measurement of a Pt-Fe sample containing 1 at.% Fe, where all the impurities are magnetic [29], leads to a value for A of 3.5 μJ K/mole. The host magnetic contribution being proportional to the concentration of magnetic impurities [17], we may estimate it to be 35 erg.K/mol per atomic per cent of magnetic impurities in Pt-Fe and in Pt-Co. For all the samples, this corresponds to about 7% of the nuclear specific heat measured as may be calculated for the Pt-Co 2.6 at.%, where all the impurities are magnetic. The results that appear in fig.8 have been corrected by this same ratio for all the samples.

- A unique value of the hyperfine field has been attributed to all the magnetic atoms. However, for others exchange enhanced metal based alloys in which all the impurities are magnetic, a distribution of hyperfine field has been observed [30]. This was accounted for by the molecular field distribution P(H) which introduces a distribution of $\frac{\langle S_z \rangle}{S}$ and thus of hyperfine field on the impurities. However, it is shown in the Appendix that provided the moments are coupled by R.K.K.Y. interactions, the nuclear specific heat cannot distinguish between such a distribution and the case where all the impurities have the same saturated hyperfine field.

- The hyperfine field value of 210 kOe obtained here is slightly different from the value of 180 kOe obtained by nuclear orientation [5]. However, the external field of 4 kOe applied in those experiments was not sufficient to saturate the 2 at.% Co sample, as observed in the magnetization measurements on the sample containing 2.6 at.% Co [11]. Furthermore the value of 210 kOe determined here agrees very well with the value of 216 kOe deduced from the comparison of magnetic and nuclear orientation measurements in dilute samples under fields up to 50 kOe [11].

- The result of polarized Mössbauer experiments [15] seems also to give a different value, - 112 kOe, for the hyperfine field on Co nuclei. But in spite of the low concentration of Co, estimated to be 0.1 at.%, all the Co impurities have been assumed to be magnetic. However, this measurement gives a mean value for the hyperfine field and may also be explained using a 1-0 model. The polarization may be accounted for by the existence of a fraction $c_m/c \simeq 0,4$ of magnetic impurities with a field of 210 kOe.
According to fig. 9, this corresponds to a concentration around 0.3 at.%, which differs from the estimated one, but which agrees much better with the ordering temperature that may be deduced from the Mössbauer spectrum [15 - 11].

V - ONE IMPURITY EFFECT ANOMALY

The excess specific heat ΔC divided by the concentration $c-c_m$ of isolated Co atoms (as given by table I) is reported in fig. 10 for the 0.31 at.% sample after substraction of the nuclear Schottky contribution. The entropy has been evaluated by a graphical determinations of the area under the curve $\Delta C/(c-c_m)$ up to 4K and extrapolating with a I/T law above 4K. From R log (2 S + 1), the value of S is found to be about 2. If ΔC was divided by the total concentration, this value would be around 1, in agreement with the previous estimations [12 - 31].

Phenomenologically, it is possible to compare the behaviour of the Pt-Co anomaly to that of Cu-Cr [32], which has approximately the same T_M, as may be seen in fig. 10. In the case of Cu-Cr the excess specific heat ΔC has been divided by the total Co concentration since the fraction of magnetic impurities is very small in the range of concentration

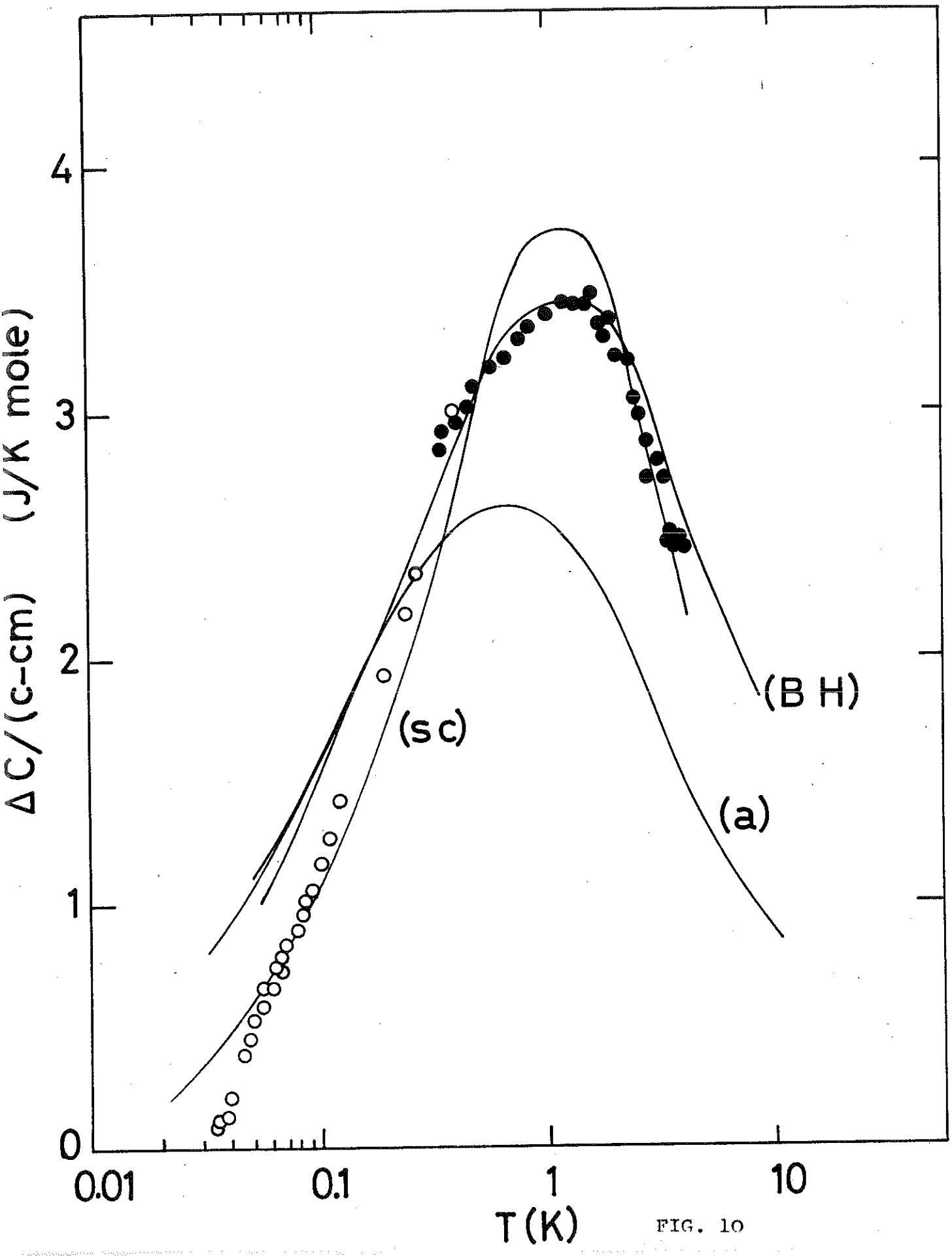

FIG. 10

studied. Some tentative fittings to theoretical curves have been made to explain the experimental results on Cu-Cr and Cu-Fe. Bloomfield and Haman's curve fits sucessfully the Cu-Cr results[33] when normalized to spin 3/2. Schweizer's curve agrees also with the Cu-Fe experimental points [34]. Figure 10 shows those curves normalized to spin 2. The values of T_K obtained are respectively 4.5K and 3K. Nevertheless the validity of such fittings is subject to discussion. Indeed both models assume a good localized moment on the impurity ($U/\Delta \gg 1$) and so predicts a minimum in the resistivity which is not observed in Pt-Co [4 - 35].

Some other remarks should be made. Above T_M the one impurity effect anomaly seems to become more extended in temperature when the concentration rises (fig.4). This may just be due to the contribution of the high temperature tail of the ordering anomalies situated at lower temperatures (coming from the fraction of impurities which remains magnetic) but also to the existence of a distribution of T_K and so of T_M increasing with the concentration[28].

According to the results of this paper, the effect of an external magnetic field on the specific heat has to be understood differently in the Pt Co and in the Pd-Co alloys [13 - 14]. For the last system the tail of the anomaly observed above 1K is due to an ordering anomaly ($T_K \ll 1K$), and the application of an external field just changes the distribution P (H) of molecular field. For Pt-Co however, the tail arising from a one impurity effect anomaly , the field destroys gradually the Kondo or spin fluctuation state and the anomaly approches a Schottky one, as in Cu-Cr [33].

VI - MAGNETIC CONTRIBUTION ABOVE 0.3K

Knowing the proportion of magnetic atoms, it is possible to come back to the results of the more concentrated samples (c >0.6 at %) above 0.3K. The excess specific heat ΔC may be considered as the sum of two terms : ΔC_1 due to the isolated Co atoms and ΔC_2 due to the magnetic ones.
For the concentration c° = 0.31 at.% the magnetic contribution may be neglected since the ordering temperature is about 0.2K and $\Delta C_1^\circ = \Delta C^\circ$. For larger concentrations c, ΔC_1 is taken to be proportional to ΔC°, with a proportionality factor given by the ratio of non magnetic cobalts in the respective concentrations c and c°.

$$\Delta C_1 = \Delta C^\circ \quad \frac{1 - c_m/c}{1 - c_m^\circ/c^\circ} \qquad (10)$$

with c_m/c given by table 1.

Substrating this calculated ΔC_1 from the experimental ΔC yields the ΔC_2 which are plotted in a reduced diagram [36] $\Delta C_2/c_m$ versus T/c_m in fig. 11. Below the maximum, the superposition of the points on a straight line is rather good. The magnetic specific heat ΔC_2 is linear in temperature up to the ordering temperature

$$\Delta C_2 = \gamma_m T \, . \qquad (11)$$

γ_m is roughly independent of the concentration in the whole range of concentration. Its value, $\gamma_m \simeq 7 mJ/K^2$ mole, and the superposition of the curves in the reduced diagram are comparable to those obtained for the Cu-Mn system. Thus, it seems that R.K.K.Y type of interactions between magnetic impurities are responsible of this behaviour, but this is relatively surprising since the ferromagnetic character is expected to be preponderant for the higher concentrations.

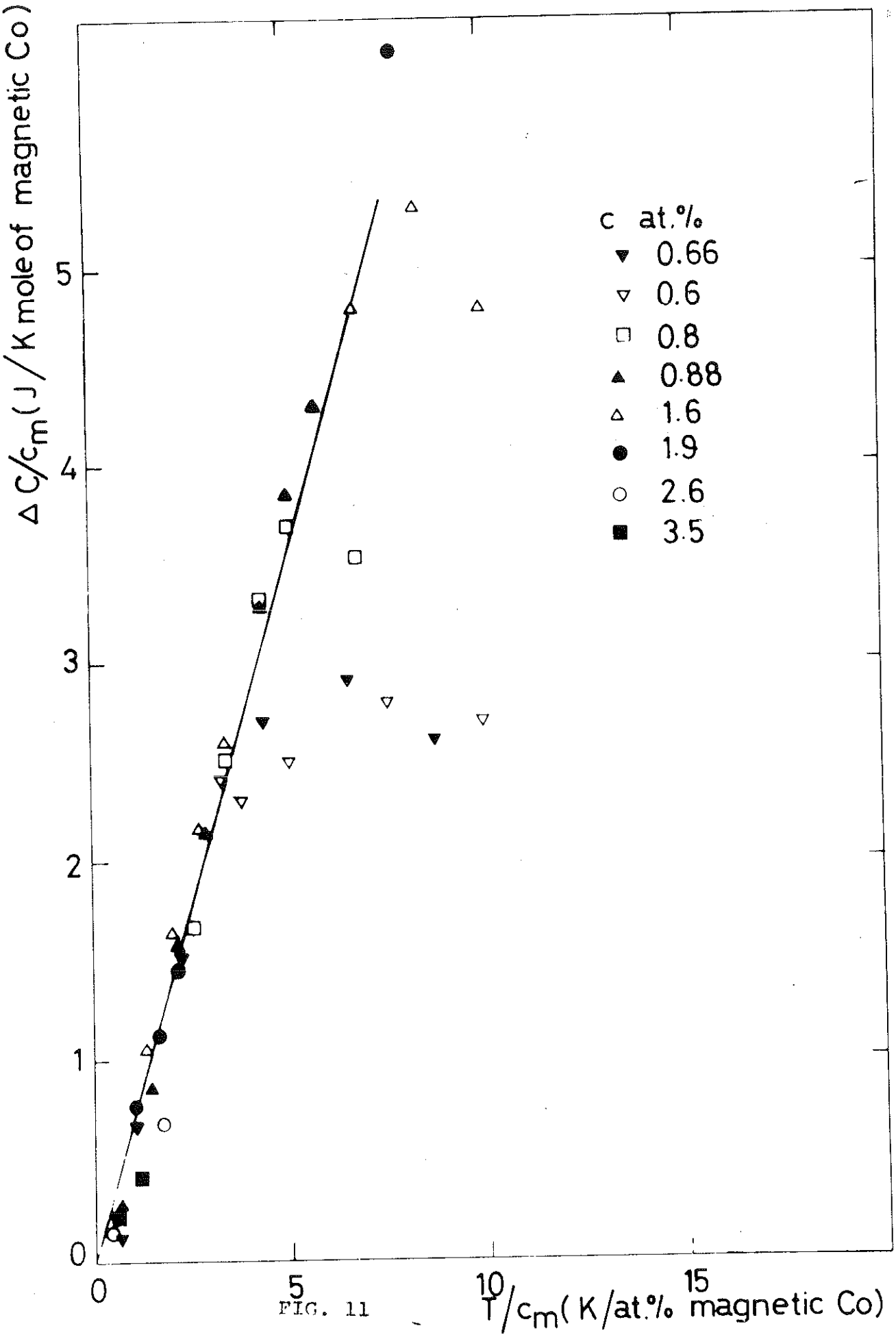
ΔC/cm (J / K mole of magnetic Co)
T/cm (K/at.% magnetic Co)
c at.%
0.66
0.6
0.8
0.88
1.6
1.9
2.6
3.5
0
1
2
3
4
5
0
5
10
15

FIG. 11

C O N C L U S I O N

-:-:-:-:-:-:-:-:-

The low temperature specific heat measurements of the Pt-Co system show the existence of two different types of impurities.

- Non magnetic impurities which produce a one impurity effect anomaly around 1.2 K, not far from the critical temperature T_K = 1.6 K determined by nuclear orientation and magnetization measurements.

- Residual magnetic impurities which order much below T_K and are easily detected by their magnetic hyperfine contribution.

The hyperfine field of the magnetic cobalt atoms is found to be 210 kOe, nearly the same as in f.c.c. ferromagnetic cobalt, thus corresponding to the same maximum moment of 1.7 μ_B. In the giant moment of 3.6 μ_B determined by the magnetization measurements, the excess is due effectively to the host polarization around the impurity as in other giant moment systems like Pd-Fe and Pd-Co.

For the lowest concentrations, the fraction of these magnetic impurities varies as c^2, the square of the total Co concentration. Thus, even in a giant moment system, the "residual magnetism" appears much below T_K in the same way than in classical "Kondo alloys" as Cu-Fe.

A P P E N D I X

The concentration c_m of magnetic impurities has been deduced from equation (5)

$$A = c_m R \frac{I(I+1)}{3} \gamma^2 . \hbar^2 . H^2_{eff/k^2}$$

assuming a unique and same hyperfine field value for all the magnetic impurities. However, this is not the case when the magnetic impurities are coupled by RKKY interactions since the distribution P(H) of molecular field leads to a distribution $p(H_{eff})$ of hyperfine field. Nevertheless the existence of such a distribution does not modify the estimation of c_m as will be shown below.

Indeed, when working with dilute alloys where the contribution of the conduction electrons to the hyperfine field may be neglected, the hyperfine field H_{eff} will be proportional to the mean value of the z component of the electronic spin S :

$$H_{eff} = H_{eff_o} . \frac{\langle S_z \rangle}{S} \qquad (I2)$$

where H_{eff_o} is the saturation hyperfine field and the z direction is defined by direction of the molecular field produced on the site of one magnetic impurity by all the others. Assuming for simplicity S = I/2, the equation (I2) becomes :

$$H_{eff} = H_{eff_o} . \tanh (\mu H / k_T) \qquad (I3)$$

where μ is the electronic moment, H the molecular field and T the temperature. This equation shows that if there is a distribution function P(H) of molecular field, there should exist also a corresponding distribution $p(H_{eff})$ of hyperfine field, where H_{eff} varies from zero to H_{eff_o}. Even more, according to

equation (I3) $p(H_{eff})$ will be temperature dependent even for a temperature independent P(H).

Another way to see this is by recalling that the existence of a magnetic contribution to the specific heat γT, where γ is concentration independent, is due to the ordering of electronic spins located in sites of near zero molecular fields. For such impurities, $\frac{\langle S_z \rangle}{S}$ is different from one and according to equation (I3) the hyperfine field on their nuclei will be different from the saturated value H_{eff_o}.

Let us see now the influence of this hyperfine field distribution on the coefficient A of equation (5). Assuming also the value I/2 for the nuclear spin, its energy will be

$$e = - \frac{\mu_I H_{eff}}{2} \tanh (\mu_I . H_{eff/kT} \quad (I4)$$

where μ_I is the nuclear magnetic moment. The temperature derivative of this expression gives the nuclear Schottky anomaly in the specific heat, the high temperature tail of which is observed in our experiments. Indeed for 3d impurities, the condition $kT >> \mu_I . H_{eff}$ is fulfilled above 40 mK and equation (I4) will be dominated by the term

$$e = \frac{\mu^2_I . H^2_{eff}}{4kT} \quad (I5)$$

And using H_{eff} given by equation (I3)

$$e = -k \frac{\mu^2_I . H^2_{eff}}{4k^2 T} \tanh^2 (\mu H/kT) \quad (I6)$$

Considering now the distribution P(H), the total energy of the nuclear system for one mole of the alloy, will be :

$$E = - \frac{A}{T} \int_{-\infty}^{+\infty} P(H) . \tanh^2 (\mu H/kT) dH \quad (I7)$$

with A given by (5) or :

$$A = c_m . R \frac{\mu^2 I H^2 eff_o}{4k^2} \qquad (18)$$

c_m being the magnetic impurity concentration and R the universal gaz constant. Using the normalization condition

$$\int_{-\infty}^{+\infty} P(H).dH = 1 \qquad (19)$$

equation (17) becomes :

$$E = - \frac{A}{T} \left[1 - \int_{-\infty}^{+\infty} P(H) \ \mathrm{sech}^2 \ (\mu H/kT) dH \right] \qquad (20)$$

Working at temperatures much below the ordering temperature T_o of the alloy, where the magnetic γT term is observed, we are able to make the same simplifications that leads to this γT contribution. In other words, the hyperbolic function in equation (20) will be negligibly small except for very small values of H, where P(H) may be substituted by the constant value P(o). Then :

$$E = - \frac{A}{T} + 2 . \frac{Ak \ P(0)}{\mu} \qquad (21)$$

This may also be expressed using the magnetic coefficient γ by :

$$E = - \frac{A}{T} + \frac{12 \ A\gamma}{\pi^2 \ c_m . R} \qquad (22)$$

Thus, the distribution P(H) of molecular fields just shifts, by a constant value, the total energy of the nuclear system. The nuclear specific heat will then simply be :

$$C = A/T^2$$

with A given by (5) or (18). In other words the nuclear specific heat will be insensitive to the distribution of hyperfine field and will give the same result as if all the impurities

had the same saturated hyperfine field H_{eff_o}. This result is obtained equally in the general case of spins different from I/2, with the use of Brillouin functions.

ACKNOWLEDGMENTS

We thank B. PICOT for his assistance in performing experiments and the metallurgical group of the laboratory for the preparation of the samples.

-- FIGURE CAPTION --

Figure 1 - The specific heat of pure Platinum and of seven Pt-Co samples measured above 0.3K.

Figure 2 - The specific heat C divided by the temperature T as a function of T^2 for pure Pt. The insert shows the scattering of the experimental points.

Figure 3 - The excess specific heat ΔC of the alloys obtained by substracting the pure platinum contribution for $T > 0.3K$.

Figure 4 - The excess specific heat ΔC divided by the concentration c of Co atoms as a function of the temperature, for $T > 0.3K$. The error bars are given for the 3 less concentrated alloys.

Figure 5 - The specific heat of the 5 more concentrated samples as measured below 0.5K

Figure 6 - The product CT^2 of the measured specific heat by the square of the temperature as a function of T^3 for $T < 0.2K$. The temperatures of 0.1 and 0.2K are indicated by arrows.

Figure 7 - The coefficient A of the $1/T^2$ term of the nuclear Schottky anomaly as a function of the cobalt concentration. The broken lines represent linear and quadratic dependences in this log.log. diagram.

Figure 8 - The nuclear Schottky anomalies versus temperature. The term linear in temperature and the matrix contribution have been substracted from the total specific heat. The full lines representing the calculated Schottky anomalies with H_{eff}=210kOe provide the values of c_m reported in figure 9. Also shown for the 2.6 at.% a tentative fitting corresponding to 180 and 240 kOe for the hyperfine field (—·—) and the A/T^2 term.

Figure 9 - The fraction c_m/c of the magnetic Co concentration to the total concentration as a function of the total concentration c, determined from our results (O) and magnetization measurements (□). The full lines represent P_z for the different values of Z.

Figure 10 -The excess specific heat ΔC divided by the concentration $c-c_m$ of isolated Co atoms for the 0.31 at.% sample, showing the one impurity effect anomaly. Filled circles are results obtained with the He^3 apparatus, the others being those obtained with the demagnetization apparatus. Curve a shows the anomaly already observed in Cu-Cr (32) and associated with the Kondo effect, curve B-H, Bloomfield and Haman's prediction for the Kondo anomaly normalized to spin 2 and curve Sc, Schweitzer's prediction.

Figure 11 -The reduced diagram of the magnetic contribution $\Delta C_2/c_m$ against T/c_m. Concentrations of 1.6, 1.9 and 3.5 at.% are obtained from Wheeler's results (12).

REFERENCES

1- J. CRANGLE and W.R. SCOTT, J. Appl. Phys. 36, 921 (1965)

2- L. D. GRAHAM and D.S. SCHREIBER, Phys. Rev. Lett. 17, 650 (1966)

3- L.D. GRAHAM and D.S. SCHREIBER, J. Appl. Phys. 39, 963 (1968)

- L. SHEN, D.S. SCHREIBER and A.J. ARKO, Phys. Rev. 179, 512 (1969)

4- P. LEDERER and D.L. MILLS, Phys. Rev. I65, 837 (1968)

A.B. KAISER and S. DONIACH, Int. J. Magnet. I, II (I970)

5- J.C. GALLOP and I.A. CAMPBELL, Solid State Comm.6,831 (I968)

6- J. L. THOLENCE and R. TOURNIER, Phys. Rev. Lett. 25, 867 (1970)

7- J.L. THOLENCE and R. TOURNIER, Suppl. J. de Physique 32, C1 - 211 (1971)

8- R. TOURNIER and A. BLANDIN, Phys. Lett. 24, 397 (1970)

9- P. COSTA-RIBEIRO, J. SOULETIE and D. THOULOUZE, Phys. Rev. Lett. 24, 900 (1970)

10- E. BOUCAI, B. LECOANET, J. PILON, J.L. THOLENCE and R. TOURNIER, Phys. Rev. B3, 3834 (1971)

11- B. TISSIER, R. TOURNIER, Solid State Comm. 11, 895 (1972)

12- J.C.G. WHEELER, J. Phys. C. 2, 135 (1969)

13- B.M. BOERSTOEL and C. VAN BAARLE, J. Appl. Phys. 41, 1079 (1970)

14- J.E. VAN DAM and C.J. VAN DEN BERG, Phys. Stat. Sol. 3, 11 (1970)

15- T. ERICSON, M.T. HIRVONEN, T.E. KATILA and V.K. TYPPI, Sol. Stat. Comm. 8, 765 (1970)

[16]- F.J. DU CHATENIER and J. DE NOBEL, Physica 32, 1097 (1966)

[17]- D. THOULOUZE, Thesis (unpublished)- University of Grenoble, France (1968)
J. Appl. Phys. 39, 1320 (1968)

[18]- P. COSTA RIBEIRO, J. SOULETIE, D. THOULOUZE R. TOURNIER, Suppl. J. de Physique 32, C1 753 (1971)

[19]- O. BETHOUX, M. FERRARI, B. CORNUT, Rev. Appl. Phys. 5, 865 (1970)

[20]- K.H. GOBRECHT , J.J. VEYSSIE, and L. WEIL, Acad. Sci. Fennicae 210, 63 (1966)

[21]- K.H. GOBRECHT and M. SAINT-PAUL , Proceedings of the Third International Cryogenic Engineering Conference at Berlin 235 (1970)

[22]- D. THOULOUZE, J.KEYSTON, A. LACAZE, Cryogenics 8, 295 (1968)

[23]- P. COSTA-RIBEIRO, J. SOULETIE and B.PICOT, to be published

[24]- B.M. BOERSTOEL, J.J. ZWART and J. HANSEN, Physica 54, 442 (1971)

[25]- A.A. MARADUDIN, E. MONTROL and G.H. WEISS, Solid State Physics, Suppl. 3, F. Seitz and D. Turnbull eds. (Academic Press, N.Y. 1963) Chap. V.

[26]- A.C. GOSSARD, A.M. PORTIS, M. RUBINSTEIN, and R.M. LINDQUIST, Phys. Rev. 138, A. 1415 (1965)

[27]- S. EHARA, J. Phys. Soc. Japan 19, 1313 (1964)

[28]- R. TOURNIER, to appear in the Proceedings of the 13th Int. Conf. on Low Temp. Phys. BOULDER, Colorado (1972)

[29]- J.W. LORAM et al, Phys. Rev. B., 5, 3659 (1972)

[30]- W.L. TROUSDALE, G. LONGWORTH, T.A. KITCHENS, J. Appl. Phys. 38, 922 (1967)

[31]- B.M. BOERSTOEL, Thesis, Leiden 1970

[32]- B.B. TRIPLETT and NORMAN E. PHILLIPS, Phys. Rev. Lett. 27, 1001 (1971)

[33]- P.H. BLOOMFIELD and D.R. HAMMAN, Phys. Rev. 164, 856 (1970)

- B.B. TRIPLETT Thesis, Berkeley (1970)

[34]- J.W. SCHWEIZER et al., to be published

[35]- O. LABORDE, P. RADHAKRISHNA (to be published)

[36]- J. SOULETIE and R. TOURNIER, J. Low Temp. Phys. 1, 95 (1969).

L'EFFET DES INTERACTIONS DANS LE Zn-Mn ET VALEUR DU CHAMP HYPERFIN SUR LE Mn

Les alliages de Manganèse, comme ceux de Cobalt, se prêtent bien à la mesure de la chaleur spécifique nucléaire, vu la valeur importante du moment nucléaire du Mn. Les interactions à courte distance jouent probablement un rôle important dans le Al-Mn ($T_K \simeq 10^3$K), mais les difficultés métallurgiques associées à la fabrication de cet alliage ont rendu impossible une telle étude. L'effet des interactions à longue distance doit aussi être observé sur le Zn-Mn qui, malgré quelques problèmes, s'avère être un système métallurgiquement plus stable.

Des mesures de résistivité électrique [1] et d'orientation nucléaire[2] sur le système Zn-Mn donnent $T_K \simeq 0{,}25$K. En estimant la dépendance de la température d'ordre avec la concentration à 20K par %[3], nous pouvons évaluer la concentration "critique", autour de laquelle des effets non linéaires en concentration pourraient être observés, à 0,01% at. Effectivement, l'existence jusqu'à 0,02% at. d'une fraction prépondérante d'impuretés magnétiques parait être confirmée par une dépendance linéaire avec la concentration du maximum de l'anomalie observée par des mesures de chaleur spécifique entre 0,4 et 3K (T_{max} = 0,4K pour 0,02% at. et T_{max} = 1K pour 0,05% at.)[3].

Néanmoins, des effets non linéaires en concentration ont été observés jusqu'à 0,8% at. dans le Pt-Co, où la concentration "critique"définie comme celle pour laquelle $T_{ordre} = T_K$ serait de l'ordre de 0,1% at. Il parait donc possible d'observer

sur le Zn-Mn l'existence de tels effets de concentration, pour des concentrations supérieures à cette "concentration critique" de 0,01% at. et correspondant mieux à la gamme de sensibilité de notre appareil.

Des mesures de chaleur spécifique ont été effectuées sur 4 échantillons de Zn-Mn, préparés par le groupe de métallurgie du laboratoire à partir de Zn Asarco 99,999% et de Mn Johnson Matthey 99,999% suivant la procédure décrite dans la référence 3 et avec des concentrations nominales de 0,2, 0,1, 0,05, et 0,03% at. Les analyses spectroscopiques ont donné néanmoins des concentrations réelles bien inférieures : 0,17, 0,082, 0,042 et 0,024% at.
Des anomalies observées dans les mesures d'aimantation des alliages moins concentrés ont conduit à craindre l'existence d'une ségrégation produite au cours du refroidissement des alliages. Les résultats présentés ci-dessous semblent indiquer que de telles craintes étaient sans fondement. Trois conclusions intéressantes peuvent être dégagées de nos mesures.

(1) Pour les deux concentrations plus élevées (1700 et 820 ppm) les points expérimentaux portés dans le diagramme $CT^2(T^3)$ se trouvent sur deux droites de même pente, confirmant par là, l'existence d'interactions du type RKKY entre impuretés magnétiques[34]. La valeur du coefficient γ du terme linéaire en température correspondant est de $4,7 \pm 0,3$ mJ/K^2 mole, valeur supérieure à celle déduite des résultats de Smith[4] (4,1 mJ/K^2 mole) et de Martin [3] (3,7 mJ/K^2 mole).

(2) Pour ces deux concentrations, la contribution obtenue en soustrayant le terme γT de la chaleur spécifique mesurée, est bien décrite par une anomalie Schottky correspondant à un champ effectif H_{eff} = 225 Koe sur les noyaux de manganèse (fig.1). Il s'ensuit que pour ces 2 concentrations toutes les impuretés sont magnétiques et ont le même champ hyperfin.
Ce champ est supérieur de 20% à celui déterminé en orientation nucléaire d'après la valeur à saturation obtenue par extrapolation de la courbe donnant le champ hyperfin H_{eff} en fonction du champ appliqué sur un alliage contenant moins de 1ppm de

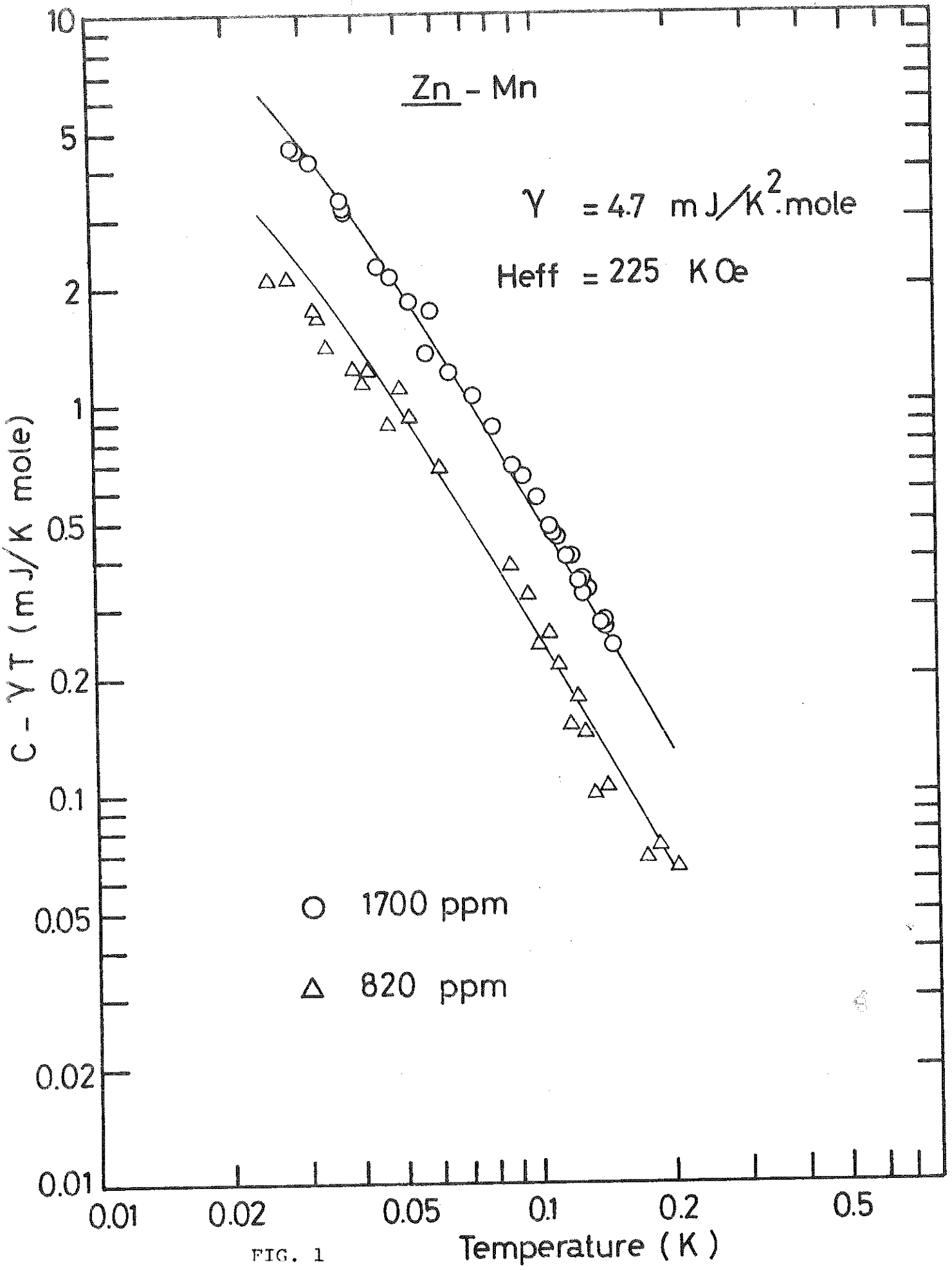
Zn - Mn
γ = 4.7 mJ/K².mole
Heff = 225 KOe
1700 ppm
820 ppm
C - γT (mJ/K mole)
Temperature (K)
10
5
2
1
0.5
0.2
0.1
0.05
0.02
0.01
0.01
0.02
0.05
0.1
0.2
0.5

FIG. 1

Mn[2]. Cet écart entre le champ effectif à saturation d'une "impureté isolée" déduit par orientation nucléaire et le champ effectif mesuré par la chaleur spécifique nucléaire sur des impuretés rendues magnétiques par interaction a été aussi observé sur le Pt-Co. En effet, la saturation de"l'impureté isolée" est difficile à atteindre en champ extérieur[5,6] et l'extrapolation des champs hyperfins effectuée n'est probablement pas exacte.

(3) Pour les deux échantillons moins concentrés (420 et 240ppm) la chaleur spécifique mesurée, une fois déduit le terme γT, est supérieure à l'anomalie Schottky prévue si toutes les impuretés étaient magnétiques et portaient le champ effectif de 225KOe déterminé précédemment (fig.2). L'excès observé doit probablement être attribué à la contribution de l'anomalie à une impureté située autour de T_K , qui est due à l'existence d'une fraction d'impuretés non magnétiques.

La proximité des anomalies Schottky nucléaires des impuretés magnétiques et des anomalies à 1 impureté des impuretés non magnétiques d'une part, et la limite de sensibilité de notre système de mesure d'autre part empêchent de refaire pour le Zn-Mn une analyse aussi détaillée que pour le Pt-Co. Nous pouvons néanmoins affirmer l'existence d'une anomalie de chaleur spécifique autour de 0.1K dans l'alliage Zn-Mn.

L'existence d'une telle anomalie a été aussi mise en évidence par des mesures récentes de chaleur spécifique entre 0.7 et 4K. En effet, Smith[4] obtient une superposition de courbes $\Delta C/c$ en fonction de T, pour des concentrations de 60 et 112 ppm, permettant de conclure à l'existence d'une anomalie à une impureté dont le maximum doit se trouver à des températures bien inférieures à 0,7K.

Il est intéressant de noter que l'observation de cette anomalie impliquant l'existence des impuretés non magnétiques a été faite sur des alliages 200 et 500 ppm pour lesquels la température d'ordre est proportionnelle à la

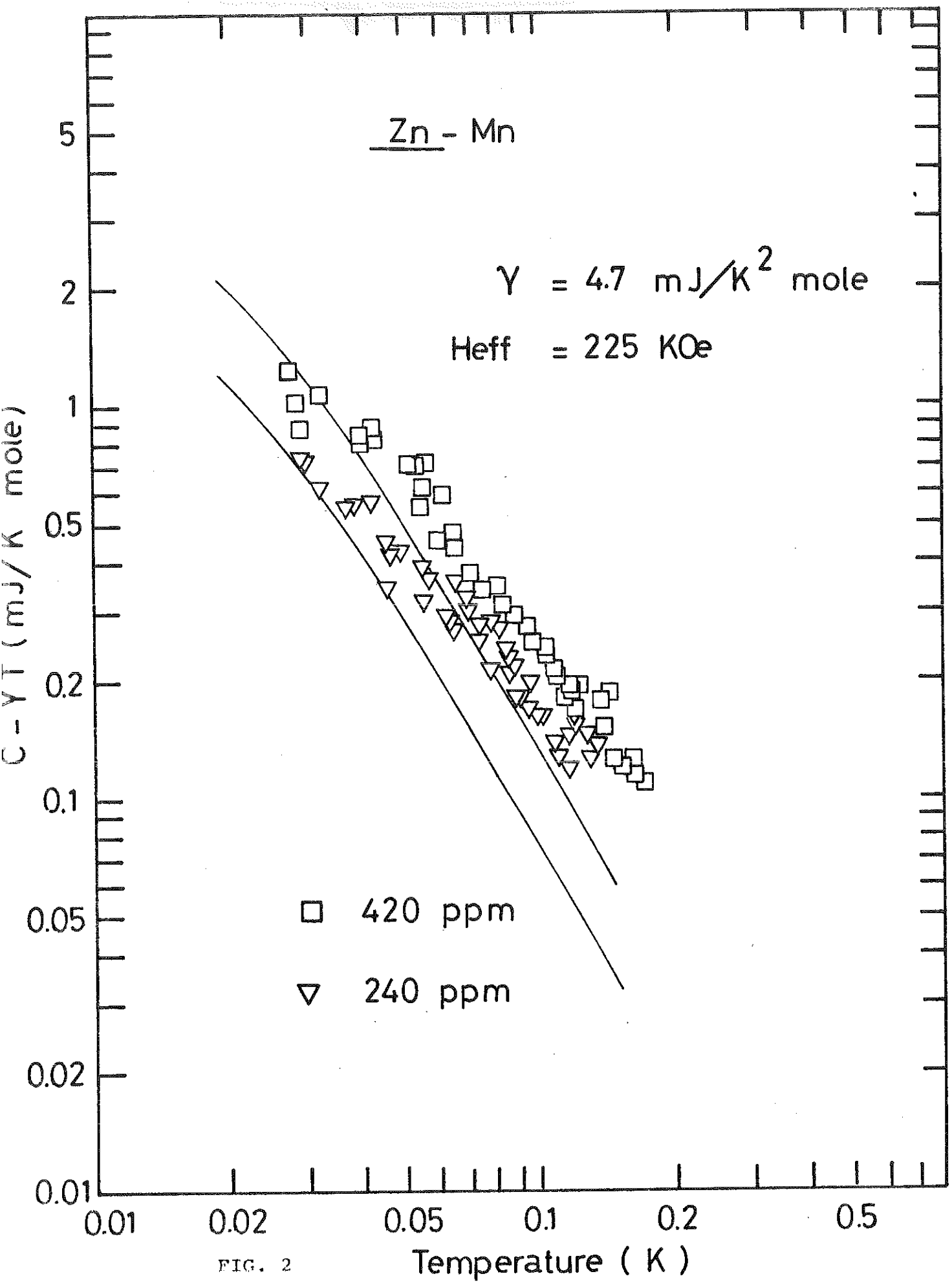
Zn - Mn
γ = 4.7 mJ/K² mole
Heff = 225 KOe
420 ppm
240 ppm
C - γT (mJ/K mole)
Temperature (K)
5
2
1
0.5
0.2
0.1
0.05
0.02
0.01
0.01
0.02
0.05
0.1
0.2
0.5

FIG. 2

concentration[3]. Ceci provient probablement de ce que la température d'ordre est donnée par les impuretés qui sont à l'intérieur du rayon de corrélation et est donc indépendante des impuretés qui se trouvent sur des sites où le champ moléculaire est proche de zéro. Une fraction de ces dernières peuvent alors donner origine à l'anomalie à 1 impureté.

R E F E R E N C E S

(1) R.S. NEWROCK et al, J. Low Temp. Phys. 5, 701 (1971)

(2) J.D. MARSH, Phys. Letters, 334, 207 (1970)

(3) D.L. MARTIN, Phys. Rev. 167, 640 (1968) et 186, 642 (1969)

(4) F.W. SMITH, à paraître

(5) B. TISSIER et R. TOURNIER, Sol. State Comm. 11, 895 (1972)

(6) F. FLOUQUET, communication privée.

- C O N C L U S I O N -

-:-:-:-:-:-:-:-:-

Les mesures de chaleur spécifique à très basse température nous ont permis d'étudier l'effet des interactions sur le comportement magnétique des impuretés dans quelques alliages dilués. Les effets observés dépendent de la valeur de la température caractéristique T_K de l'alliage, mesurée aux concentrations évanescentes.

Dans le cas du Cu-Mn pour lequel $T_K << 10^{-2}K$, la mesure d'un échantillon contenant 0.9% at. de Mn a permis de séparer la contribution nucléaire de l'impureté de celle de la matrice. Le champ hyperfin sur le Mn déduit de cette mesure (290 ± 10KOe) se trouve être le même, à l'erreur de mesure près, que celui déterminé par orientation nucléaire dans un échantillon contenant seulement de l'ordre du ppm de Mn (280 ± 10KOe). L'interaction entre impuretés ne semble donc pas affecter la valeur du moment porté par le Mn dans cette gamme de température et de concentration.

Pour les alliages de Co dans l'Au, avec $T_K >> 1K$, l'étude de la variation de la contribution nucléaire avec la concentration, montre que l'effet des interactions entre impuretés proches voisines est prépondérant et fait apparaître un moment magnétique correspondant à un champ hyperfin de 190KOe sur les atomes de Co appartenant à des groupes d'au moins 3 atomes proches voisins. La contribution linéaire en température, γT, peut être séparée en un terme indépendant de la concentration et caractéristique de l'interaction RKKY entre impuretés magnétiques, et de deux

autres termes variant l'un comme la concentration, l'autre comme le carré de la concentration et pouvant être respectivement associés à la contribution des impuretés non magnétiques isolées et en paires. En se plaçant dans le modèle LSF et en supposant un fort couplage de Hund, ces 2 derniers termes permettent de déterminer des valeurs de T_K de 700 et 50K respectivement associés aux impuretés isolées et en paire.

L'importante augmentation de la contribution nucléaire observée lors de l'introduction d'impuretés de Fe dans l'Au-Co montre que la fraction d'impuretés de Co non magnétiques dans l'Au-Co est prépondérante, comme prévue si les impuretés magnétiques sont celles appartenant aux groupes d'au moins 3 atomes de Co. La variation avec la concentration de la contribution nucléaire à la chaleur spécifique a été traitée dans un modèle de champ moléculaire et a mené à associer les valeurs de 14 et 200K aux T_K des paires et isolés de Co. L'écart existant entre les valeurs de T_K déterminées par les mesures de chaleur spécifique effectuées sur l'Au-Co d'une part et celles obtenues par susceptibilité sur l'Au-Co et chaleur spécifique sur l'Au-Co-Fe d'autre part, met en doute la validité du modèle LSF pour décrire le comportement de ces alliages.

Contrairement à ce qui se passe pour le fer, l'introduction de 5% at d'impuretés de Ni dans un alliage $\underline{Au}\text{-Co}_{1,5\%}$ n'a aucun effet sur le comportement magnétique du Co, la chaleur spécifique de l' Au-Co-Ni étant la somme de celle de l'Au-Co et de l'Au-Ni.

Pour des alliages avec $10^{-2}K \lesssim T_K \lesssim 1K$, comme Pt-Co et Zn-Mn, l'effet des interactions entre impuretés à longue distance sont dominants. Pour le Pt-Co, la contribution nucléaire permet de compter le nombre d'impuretés magnétiques dans l'alliage et l'étude en fonction de la concentration de Co montre que ce nombre croit avec le carré de la concentration totale, pour les faibles concentrations, les impuretés magnétiques portant un champ hyperfin de 210KOe. Ces résultats sont en très bon accord avec les mesures d'aimantation effectuées par M. Tissier sur les mêmes échantillons et les atomes magnétiques sont associés aux atomes distants de moins de 8Å d'un autre voisin du même type. La contribution des impuretés non magnétiques produisent une anomalie à une impureté dont le maximum se situe autour de 1,2K ($T_K \sim 1,6K$), comme le montrent les mesures de M. Saint-Paul.

Pour le Zn-Mn ($T_K \sim 0,2K$), l'anomalie à une impureté produite par les Mn non magnétiques et la contribution nucléaire Schottky des atomes magnétiques, sont superposées pour les deux concentrations les plus faibles mesurées. Pour les échantillons de plus forte concentration, l'anomalie Schottky est seule présente, toutes les impuretés étant magnétiques, et permet de déterminer un champ hyperfin de 225 KOe sur le Mn.

Dernière page d'une thèse

VU

Grenoble, le

Le Président de la thèse

VU, et permis d'imprimer,

Grenoble, le

Le Président de l'Université
Scientifique et Médicale